COMPATIBILISATION BY CHAIN COUPLING AGENTS: ENGINEERING POLYMERS/THERMOTROPIC LIQUID CRYSTALLINE POLYMER BLENDS

A THESIS

SUBMITTED TO THE

UNIVERSITY OF PUNE

FOR THE DEGREE OF

DOCTOR OF PHILOSOPHY

(IN CHEMISTRY)

BY

RAJKUMAR PATEL

CHEMICAL ENGINEERING & PROCESS DEVELOPMENT DIVISION

NATIONAL CHEMICAL LABORATORY

PUNE- 411008

INDIA

JULY 2005

Dedicated to Parents

CERTIFICATE

Certified that the work incorporated in the thesis, **"Compatibilisation by Chain Coupling Agents: Engineering Polymers/Thermotropic Liquid Crystalline Polymer Blends"** submitted by **Mr. Rajkumar Patel**, for the Degree of **Doctor of Philosophy**, was carried out by the candidate under my supervision in the Chemical Engineering and Process Development Division, National Chemical Laboratory, Pune 411008, India. Material that has been obtained from other sources is duly acknowledged in the thesis.

Dr. S. Ponrathnam

(Research Supervisor)

Acknowledgment

I express my sincere gratitude to Dr. Surendra Ponrathnam for his invaluable guidance. His continuous encouragement and specifically to be a "self-critic" is source of inspiration for me. I do not have words to express my feelings about his hard work and dedication towards research. I consider myself fortunate for having had a chance to work with him. I am grateful to him much more than words can express.

I am very much obliged to Dr. C. R. Rajan for inspiring discussions, continuous personal and professional help through out my doctoral research period.

I express my immense sense of gratitude to Dr. B. D. Kulkarni, Head, Chemical Engineering Division, National Chemical Laboratory, Pune, for his encouragements, scientific discussions and providing me opportunity to apply for SRF through him.

I will always remain indebted to Dr. Sudhir S. Kulkarni for the immense help he had rendered to me. His inspiration had eventually created my interest in this field of research. I express my sincere thanks to Dr. Upendra Natrajan for introducing me to the field of nanocomposites I sincerely thank Dr A. Lele for extending co-operation in carrying processing work in polymer processing centre. I am extremely thankful to Mr E. Deenadayalan .for assisting me working in processing and testing equipments in PPC as well as for valuable scientific discussion. I am thankful to Dr. D. R. Saini for scientific discussions. I deeply acknowledge Dr .A. Gaikward for this invaluable and timely help in obtaining SEM results. I am thankful to Dr. C. Ramesh for allowing me to run X-ray diffraction. I am thankful to Dr. Gurushwamy Kumaraswamy, who trained me in Aries instrument. I would like to acknowledge Dr.(Ms.) J. Jog for use of polarised light optical microscopy. I am thankful to Mr. H. Pol for his safety instructions. I would like to acknowledge Ms. Dhobale for training me to operate Leica's microtoming instument. I am obliged to Dr. R. S. Ghadge for scientific discussions. I would like to acknowledge Dr.(Ms.) Smita Mule for assisting me to operate instruments like DSC, PLOM, and IR.

I would like to acknowledge Mr. Gnaneswar for assisting in scanning NMR. .I would like to acknowledge Mr. Mahendra for his help to repair Parr reactor. I am obliged to Mr. Borker for his timely help to repair DSM microcompounder.

I have had the privilege of working with our wonderful labmates, Arika, Anjali, Om Prakash, Sunita, Suresh, Kamal, Vikas, Vaishali, Varsha, Rethi, Tara Shanker, Pallavi, Meghana, Avinash, Sarika, Supriya, Kiran, Ganesh, Hari, and Trupti especially each of whom accomplished a great deal. I am also thankful to Laha, Amitabh, Nayan, Renuka, Jeetu, Rajeev, Bhaben, Deba, Subhangi, Ajit, Akhilesh,, Anuj, Rajkiran Mahajan, Sandeep, Madhuri and Jaya for their help. It is difficult to name all friends who have contributed a lot. I thank them very much. I am extremely thankful to Akhilesh and Abhey for allowing me to stay with them during my initial period at National Chemical Laboratory.

I am thankful to Satheji for his help throughout this research work. I am thankful to Mr. Bhugang for drawing figures.

I deeply acknowledge the help of Banerjee, Bhalerao, Girme, Giri, Radhakrishnan, Ravi, Radha, Subbi, Shekhar, Shukla, Dhupe and Naravane.

I thank the staff of library, civil engineering, workshop, glass blowing, centre for material characterisation, administration and security.

I express my sincere gratitude to Dr. Debendra Pradhan because of whom I came to National Chemical Laboratory.

No words can express my gratitude towards my mother, brothers, bahus and in-laws. The care of my wife, Mili and smile of my daughter, Gayatri could relive my restlessness during this works.

The senior research fellowship by Council of Scientific and Industrial Research, New Delhi, India during this period is duly acknowledged. The financial aid given by Department of Biotechnology and Ministry of Information and Technology is duly acknowledged.

Finally, I feel sense of respect for Dr. Paul Ratnaswamy, former director and Dr. S. Sivram, Director, National Chemical Laboratory, Pune for permitting me to submit this work in the form of thesis.

Rajkumar Patel

TABLE OF CONTENTS

CHAPTER 1

GENERAL INTRODUCTION

CHAPTER 2

POLY(ETHYLENE TEREPHTHALATE-CO-OXYBENZOATE)-BLOCK-POLY(PHENYLENE SULPHIDE) AND POLYSULPHONE

CHAPTER 3

COMPATIBILISATION OF PPS/PET-OB BLENDS

CHAPTER 4

COMPATIBILISED POLYSULPHONE/POLY(ETHYLENE TEREPHTHALATE-CO-OXYBENZOATE) BLENDS

CHAPTER 5

THERMOTROPIC LIQUID CRYSTALLINE POLYMER-CLAY NANOCOMPOSITES BY MELT PROCESSING

LIST OF FIGURES

LIST OF TABLES

LIST OF SCHEMES

LIST OF ABBREVIATIONS

PPS	**Poly(phenylene sulphide)**
PSU	**polysulphone**
DCTPSU	**Dicarboxyl terminated polysulphone**
DCTPPS	**Dicarboxyl terminated poly(phenylene sulphide)**
PET-OB	**Poly(ethylene terephthalate-co-oxybenzoate)**
OB	**Oxybenzoate**
DCTPET-OB	**Synthesis of dicarboxyl terminated poly(ethylene terephthalate-co-oxybenzoate)**
TLCP	**Thermotropic liquid crystalline polymer**
Vectra A950	**Copolyester of hydroxy naphthoic acid and hydroxy benzoic acid**
BCP-1	**Poly(phenylene sulphide)-*block*-poly(ethylene terephtha-late-co-oxybenzoate)**

BCP-2A	**Polysulphone (n≈4)-*block*-poly(ethylene terephthalate-co-oxybenzoate)**
BCP-2B	**Polysulphone (n≈6)-*block*-poly(ethylene terephthalate-co-oxybenzoate)**
BCP-2C	**Polysulphone (n≈8)-*block*-poly(ethylene terephthalate-co-oxybenzoate)**
ΔHm	**Heat of fusion**
ΔHc	**Heat of Crystallisation**
α	**Degree of crystallinity**

CHAPTER-1

General introduction

Rajkumar Patel

National Chemical Laboratory

CHAPTER 1

1. General introduction

Polymer science and technology has undergone enormous expansion over the last few decades.[1-5] First, was the development of new polymers from a seemingly endless variety of monomers. Next, random copolymerisation was used as an effective technique for tailoring or modifying polymers. Later, more controlled block and graft copolymerisation was introduced. The list of new concepts in polymer synthesis has not been exhausted. However, it has become clear that new chemical structures or organisation are not always needed to meet new needs or to solve old problems.

1.1. Polymer blends, alloys and composites

Mixing two or more polymers together to produce a blend (or 'alloy') is one well established strategy for achieving a specified portfolio of physical properties, without the need to synthesise specialised polymer systems.[2-7] The subject is vast and has been the focus of much work, both theoretical and experimental.

More recently, an extraordinary research effort in polymer blends and alloys, in both academia and industry, has led to a mushrooming growth of the patent and scientific literature. A number of books, reviews and congress proceedings covering all aspects of the preparation, phase behaviour and applications of the different types of blends have been published.[1-15] The earlier development in polymeric materials involved synthesis of new homopolymers and copolymers for tailoring properties. The realisation that new molecules are not always required to attain desired properties and that blending can be employed more readily has lead to the commercial as well as scientific interest in blend technology. Polymer blends are mixtures of chemically different polymers and/or

copolymers. They are mainly multiphase systems with the structure dependent on composition and processing conditions.

Polymer alloys are polyblends in which a large interpenetration of domains is secured by either chemical or physical means. 'Blends' are a direct result of the blending action and 'alloys' are the final blends of well-defined morphology and set of properties. As raw material cost contributes from 35 to 80 percent of the finished article, the future of polyblends lies in their attractive cost/performance ratio. The primary advantages in employing polymer blends or alloys are as follows: (a) higher performance at a reasonable price: (b) modification of performance as a market develops; (c) extending the performance of expensive resins; (d) reuse of plastic scrap; (e) generation of unique materials with respect to processability and/or performance.

Blends/alloys can be developed at a much faster rate than new polymers allowing manufacturers to respond rapidly to changing market requirements, since their properties are a function of composition. For these reasons the growth rate of polymer blends/alloys is about 40 % per year compared to the 10 % growth rate of the entire polymer industry. There are an increasing number of patents filed in the area and about 295 blends/alloys are commercially available.[2] The development of polymer blends/alloys requires a sound scientific basis and offers opportunities for interesting fundamental work. The interest amongst scientists in this fast growing area is evidenced by the large number of research papers, books and symposia held.

1.1.1. Methods of blending

The manner in which two polymers are mixed together is of vital importance in controlling the properties of blends and to the ensuing properties of blends. Most

common techniques for preparing blends are melt-mixing, solution blending and co-precipitation.[4,5] Preparation of polymer blends can be accomplished by: (i) mechanical mixing; (ii) solvent casting; (iii) co-precipitation; (iv) latex blending; (v) interpenetrating polymer networks (IPN) technology.

(i) Mechanical mixing of two polymers in the molten state under shear is usually achieved with the help of DSM microcompounder (double screw). For economic reasons mechanical blending predominates.

(ii) Solvent casting involves dissolving the polymers in common solvent and the subsequent evaporation of solvent.

(iii) Co-precipitation involves dissolving the polymers in a common solvent and the subsequent removal of solvent by precipitation using an appropriate non-solvent.

(iv) Latex blending involves mixing the lattices of two polymers and spraying the mixture followed by drying.

(v) Interpenetrating polymer networks (IPN) technology involves the polymerisation of a monomer in the presence of another polymer.

1.1.2. Types of blends and composites: *Terminology*

In case of blends and composites various terminologies are used. Those are as follows:

Polymer blend: A mixture of at least two polymers or copolymers.

Homogeneous blend: A mixture of two homologous polymers, usually narrow molecular weight distribution fractions of the same polymer.

Miscible polymer blend: Polymer blend homogeneous down to the molecular level, associated with the negative value of free energy of mixing; $\Delta G = \Delta H \leq 0$.

Immiscible polymer blend: Any polymer blend whose $\Delta G = \Delta H \geq 0$.

Compatible polymer blend: A term indicating a commercially attractive polymer mixture with enhanced physical properties over the constituent polymers.

Polymer alloy: An immiscible polymer blend having a modified interface and/or morphology.

Compatibilisation: A process of modifying interfacial properties of an immiscible polymer blend, leading to the creation of a polymer alloy.

Composites: Composites consist of a thermoplastic matrix and reinforcing fibres as dispersed phase.

Macrocomposites: Inorganic materials like glass fibres or carbon fibres are used as reinforcement.

Microfibrillar Composites (MFCs): Upon drawing and annealing, the components of the immiscible blend are oriented and microfibrils are formed. Bundles of highly oriented microfibrils act as reinforcing elements in MFCs.

Molecular composites: Rigid rod molecules (eg. liquid crystalline polymer) are used as reinforcement dispersed phase within flexible coil matrix (eg. thermoplastic matrix)

1.2. Miscibility in blends and composites

Polymer blends can be characterised by their phase behaviour as being either miscible or immiscible. Immiscible blends show multiple amorphous phases with each phase consisting of essentially pure components whereas the phases of partially immiscible blends may contain some of each component. Blends can also be completely miscible and have only one amorphous phase. The mechanical, thermal, rheological and other properties of a polymer blend depends strongly on its state of miscibility.[1-5]

Only a few polymer blends are truly miscible on a molecular scale, poly(phenylene oxide)/polystyrene (PPO/PS) and poly(vinyl chloride)/polycaprolactam (PVC/PCL) are examples of such systems. Miscible systems exhibit a single glass transition temperature (T_g) located between the T_g values of the two components and are expected to behave like single component polymers. They are generally transparent and can be moulded without streaking. The heat distortion temperatures (HDT) of miscible blends vary smoothly with composition and thus are easy to predict and to control.

Most polymer mixtures are immiscible and form multiphase systems. The interface between two adjacent phases is not clear-cut. There are composition gradients whose levels depend on the intensity of mixing and on solubility parameter values (δ) of the polymers. These sometimes require compatibilisation in order to decrease the degree of immiscibility or to improve compatibility by mechanical or chemical means. Compatibilisers are generally graft or block copolymers of a mutually 'compatible' polymer or plasticiser and lead to the formation of alloys where interpenetration of domains is achieved to a greater extent.

Compatibilisation of blend components is a major consideration while designing blends and is often the primary criterion for commercial success. The major future challenges and developments for compatibilisation technology lie in three main areas of blending: engineering polymer blends, superior commodity polymers and polymer recycling.

Blends are considered as compatible when they possess a desirable set of properties. Interfacial behaviour is important to polymer blends (Fig. 1.1). Compatibilisation can interact in complex ways to influence final blend properties[13]: (i)

reduce the interfacial tension in the melt, causing an emulsifying effect and leading to an extremely fine dispersion of one phase in another; (ii) increase the adhesion at phase boundaries giving improved stress transfer; (iii) stabilise the dispersed phase against growth during annealing, which would modify the phase boundary interface.

1.3. Methods of compatibilisation

A number different approaches have been established for compatibilisation:[4,5] (1) Achievement of thermodynamic miscibility; (2) Addition of block or graft copolymers; (3) Addition of functional/reactive polymers; (4) *In situ* grafting/polymerisation (reactive blending).

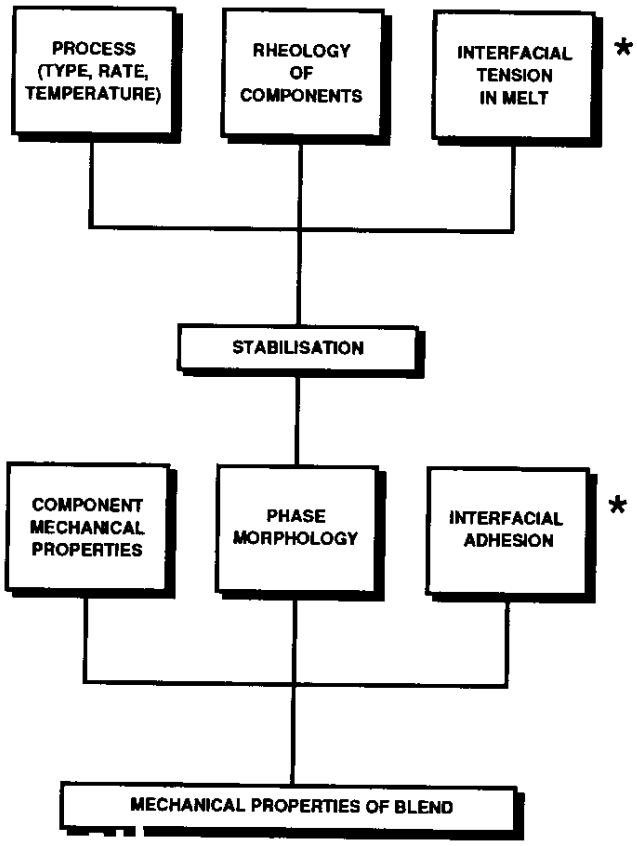

Figure 1.1: Influence of interfacial behaviour in polymer blends

1.3.1. Thermodynamic miscibility

Miscibility between polymers is determined by a balance of enthalpic and entropic contributions to the free energy of mixing. While for small molecules the entropy is high enough to ensure miscibility, for polymers the entropy is almost zero, causing enthalpy to be decisive in determining miscibility. The change in free energy on mixing (ΔG) is written as: $\Delta G = \Delta H - T\Delta S$. Here, H is enthalpy, S is entropy and T is temperature. For spontaneous mixing, ΔG must be negative, and so $\Delta H - T\Delta S < 0$.

Exothermic mixtures ($\Delta H < 0$) will mix spontaneously, whereas for endothermic mixtures miscibility will only occur at high temperatures. For two-component blends it is possible to construct a phase diagram, which may exhibit lower or upper critical solution temperature (LCST or UCST), as seen in Fig. 1.2. In practice, LCST behaviour is more commonly seen, with phase separation occurring as temperature increases, because the intermolecular attractive forces responsible for the miscible behaviour tend to disappear, as internal energy of the molecules becomes high enough to overcome them.

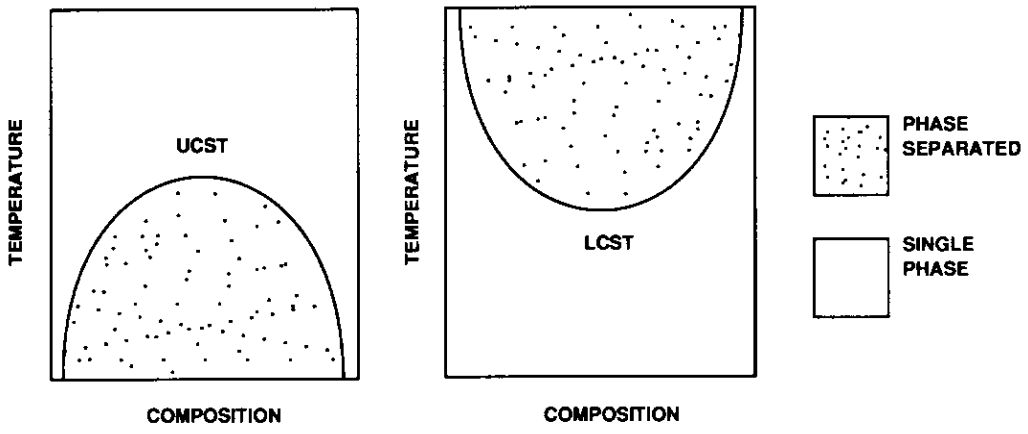

Figure 1.2: Schematic diagrams of binary blends showing LCST and UCST behaviour

1.3.2. Addition of block and graft copolymers

The addition of block or graft copolymers represents the most extensively researched approach to compatibilisation of blends, as seen in Fig. 1.3. The block and graft copolymers with segments chemically identical to the blend components are obvious choice as compatibilisers. The copolymer should meet certain structural and molecular weight requirements in order to locate it preferentially at the interface.

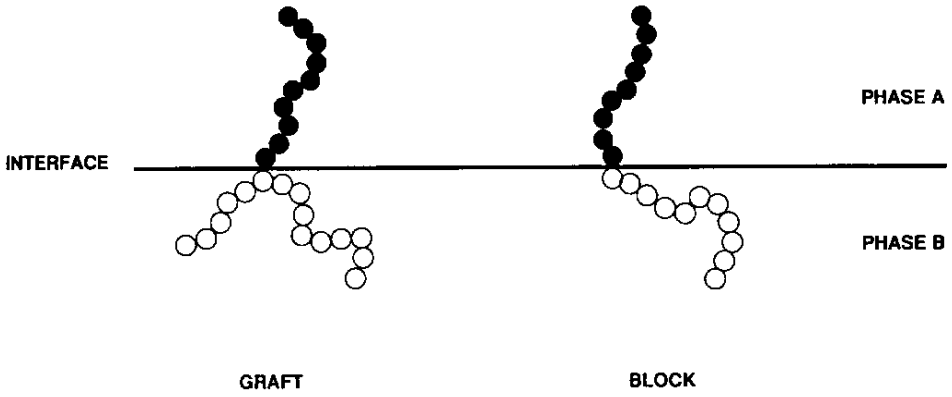

Figure 1.3: Schematic diagram showing location of block and graft copolymers at phase interfaces

The effect of different copolymer types on the compatibility of polyethylene(PE)/polystyrene(PS) blends has been studied extensively by Fayt et. al.[15] The superiority of the tapered diblock over others might be due to its ability to quantitatively locate at the PE/PS interface and consequently form a more efficient barrier against the subsequent breakup of the elongated structures of the co-continuous phase morphology. Using ultimate tensile strength of the blends as a measure for effectiveness of compatibiliser, they concluded that: (a) Block copolymers are effective than graft copolymers; (b) Diblock copolymers are more effective than triblock or star-

shaped copolymers; (c) 'Tapered' diblock copolymers are more effective than pure diblock copolymers.

Paul[16] suggested that solubilisation of a discretely dispersed homopolymer into its corresponding domain of a block copolymer compatibiliser only occurs when the molecular weight of homopolymer equals or is less than that of the corresponding block. Gaylord[17] offered the pragmatic view that a balanced molecular weight is needed for copolymer compatibilisers i.e., the segment needs to be long enough to anchor to the homopolymer (i.e. to solubilise) but short enough to minimise the amount of compatibiliser needed, and hence be cost-effective.

The requirement that the copolymer should locate preferentially at the blend interfaces also has implications for the molecular weight of the compatibiliser.[18] Both the thermodynamic 'driving force' to the interface and the kinetic 'resistive force' to diffusion increase with molecular weight, suggesting that high molecular weight copolymers may be used if sufficiently long times are available during the process, but that lower molecular weights must be used if the available diffusion times are short.

1.3.3. Addition of functional polymers

Many workers have described the addition of functional polymers as compatibilisers. A polymer chemically identical to one of the blend components is modified to contain functional (or reactive) units, which have some affinity for the second blend component. This affinity is usually the ability to chemically react with the second blend component, but other types of interaction (e.g.: ionic) are possible. The functional modification may be achieved in a reactor or via an extrusion-modification process. Thus, on grafting maleic anhydride or similar compounds to polyolefins, the

resulting pendent carboxyl groups acquire the ability to form a chemical linkage with polyamides via their terminal amino groups.

1.3.4. Reactive compatibilisation

A comparatively new method of producing compatible thermoplastic blends is via reactive blending, which relies on *in situ* formation of copolymers or interacting polymers at the interface of blends during melt blending.[4,19-21] Compared to batch-type melt mixers, continuous processing equipments such as single- or twin-screw extruders are often preferred for reactive blending. Continuous processing equipments have several advantages like excellent temperature control, continuous production as well as the provision for the removal of unwanted reaction products by devolatilisation.

Reactive blending mechanisms exploited are: (i) Formation of *in situ* graft or block copolymer by chemical bonding reactions between reactive groups on component polymers by free radical initiators; (ii) Formation of a block copolymer by an interchange reaction in the backbone of components, as in condensation polymers; (iii) Mechanical scission and recombination of component polymers to form graft or block copolymers; (iv) Promotion of reaction by catalysis.

1.4. Characterisation of polymer blends and composites

It is important for those developing new polymer blends are to measure degree of miscibility and interaction of phases, as these significantly influence properties and behaviour of the blend.[2-5]

1.4.1. Mechanical properties

Since plastics are primarily used for structural applications, the mechanical properties of these materials are of great importance. Important parameters affecting

polymer properties are time, temperature and humidity. The inter-relation between structure, properties and processing is presented in Table 1.1.

Table 1.1: Processing-structure-property relations in polymers and polymer blends

Molecular architecture	* Molecular weight/ * Molecular weight distribution * Linearity/rigidity * Molecular interactions * Packing ability
Inherent polymer properties	* Glass transition temperature * Crystallising ability * Melting/softening temperature * Melt viscosity * Elasticity
Processing conditions	* Pressure/temperature/quench rate * Shear or extension * Heat deflection temperature (HDT)
Structure	* Degree of crystallinity * Orientation (crystalline/amorphous) * Crystalline morphology * Crystalline size distribution * Fibre orientation
Product properties	* Tensile strength * Impact strength * Flexural modulus

Stiffness of material is usually expressed by modulus of elasticity. Tensile properties are related to the properties describing the atomic bond strength. Properties of polymers are dominated by strength of carbon-carbon bond. Properties determined under flexural loading most closely duplicate stresses experienced under practical applications. Specimen is extended at a predetermined, constant rate and resulting stress (load acting at upper jaw) is determined. Flexural property is material response to a combination of tensile and compressive forces. Impact strength is the ability of material to absorb impact energy. Impact strength of blend depends on its interfacial behaviour.

1.4.2. Thermal properties

Thermal analysis techniques are very useful in the characterisation of polymeric materials. Several structural transitions can occur in polymers during heating. These

transitions are melting and crystallisation, glass transition, crystal transformations, decompositions and other chemical reactions, volatilisation and annealing effects.[6,7] Other thermal properties of polymers under heat are heat distortion temperature and linear coefficient of thermal expansion. For characterisation of polymer blends the most important transitions are the glass transition temperature and the melting point.

Structural changes are usually associated with changes in heat adsorption or emission and are measured using differential scanning calorimetry (DSC). DSC can measure changes at constant heating or cooling rates. The differences in heat loss or gain between the sample and the reference cells are measured in a differential scanning calorimeter. The heat input needed to maintain both cells at the same temperature is measured.

Glass transition temperature: The glass transition temperature (T_g) is neither a thermodynamic transition, such as the melting transition, nor a sharp temperature point. T_g is a characteristic material constant. T_g is influenced by degree of crystallinity and molecular weight. It is the transition associated with the change in the specific heat capacity and thus is related to the freedom of molecular motions. The sudden change in heat capacity at T_g is manifested as a step on the temperature versus differential heat absorbed curve. The material has different mechanical and other properties on either sides of this transition. In physical blends of two polymers each polymer retains its own transition temperature. The presence of single glass transition temperature for a blend is an indication of homogeneity on a molecular level and thus mechanical integrity.[3-5] The measurement of glass transition temperature can therefore assist in the determination of compatibility of amorphous polymer blends.

Heat deflection temperature: Heat deflection temperature (HDT) is the point at which the 10.2 cm long test bar deflects by 0.025 cm.

Linear thermal expansion coefficient: Thermal shrinkage is a material property of the solidifying polymer. To obtain the correct dimensions of precision (dimensional stability) moulded parts, the mould shrinkage must be taken into account. Polymer with low coefficient of thermal expansion can easily be moulded into discrete shapes. The highly oriented thermotropic liquid crystalline polymers have lower coefficient of thermal expansion than thermoplastics. Thermomechanical analyser (TMA) is used for measuring heat distortion temperature.

1.4.3. Melting and crystallisation behaviour of blends

Blends with crystallisable components have received increasing attention both for fundamental and practical reasons.[22] The two components may influence each other giving rise to very interesting effects such as: (i) depression of the equilibrium melting temperature; (ii) decrease or increase of the crystallinity and of the rate of crystallisation; (iii) drastic change in morphological quantities such as lamellar thickness; (iv) change in the size and shape of the spherulites.

The following morphologies may be encountered in alloys with one crystallisable component: (a) the spherulites of the crystallisable components grow in a matrix consisting mainly of the non-crystallising polymer; (b) the non-crystallisable component may be incorporated in the interlamellar regions of the spherulites of crystallisable polymer and the spherulites fill all the available volume; (c) the noncrystallisable component may be included within the spherulites of the crystallisable polymer forming domains having dimensions larger than the interlamellar spacing.

For blends having both crystallisable components the most probable morphologies are: (i) crystals of the two components are dispersed in an amorphous matrix; (ii) one component crystallises according to a spherulite structure while other crystallises in a simpler structure; (iii) both components exhibit separate spherulitic structures; (iv) the two components crystallise giving rise to the formation of mixed spherulites containing lamellae of both polymers.

The crystallisation kinetics of a polymer crystallising from a mixture containing another polymeric component may be strongly influenced by composition, particularly when the two polymers have a certain degree of compatibility in the melt. The dispersed phase may influence the shape, size and growth rate of the spherulite texture.

A substantial depression in the melting temperature of crystalline component has been often observed in crystallisable blends. This effect is particularly relevant in blends where the two components are compatible in the amorphous state. The melting point depression has been observed also in systems, which are not compatible in the molten state. In such cases the melting point depression must be attributed to kinetic and morphological effects of the noncrystallisable polymer producing a reduction in crystal size, lamellae thickness or crystal perfection.

1.4.4. Phase morphology

The morphological studies are very important in order to establish how the processing condition may govern the morphological features and hence the end-use properties of these blends.[23] The basic modes of dispersion are: (i) ribbons and lamellae (stratified morphology), (ii) rods and fibrils and (iii) droplets. The overall morphology, ie, the modes and the state of dispersion of different phases in mixture of incompatible

molten polymers depends on the blend compositions, starting particle size, molecular weight distribution of individual components, and blending method adopted.

Scanning electron microscopy (SEM) gives information on surface topography of the materials. It can reveal the level of interfacial adhesion of different phases in polymer blends. The shape, size and degree of mixing of dispersed phase can be investigated by SEM. Transmission electron microscopy (TEM) provides information on the fine structure of materials down to atomic or molecular levels. Polarised light optical microscopy (PLOM) is useful in the study of morphology of blends in the molten state, the size and shape of spherulites of matrix polymer in the presence of another polymer. Light scattering, neutron scattering, x-ray scattering and spectroscopy can give quantitative information regarding interaction between the phases.

1.4.5. Rheological behaviour

In two-phase blends, the component forming the discrete phase (droplets or long ribbon) is dispersed in the continuous phase (Fig. 1.4). The dispersed phase is usually not uniform in size and shape and the average size depends on blending conditions such as mixing equipments, time of mixing etc.[24] A number of variables affect blend properties (Fig. 1.5).

The rheological behaviour of polymer blends is closely related to the deformation of the droplets in the continuous phase. Much of the work carried out on the rheology of heterophase systems deals with the deformation of Newtonian droplets suspended in a Newtonian fluid.[25] Moreover, the behaviour of droplets in non-uniform shear flow depends on the location of the droplets in the plane of shear. The deformation and the orientation angle of the droplets are expressed as a function of the viscosity ratio of the droplet and the suspending medium, the droplet radius, the interfacial tension and the rate

of deformation. A study on droplet deformation performed by Chin and Han[26] showed that increased droplet deformations occur on increasing the medium viscosity, the initial droplet size or the elongational rate and on decreasing the interfacial tension.

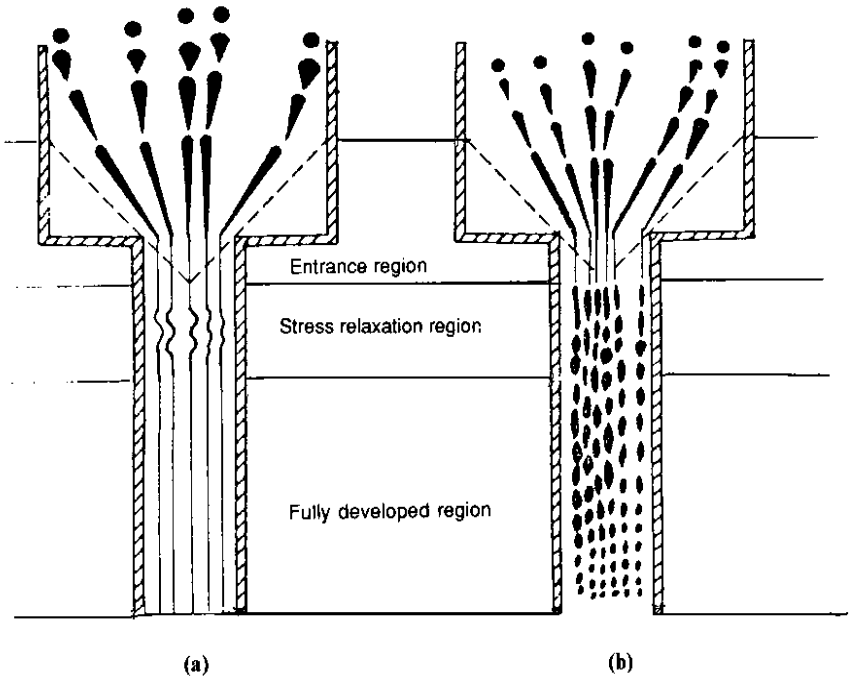

Figure 1.4: Schematic representation of molten two-phase dispersed polymer blend flowing through a capillary. (a) fibre-like domain; (b) droplet-like domains

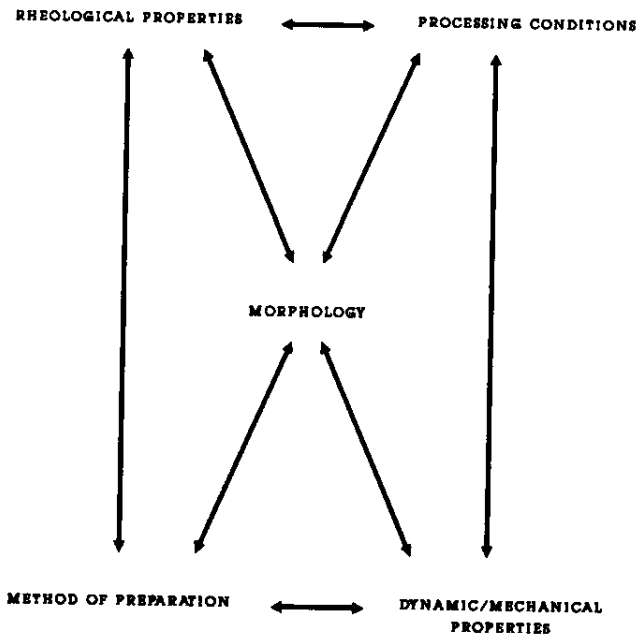

Figure 1.5: Properties of polymer blends

1.5. *In situ* fibre composites from polymer blends

Fibre-reinforcement has been used for many years to increase the engineering performance of thermoplastics. There are three different types of composites: (i) Macro-composites; (ii) Microfibrillar reinforced composites (MFCs) and (iii) *In situ* molecular composites.

1.5.1. Macro-composites

In macro-composites, inorganic fibres and fillers like glass fibres, carbon fibres are used as reinforcements. The use of solid fibres in thermoplastics causes a substantial increase in melt-viscosity and lowers the ease of processing. The *in situ* generation of reinforcing species offers advantages over the addition of solid fibres and fillers.

1.5.2. Microfibrillar reinforced composites (MFCs)

A new type of polymer composite called microfibrillar reinforced composite (MFC)[27-29] has been developed recently. With respect to the size of the reinforcing elements, MFCs take an intermediate position between the two extreme groups of polymer composites, macrocomposites and molecular composites. Unlike classic composites, MFCs are formed from two immiscible (e.g.: polyamides/polycondensates system), crystallisable homopolymers by drawing the polymer blend and then annealing. Upon drawing, the components of the blend are oriented and microfibrils are formed. The structural perfection develops during subsequent annealing. The temperature and duration of annealing have been shown to significantly affect the structure and properties of the blend. If the annealing temperature is set in between the melting temperatures (T_m) of the two components, the low melting component melts to form an isotropic matrix while the microfibrillar regions involving the component with higher T_m preserve their

orientational and morphological characteristics. The resulting material is referred to as a microfibrillar-reinforced composite (MFC). Bundles of highly oriented microfibrils act as reinforcing elements in MFC.

1.5.3. *In situ* molecular composites

The rigid-rod polymeric materials fabricated from the liquid crystalline state far exceed the strength and modulus properties of structural metals used currently in advanced aircraft and aerospace systems.[4,30-40] It is very easy to produce fibres and films from these rigid materials. It is however difficult to laminate liquid crystalline polymeric materials to obtain large bulk specimen due to its anisotropic nature as well as the close proximity of glass transition temperature (T_g) to its decomposition temperature.

One of the solutions is to blend these materials with flexible coil polymers. Thus, a molecular composite is defined as rigid-rod molecules molecularly dispersed in a matrix of flexible coil polymer such that the rods act as the reinforcing elements. Compared to conventional fibre composites, these molecular composites show excellent dimensional stability as well as very good fracture and impact toughness. The high modulus and strength of rigid-rod LCPs is transferred to the flexible thermoplastic matrix to form a virtually ideal *in situ* molecular composite. Thus, molecular composites based on thermoplastic as matrix and liquid crystalline polymers as reinforcement offer exciting engineering technologies in the field of structural materials.

1.6. Coupling reactions involving functional polymers

Coupling reaction is used for two types of application. One is for the chain extension of polymers i.e. molecular weight boosting and the other is synthesis of block copolymers with a random distribution of blocks. The synthesis of high molecular weight

polymers by step growth polymerization requires high degree of conversion, this means high temperature, long reaction time, and low pressure to distill off the last traces of reaction by product i.e. water. Such condition leads to some undesired side reaction.

To overcome this drawback a coupling agent may be added in the last steps of the reaction. This coupling agent should be able to give a rapid polyaddition with the end groups of the growing chains, so that high molecular weight copolymer can be obtained using lower temperatures, shorter reaction times and no vacuum. With coupling agents of functionality more then two, the process leads to highly branched or cross-linked products. With difunctional coupling agent, high molecular weight linear copolymers are produced and the process is often termed chain extension.

This strategy is used to prepare block copolymer by coupling end functional polymer. Diisocyanates are probably the most used coupling agents as they give rapid reactions with a number of protic nucleophiles, particularly hydroxy,[41,42] amino or carboxy end groups, which are very common polymer end groups. The amount of coupling agent used is low and with the exception of its role of connecting units, exerts little or no influence on the properties of the final block copolymers. At high reaction temperatures problems due to side reactions arise with diisocyanates. It undergoes a trimerisation reaction, which produce branched polymers.[43]

Inata and Matsumura have examined a number of coupling agents for high temperature reactions with the carboxyl end groups of PET and PBT.[44] The best coupling agents are bisoxazoline.[44,45,49] Reaction leads to the formation of ester amide linkage between prepolymer chains.[46] This approach has been applied to the chain extension of

recycled PET[47] and dicarboxyl polyamide-12.[48] No side reaction has been detected in the reaction between 2,2'-bis(2-oxazoline) and dicarboxypolyamide-12.[48]

The reactions of bisoxazolines with carboxy groups[50] and of bisoxazoline with amino groups[51,52] have been applied to the synthesis of block copolymers in the bulk at high temperature. Thus, bisoxazolinone acts as coupling agent in the synthesis of polyoxyethylene/polyamide-12 block copolymers.[53] The chain extension of carboxyl terminated oligomers with bisoxazolines is another way to synthesise polyether/polyamide block copolymers.[54]

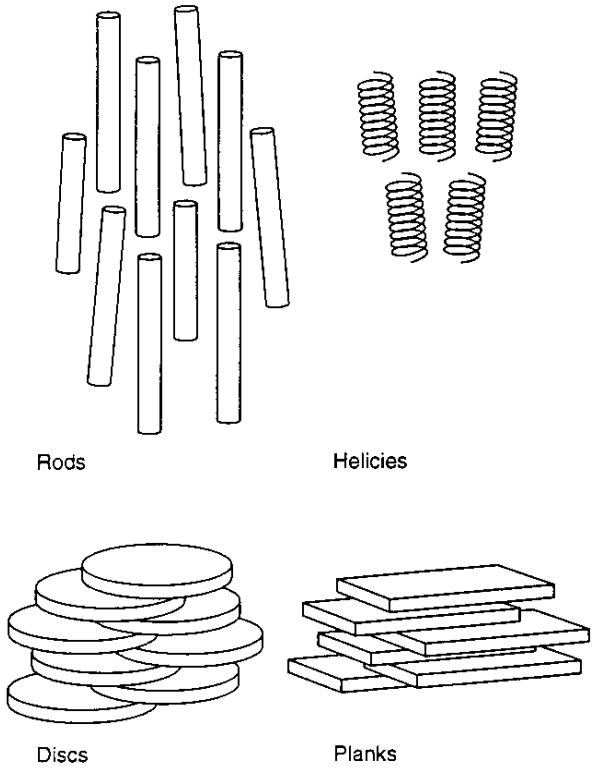

Figure 1.6: Anisotropic units giving rise to liquid crystal phases

1.7. Liquid crystalline polymers

Liquid crystalline polymers (LCPs) are a relatively new class of engineering plastics, which have attracted significant interest in the last two decades. [30-40,55-58] de

Gennes,[30] Onsager[31] and Flory[32] predicted some 40 years ago that the incorporation of liquid crystallinity would result in very interesting and exciting performances in plastics and fibres. A liquid crystal is quite simply a state of matter between the liquid and crystalline states. A liquid crystal is an ordered fluid. Structural elements, which act as rigid rods, are essential in the polymer chain to form liquid crystal phases. Rods, discs, planks and helices are well-documented examples Fig. 1.6).

1.7.1. Lyotropic liquid crystalline polymers

Polymers in which liquid crystalline properties are induced in the presence of a solvent are called *lyotropic* (Example: Kevlar). In these, the liquid crystallinity is observable within definite range of concentration in solution. These are the first generation liquid crystalline polymers. Lyotropic liquid crystal polymers can be processed from solutions in highly polar solvents by wet spinning methodologies.

1.7.2. Thermotropic liquid crystalline polymers

These are the second-generation high performance polymeric systems. In these, the ordered liquid crystalline molten state is observed over a temperature range above the crystalline solid state and below the formation of a normal molten state with a random arrangement of chains. Thermotropic liquid crystalline polymers need to be processed from the ordered molten state to have the inherent high performances frozen in the solid state. Thermotropic liquid crystals can be classified into 3 types according to the arrangements of their molecules. They are: (i) smectic, (ii) nematic and (iii) cholesteric phases (Fig. 1.7). Cholesteric phase is induced by the presence of an optically active centre in the liquid crystal or by the addition of an optically active compound to a nematic liquid crystalline (LC) polymer.

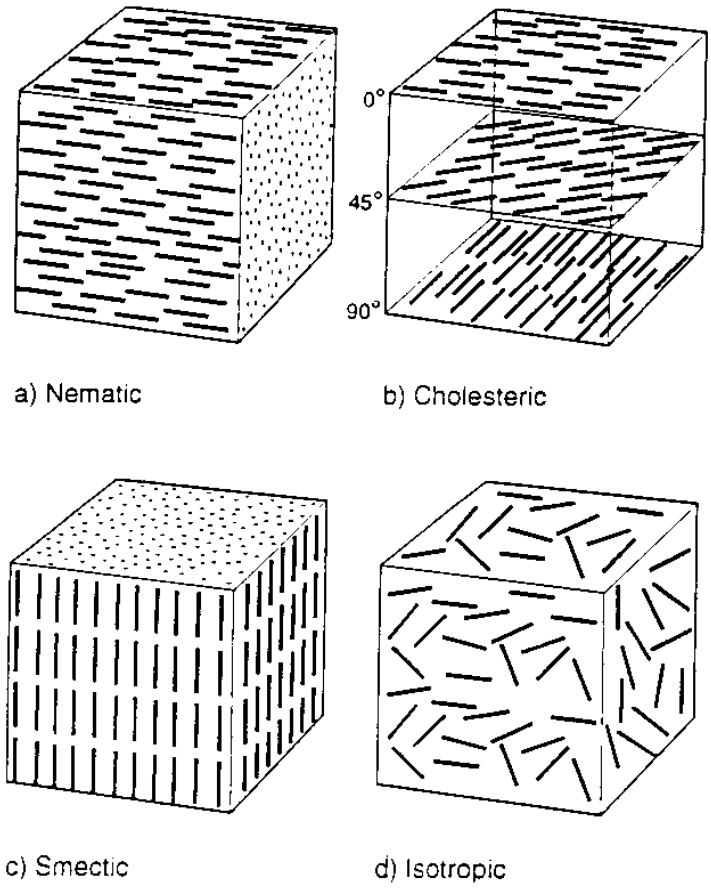

Figure 1.7: Comparison of three liquid crystal phases (a, b and c) with isotropic state (d)

Cholesteric LC polymers show reflection of colours. Thermotropic liquid crystalline polymers (TLCPs) would exhibit one of the above liquid crystalline structures. There are two main ways by which anisotropic LC building block can transferred into a polymer: by joining end to end to form a main chain TLCP or by dangling from the side of a normal polymer chain to form a side chain TLCP (Fig. 1.8). "Main-chain" LCPs have already met commercial applications as high modulus materials, whereas "side-chain" LCPs are currently very actively investigated in view of their potential applications in optoelectronics. The most important TLCPs for blending with bulk polymers are thermotropic main chain TLCPs that exhibit a liquid crystal phase within

the processing window of the bulk polymer but which then solidify on cooling to room temperature.

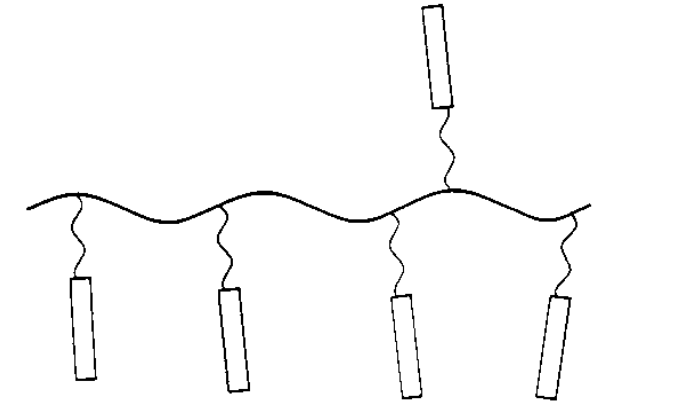

Figure 1.8: Types of liquid crystal polymers

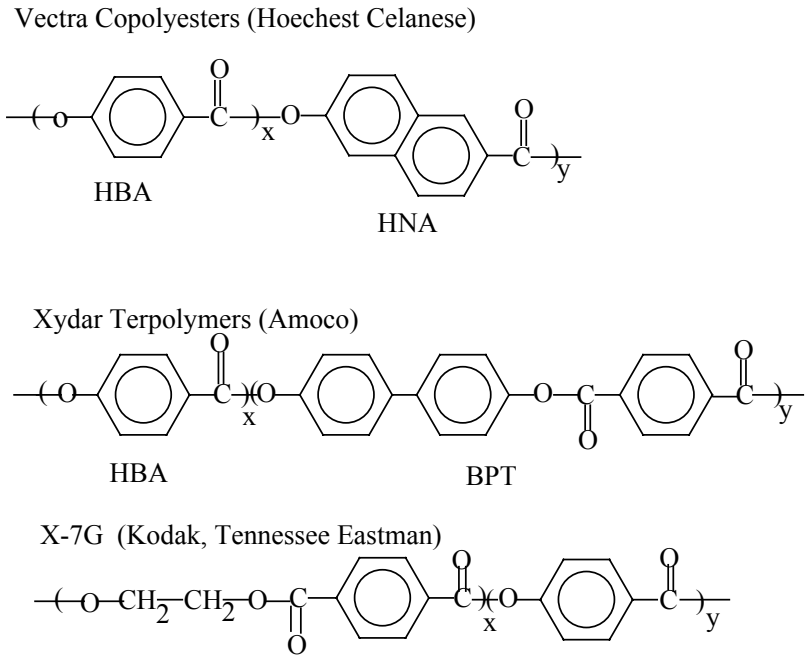

Figure 1.9: Commercially available TLCPs

As with any polymer, a LCP can either crystallise on cooling or go through a glass transition temperature. Hence, at room temperature, the structure of the TLCP is that of an ordered glass or a semi-crystalline polymer. The chemistry of commercial TLCPs has been dominated by aromatic polyamides (e.g. Du Pont's Kevlar) and aromatic polyesters (e.g. Hoechst Celanese's Vectra or Amoco's Xydar) (Fig. 1.9). Other commercial types have been synthesised (e.g. liquid crystal polycarbonates, liquid crystal polyphosphazines and liquid crystal siloxanes).

Table 1.2: Commercially available thermotropic liquid crystalline polymers (TLCPs) and their physical properties.

Trade name	Company	Compn.	T_m ^oC	T_g ^oC	PT ^oC
VECTRA A	Hoechst Celanese	HNA(27%), HBA(73%)	283	105	320-340
VECTRA B	Hoechst Celanese	HNA(58%), TPA(21%), 4AP(21%)	280	110	300-330
X7	Eastman Kodak	PET/HBA (HBA 40, 60 or 80%)	250-300	70, 143	270-350
RODRUN	Unitika	PET/HBA	250	70, 143	270-350
LX-series	duPont	TA, HQ, PHQ	310	195	270-350
ULTRAX KR	BASF	Unknown	-	-	340-360
XYDAR	AMOCO	BP, HBA, TA	412	-	>420
VITREX SRP	ICI	HBA, HQ, IA	280	-	300-350
KU-9211	Bayer	HBA, TA, HQ, IA, BP	-	198	330-360

PT=processing Temperature; HNA=2-hydroxy-6-naphthoic acid; HBA=4-hydroxy benzoic acid; TPA=*tere*-phthalic acid; 4-AP=4-amino phenol; PET=poly(ethylene *tere*phthalate); HQ=hydroquinone; PHQ=2-phenyl hydroquinone; BP=4,4'-dihydroxy biphenyl; IA=*iso*-phthalic acid.

1.7.3. Properties, processing and applications of TLCPs

Thermotropic LCP materials have very good thermal, physical, dielectric, optical and mechanical properties as well as good chemical resistance, low flammability, very good dimensional stability (Table 1.2). They also show excellent processability and high melt strength. Thermotropic materials are processed by injection moulding, extrusion, thermoforming, blow moulding etc. Nematic liquid crystals possess a relatively low viscosity and can be deformed by small external forces.

Table 1.3: A comparison of properties of thermoplastics and thermotropic liquid crystalline polymers (TLCPs)

TLCPs	Thermoplastics
Anisotropic	Isotropic
Low linear thermal expansion coefficient	High linear thermal expansion coefficient
Low melt viscosity	High melt viscosity
Low mould shrinkage	Comparatively high mould shrinkage
Very good melt strength	Poor melt strength
Easy processability	Poor processability
Very good mechanical properties	Poor mechanical properties
Excellent barrier properties	Poor barrier properties

TLCPs offer many advantages over conventional thermoplastics in injection moulding such as low mould shrinkage, minimum warpage and distortion, fast cycle time, low moisture etc (Table 1.3). TLCP rods are manufactured by extrusion under conditions, which produce a strong molecular orientation in the flow direction. Rapid cooling preserves the orientation. These TLCP rods are useful in optical keyboard applications. TLCP rods have low weight, considerable flexibility, low thermal expansion coefficient and excellent tensile properties.

Oriented TLCP sheets and films are produced either by pressing the fibres at melt temperature or by extruding the solution of LCP. LCP films have very good mechanical

properties and low coefficients of diffusion and are used as high performance packaging materials. Sheets of mineral filled LCP materials have been used for thermoforming and electroplating of printed circuit boards (Table 1.4).

LCP/carbon-fibre composites have been developed and are used in aerospace industry. LCP matrices offer low viscosity for the impregnation of fibres and excellent chemical resistance. Impregnation is achieved in a cross-head die, after which the panels are prepared by compression moulding the stacked prepreg sheets.

Table 1.4: Applications of TLCPs

Area	Property	Applications
Electrical/Electronics	Low dielectric constant, high dielectric strength, arc resistance, resistance to vapour phase and wave soldering.	Connectors, capacitor housing, potentiometers, switches, Printed circuit boards.
Fibre optics	Excellent mechanical properties, inherent flame retardance, good moisture resistance and low coefficient of thermal expansion	Connectors, strength membranes and couplers
Aircraft/Aerospace	High strength to weight ratio high temperature performance, low coefficient of thermal expansion and excellent dimensional stability	Parts of space vehicles, Aircraft engines, Helicopters, Missiles
Industrial	Excellent mechanical strength, very good dimensional stability and heat resistance	Motor components, lamp housing, conveyer belt components, gears
Automotive	Resistance to automobile fluids, solvents, very good dimensional stability and flame retardance	Fuel-system components, electrical/ electronics systems
Medical	Toughness, low permeability, non-toxicity, compatibility with sterilisation techniques.	Various medical components
Chemical process	Chemical resistance, heat resistance, dimensional stability	Chemical tower pickings and in oil well logging devices.
Cookware	Toughness, heat resistance, resistance to staining and odour retention	Microwave equipment and turntables
Fibre applications	LCP fibres with excellent tensile properties, low density, thermal resistance, low creep, weatherability	Protective fabrics, gloves, clothing, ropes, sewing threads, rubber reinforcement in radial tyres, belts, cement reinforcements etc.
Other	Dimensional stability, mechanical properties and good moisture resistance	Watch components, safety equipments etc.

The liquid crystalline polymer market had probably grown to USD 10 billion in 2000, from USD 3.4 billion in 1996, according to a study that covers three broad classes - lyotropic aromatic polyamides used for fibres, thermotropic aromatic polyesters for structural parts and functional LCPs with nonlinear optical properties.

1.7.4. Polymer blends containing TLCPs

The concept of molecular composites first originated from the work of Flory[32] on the polymer rigid rods. He studied ternary blends of rigid rods (PBX type, aramids, and copolyesters) with conventional polymers in solvents. A molecular composite is defined as rigid-rod molecules molecularly dispersed in a matrix of flexible coil polymer such that the rods act as the reinforcing elements. Reinforcement through the addition of TLCPs to thermoplastics has been investigated over the last few years with some encouraging results.[31-40] The principal goal is to achieve improvements in mechanical properties by using the TLCP component to reinforce the flexible thermoplastics through the formation of fibres (Table 1.5).

Table 1.5: Applications of thermoplastics/liquid crystalline polymer blends

Area	Property	Application
Electronic	Excellent mouldability, dielectric property and good thermal stability	Molded interconnected devices, multi layer circuit boards
Automotive	Excellent processability, high use temperature	Engine parts and in under-the-hood parts
Aircraft	High use temperature, good fatigue resistance, high modulus and excellent processability	Primary/secondary structural components in aircraft
Medical	Excellent barrier properties, High use temperature and non-toxicity	Thin films with high strength finds applications in various medical equipments
Packaging	Selective permeability, excellent processability	Thin films are used for packaging applications

Blending is also considered as a possible route to overcome the highly anisotropic physical properties of TLCP that can be problematic in many applications. The challenge is to produce organic TLCP fibres *in situ* that give the required level of reinforcement at a realistic cost. The use of TLCPs in polymer blends looks attractive from a number of view points: (a) The high para-linked aromatic content gives polymers with good moduli; (b) TLCPs have very low melt viscosities allowing good flow properties and ease of processing; (c) TLCPs form fibrous structures; (d) TLCPs show excellent chemical resistance and low mould shrinkages.

1.7.5. TLCPs as reinforcement

The ability of LCPs to form fibrillar morphology within a thermoplastic matrix during melt processing makes it possible to develop *in situ* fibril reinforced molecular composites from thermoplastics/liquid crystalline polymer blends. The control of LCP's morphology, its interfacial adhesion with blend matrix, thermoplastics to LCP composition ratio are important for the achievement of maximum desirable properties. Thermoplastics/LCP blends have started to compete effectively with carbon or glass fibre reinforced composites. Techniques with high extensional flow such as spinning, extrusion and injection moulding ideally facilitate the high performance properties of the thermoplastics/LCP blends.

1.7.6. TLCPs as processing aid

The melt viscosity of LCPs is lower than that of thermoplastics. Therefore, on blending with thermoplastics, the blend viscosity drops dramatically. LCPs can act as processing aid for thermoplastics thereby reducing energy consumption. Also, other advantages such as less degradation of polymers and easy filling of complex moulds have

been demonstrated. Engineering plastics so far used as matrix for LCP blends are polycarbonate (PC),[59-65] poly(ethylene terephthalate) (PET),[66-69] poly(butylene terephthalate) (PBT),[62,71] polyamides (PA),[72,73] Poly(ether sulphone) (PES),[62,74] polyether imide (PEI),[62,75] poly(ethyl ether ketone) (PEEK),[62,74] polypropylene (PP),[75,76] polyethylene,[78] poly(vinyl chloride) (PVC),[79] poly(phenylene oxide) (PPO),[80] polystyrene (PS)[70,73,74,80] Polyarylate (PAr)[81] etc.

1.8. Polysulphone (PSU)

Polysulphone was discovered in the early 1960s. It involves reaction of the bisphenol of choice with 4,4'-dichlorodiphenyl sulphone in a dipolar aprotic solvent in the presence of an alkali.[82,83] There are mainly three types of polysulphones that are practiced commercially. Those are bisphenol based polysulphone (PSU), poly(ether sulphone) (PES) and poly(phenyleneether sulphone) (PPES).

Ulmann synthesis[84] is used to produce PSU. PSU synthesis in nondipolar aprotic solvents has been established.[85,86] Several other synthetic procedures are also possible. Polyethersulphone can be synthesised by the electrophilic Friedel-Crafts reaction of bis(4-chlorosulphonyl phenyl) ether with diphenyl ether.[87-89] Oxidative coupling of aromatic compounds via Schroll reaction has been applied successfully to synthesise a polyarylether sulphone.[90]

1.8.1. Structure, properties and applications of polysulphones

These polymers offer outstanding thermal stability and resistance to thermal oxidation because of sulphur atom in its highest oxidation state and the enhanced resonance of sulphone group present in para position. The thermal stability is further augmented by high bond dissociation energies inherent in the backbone structure. Hence,

this polymer can be melt fabricated at temperature up to 400^{o}C without any adverse effect. The high degree of oxidation stability also allows for continuous exposure to temperature in the range 150-190^{o}C, allowing greater flexibility in polymer formulation and use condition. The high glass transition temperature of PSU is due to the rigid phenyl rings in the backbone and also the sulphone group which increases T_g by providing strong dipole interaction and restricting rotation of the aromatic unit relative to the other connecting group. The sulphone group is the most hygroscopic moiety and the isopropylidine is hydrophobic. The moisture uptake at equilibrium is significantly low for PSU, as desired for most engineering applications.

The chemical structure of polysulphones is as shown in Fig. 1.10.

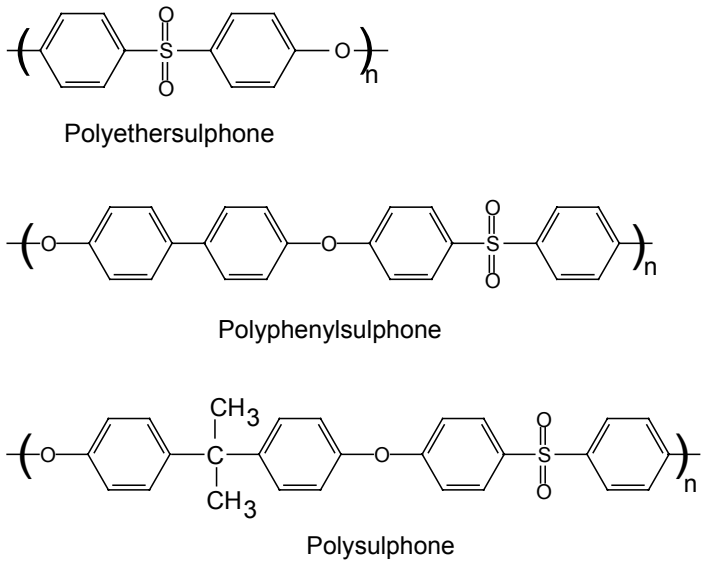

Figure 1.10: Structures of commercial polysulphones.

Polysulphones do not crystallise in spite of their regular structure. It might be expected that the stiff chain with its high T_g would only crystallise with difficulty but in itself this would not expected to inhibit it completely. The ether linkage has a bond angle of 120^{o} the C-S-C bond angle is 105^{o} and it is difficult to fit these bond angles into crystal

lattice. The relatively inert ether and sulphone back bone functionalities contribute to resistance against hydrolysis and chemical attack by acids and bases.

PSU structure is polar which is frozen at room temperature. So it has good electrical insulation properties even at high frequency. PSU has good heat deformation resistance and resistance to chemical change on heating as well. This is because of the high degree of resonance, which gives high bond strength. Hence it is capable of absorbing high degree of thermal and ionizing radiation without crosslinking. PSU is least susceptible to oxidation as sulphur is in its highest oxidation state; electrons are withdrawn from the benzene rings. As a highly polar polymer it is not dissolved by aliphatic hydrocarbons but by polar solvents such as dimethyl formamide and dimethyl acetamide.

1.8.2. Polysulphone blends and composites

Polysulphone is commercially blended with various polymers and fillers. Azak[91] established that in PEEK/PSU blends the phase separation allows PEEK to crystallise. The moduli of elasticity is approximately additive but ductility and impact strength showed an additive response.

1.8.3. Polysulphone/thermotropic liquid crystalline polymer blends

Several studies on thermal, mechanical and rheological properties, morphology and phase behaviour of blends of PSU and commercial TLCPs are reported.

1.8.4. Thermal properties

Jung et. al[92] studied blends of thermotropic liquid crystalline polyesters **(**TLCP) with polysulphone (PSU), and polyarylsulphone (PAS) by differential scanning calorimetry (DSC) and DMTA to show that T_g of PSU remains nearly invariant with

blend composition and thus that PSU is immiscible with TLCP. Hi et. al[93] used sulphonated polystyrene to compatibilise TLCP/PSU blends. This is revealed by inward glass transition shift of polymer components in DSC and DMA thermogram and by a much finer dispersion of the minor TLCP phase in these matrix polymers. Li et. al[94] studied binary blends of polyarylethersulphone and PET-OB (40/60). DSC study showed that blends are partially compatible. Two glass transition temperatures corresponding to the two components were observed. This was confirmed by SEM. Phase inversion in blends was observed when the blends contained 50 wt % or more of the TLCP, PET-OB (40/60).

Honget et. al[95] studied the blending of PSU and Vectra A 950 in a twin-screw extruder. PSU was taken as the matrix and TLCP as reinforcement. Thermal properties were not altered appreciably.

1.8.5. Mechanical properties

Golovoy et. al[96] studied the morphology, rheology and mechanical properties of blends of polysulphone with up to 65% of wholly aromatic thermotropic liquid crystalline polyester. The addition of TLCP to PSU resulted in an increase in stiffness, a small increase in tensile strength and significant improvement in processability. Injection moulded sample showed skin-core morphology with the minor TLCP phase in the skin and globular in the core. He et. al[97] studied blends of PSU with the TLCP (p-hydroxybenzoic acid-terephthalic acid-naphthalenediol-poly(ethylene terephthalate)). The tensile modulus increased and the elongation at break decreased with increasing PSU content while strength was maximum at 95:5 (PSU: TLCP) ratio. The extrudate showed skin-core morphology.

Fang et. al[98] blended polyethersulphone (PES) with commercial TLCPs, KU9221 and KU9231, and extruded the blends to form fibres. It was easier to orient TLCP domains in the extruding flow, which resulted in better *in-situ* reinforcement than that obtained by injection molding. The extruded fibres had better mechanical properties, which improved with increasing tensile ratio of melt drawing and TLCP content.

Wang et. al[99] obtained composite strand with well defined microfibrils with 30 wt % TLCP in the PES matrix which was fabricated by extrusion and subsequent drawing down to have a high tensile modulus and high tensile strength compared with the thermoplastic matrix. The heat of fusion of TLCP increased with draw down ratio, while the crystal-nematic transition temperature, T_m and T_g corresponding to matrix were essentially unaffected by draw down. Garcia et al[100] reported that the Young's moduli of PSU/TLCP blends increased with TLCP content. The notched impact strength of PSU increased at low TLCP content.

1.8.6. Morphology and phase behaviour

Garcia et. al[100] reported the PSU/TLCP blends consist of two pure amorphous phases. The morphology of the core was mainly spherical but some elongated irregular TLCP aggregates appeared mainly in the 30 and 40% TLCP blends. Xu. et. al[101] reported that PES forms an ordered structure such as spherulite like globules under suitable conditions. The microdomains and the rigid segment of the TLCP promoted the growth of the ordered polymer. Skovby et. al[102] studied thermal properties, viscoelastic behaviour, processability, and mechanical properties of PSU/TLCP blends. Composite fibres were spun from the blends, and the tensile moduli and strengths were consistent with morphology of highly oriented TLCP microfibrils with high aspect ratios dispersed

in the thermoplastic fibre. The properties increased with increasing draw ratio.

Cohen et. al[103] studied TLCP-polysulphone blends for phase separation and aggregation. In concentrated solution two kinds of segregation are observed, one rich in polysulphone and poor in polyester and vice-versa. These polymers undergo a phase separation. At 40% TLCP, the blend was composed of two isotropic phases. The kinetics of phase separation was very fast compared to that of solvent elimination from mixture. He et. al[104] studied blends of PES and PSU with TLCP which were extruded at different temperatures. SEM and image analysis showed that the viscosity ratio of the dispersed TLCP phase to continuous phase is a decisive factor determining the formation of TLCP fibrils. The extrusion temperature has a marked effect on the size of minor TLCP and aspect ratio increases with increasing extrusion temperature.

James et. al[105] studied the permeability to oxygen of thin pressed films of blends of polyether-polysulphone (PES) and TLCP over a range of composition. Fairly modest addition of the thermotropic liquid crystalline polymer (TLCP) led to a pronounced improvement in the barrier properties. This improvement was ascribed to the formation of a thin surface layer of the TLCP. The existence of this TLCP surface layer was supported by SEM examination of samples etched with dimethyl formamide. The etching did not remove all PES because it was protected from the enchant by the surface layer.

Zheng et. al[106] studied an isotropic, amorphous blend of TLCP [PET/OB (40/60)] with polyether-polysulphone (PES) prepared by solvent casting. Thermally induced phase separation took place up on heating slightly above the glass transition temperature of PES. Morphology development within phase-separated domains was qualitatively examined by light scattering and optical microscopy. Wiff et. al[107] studied a new process

to obtain fibrous thermotropic liquid crystal domains in bulk forms by proper blend processing. By blending PES with TLCP the tensile strength and fracture toughness are almost doubled. These are successfully used in aircraft interior panel. Honget et. al[95] reported the blending of PSU and TLCP, Vectra A 950, in a twin-screw extruder. The tensile strength modulus of as spun PSU/TLCP fibres increased with TLCP content and spin draw ratio. Supporting evidence by WAXD showed enhanced molecular orientation and resultant fibrillation of TLCP. Li et. al[108] reported the effect of method of blending on the phase behaviour of PES/TLCP blend. Solution cast blend are homogeneous while melt mixing blends are multiphase systems. Impact strength, tensile strength, and Young's modulus of PES-C were enhanced to some extent by the addition of 2.5 to 5% TLCP.

Engberg et. al[109] studied the microstructure, thermal expansion, and stiffness of injection molded samples of blends consisting of Vectra (TLCP) and polyethersulphone (PES), as a function of TLCP content. The stiffness of the PES/TLCP blends followed a near-lower-bound law more accurately described by the equations of Halpin-Tsai and Takayanaga whereas the coefficient of linear thermal expansion of PES/TLCP blends was predicted by the Takayanaga model. He et. al[110] reported that *TLCP* domains in TLCP/PES blend are deformed into oriented fibrils, due to a viscosity ratio of 0.0l. A quantitative comparison of TLCP droplet sizes before and after the extruder die showed that the morphology of extrudates is determined before the melt enters the die. After the die, the diameter and length to diameter ratio of LCP fibrils were increased by coalescence and further deformation by the action of extensional flow.

Yanc et. al[111] reported that the PHB-PET thermotropic liquid crystalline polymer (TLCP) could be used as toughening agent as well as a reinforcement for a PES-C matrix. The addition of a small amount of TLCP to the PES-C matrix resulted in a significant increase in fracture toughness and a reduction in flow viscosity. Cohen-Addad reported[103] the SAXS and WALS investigation of a wholly aromatic Para linked random copolyester and PSU. In concentrated solutions containing polysulphone and polyester, aggregation is observed prior to the demixing process. Two kinds of aggregates are formed: one rich in polysulphone and poor in polyester, and vice versa for the other kind. This behaviour is consistent with the observations in the solid state: these polymers undergo a phase separation. Blend films (40 wt% TLCP) are composed of two isotropic phases, an estimate of their size being a few micrometres.

1.8.7. Rheological properties

Honget et. al[95] reported the blending of PSU and Vectra A 950 in a twin-screw extruder. PSU was taken as matrix and TLCP as reinforcement. At crystal nematic transition temperature incorporation of TLCP into PSU increase melt viscosity and gave rise to large yield stress. But above this temperature melt viscosity drastically decreased and resultant yield stress was small.

Kim et. al[112] studied rheology, morphology and physical properties of ternary blend consisting of polysulphone, Vectra A 950 and Hytrel 7246. The thermoplastic elastomer (Hytrel) helps to elongate the dispersed TLCP domain and enhance the interface adhesion, which results in improved mechanical properties. Magagnini et. al[113] studied morphology and rheology of PSU/Vectra A 950 blends synthesised by melt blending. The rheology was studied in the range 290-300^{o}C.

La Mantia et. al[114] studied the rheological behaviour of PSU/VA blends with 10 % TLCP by capillary viscometer equipped with cylindrical dies having different L/D ratio. The addition of 10% TLCP into the flexible resins strongly increased their elongational viscosity and made the blends resemble neat TLCPs in their extensional flow behaviour.

Kulichikhin et. al[115] reported the rheological properties of polymer blends containing polysulphone and TLCPs. A maximal increase in the strength and initial modulus was observed for blends containing 10% TLCP.

Tanaka et. al[116] studied the rheology and morphology of polymer blends containing liquid-crystalline component in melt and solid state. Kulichikhin et. al[117] investigated blended melts of isotropic polysulphone (PSU) and LCP which differed in viscosity by more than one order of magnitude, by studying flow curves observed in cone and plate geometry. Machiles et. al[118] studied rheology of PES/TLCP blends by three different methods.

Machlies et. al[119] reported break up fibres of a TLCP above the melting temperature in various polymer by capillary instabilities experiment on single TLCP fibres and by annealing experiment on extruded TLCP/ thermoplastic blends. DSC and FTIR of TLCP/PES indicates miscibility of two components is poor.[120,121] A theoretical formula, which expresses the variation of blend viscosity, was derived to show that the calculated results agreed well with the experimental data. The formula was used to explain the abnormal variation of viscosity of TLCP/TP blends and to estimate the viscosity of these blends. He et. al[104] reported that the formation of TLCP fibrils is crucial to the performance of polyblends containing TLCPs. The deformation of the TLCP

dispersed phase needs a large viscous force, so the viscosity ratio of the TLCP to the matrix is the decisive factor controlling the formation of TLCP fibrils in the resin matrix.

1.8.8. Compatibilisation

Zhang et. al[122] reported synthesis of two block copolymers, PSU-PET and PSU-PHB in order to compatibilise PSU/TLCPA1. At just 2% loading the PSU-PET copolymer could reduce the interfacial tension of a PSU and TLCPA1 blend, which made TLCPA1 form fine microfibre phase and to be uniformly distributed in a PSU matrix.

Pospeich et. al[123] reported the study of multiblock copolymer.They compared the mechanical properties of TLCP/PSU (50/50 wt/wt) blend with pure PSU, TLCP and corresponding block copolymer (BCP). It was found that tensile strength of blend drops down bleow the level of homopolymer. In case of BCP , tensile strength is higher then pure PSU. Elastic modulus and fracture strength shows significant increase.

Haubler et. al[124] reported that the addition of PSU/TLCP multiblock copolymer, with higher molecular weight, enhanced elastic modulus and fracture strength than the corresponding value of noncompatibilised blends. They investigated the solution cast binary blend to know the basic interaction in PSU/LCP/BCP blends.In LCP/BCP blend weak interaction was observed although both have LCP phase. In PSU/BCP blend , miscibility between both phase was observed (PSU molecular weight> 8400 g/mol). This indicate that the interpenetration of the PSU phase of the block copolymer and the PSU matrix leads to an improved miscibility of the blend.In PSU/LCP/BCP (5 wt %) blend, mechanical sterength (elastic modulus and fracture strength) increases compared to PSU/LCP blend. This is supported by their morphology study. BCP acts as a compatibiliser in PSU/LCP system.Yang et. al[125] reported that compatibility of PSU and

a TLCP can be improved by adding a block copolymer of low molecular weight PSU and a rigid rod polymer. Significant improvements in tensile modulus and strength were observed. Morphological study showed that the TLCP can be finally dispersed and well bonded to an inherently incompatible PSU matrix through the presence of compatibiliser.

Kim et. al[126] reported that introducing an amorphous PSU in PPS/TLCP blends effectively enhances the elongation of the dispersed TLCP domain, which produced a positive effect in tensile strength, particularly at TLCP contents. In the incompatible PPS/LCP blends, LCP imparted a nucleating effect to the crystallization of PPS. Up to 10 wt % LCP content, the tensile properties of PPS/LCP blends were enhanced with increasing LCP content, but they deteriorated if the LCP content exceeded 20 wt%. Addition of a third component, PSF, to the 90/ 10 PPS/LCP blend promoted development of rod-like or threadlike fibrillar structure and orientation of the deformed LCP domains, which led to improvement of tensile strength up to 20%.

Yazaki et. al[127] investigated polymer blends of commercial PES with TLCP. PES oligomers, with reactive functional groups at their terminals, were added as the third component to the above blends to improve mechanical properties. The flexural modulus of the PES/TLCP blends increased almost linearly as TLCP content increased while flexural strength of the PES/TLCP blends decreased most notably when TLCP content was in the range of 20 to 60 wt%, but increased again for higher TLCP content. In contrast, the addition of the PES oligomers had little effect on flexural modulus, but flexural strength was clearly improved. The morphologies of each blend were analysed by DSC. T_m and T_c of both TLCPs remained constant when blended with PES. However,

the T_g of PES decreased slightly up on blending. The addition of the PES oligomers caused a decrease in the T_g of PES, suggesting that they were miscible in PES.

1.9. Poly(phenylene sulphide) (PPS)

Poly(phenylene sulphide) (PPS) is a high performance engineering plastic, based on aromatic monomer units.[128] It was first reported in 1897, while first commercial plant was set up in 1972 by Phillips Petroleum Company in USA to market it under the trade name Ryton. At present, 72 different grades of PPS are available. First synthetic attempt by Friedel and Crafts in 1888 and Genvresse in 1897 to synthesise PPS by reaction of benzene with sulphur in presence of aluminium chloride[129] generated oligomers. Other synthetic route involved the self condensation of cuprous p-bromo thiophenoxide reported by Lenz in 1962.[130] Although the reaction gave a linear PPS, removal of the by-product, cuprous bromide, from the polymer was difficult.

The commercial process for the production of PPS was discovered by Edmonds and Hill.[131] This involves the production of PPS from relatively inexpensive starting materials, p-dichloro benzene and sodium sulphide in a polar solvent under high temperature and pressure. Polymer produced by this method is linear, containing 150-200 repeat units, and has molecular weight in the range 15,000-20,000. Polymer obtained from this process is referred to as "virgin" PPS. We can produce moulding resins from virgin PPS by solid-state polymerisation (SSP) below melt temperature of resin.

1.9.1. Structure, properties and applications of PPS

Structurally, the polymer backbone of PPS consists of p-substituted aromatic rings inter-connected by sulphur linkages. Linear PPS has one sulphur atom between the p-phenylene units. The chemical structure of the PPS can be represented as:

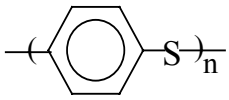

Figure 2.11: Structure of Poly(phenylene sulphide)

PPS is an unique resin in a number of ways. It combines the properties of both thermoplastic and thermosetting class of materials. Under normal conditions, PPS behaves as a true thermoplastic. The polymer can be repeatedly melted and solidified with minor changes in its mechanical properties. It can behave as a thermoset polymer when it is subjected to a process called "curing", even though the reactions involved are many times slower than that in typical thermosets.

PPS is a crystallisable polymer with crystalline melting point, T_m of 285 ^oC and a glass transition temperature, T_g of 85 ^oC. The repeating p-phenylene units impart rigidity to the polymer chain and the symmetry due to p-phenylene linkages imparts a high degree of crystallinity. PPS exhibits good thermal stability, chemical resistance, inherent flame retardance, good mechanical strength and processability. The polymer is insoluble in most organic solvents. It is soluble to a limited extent in some aromatic solvents at elevated temperatures. 1-Chloro naphthalene acts as a solvent for PPS at 206 ^oC. PPS is an inherently conducting polymer. Doping with arsenic pentafluoride increases the conducting properties of PPS and yet retains its melt-processable characteristics.[132]

"Curing" is the thermal treatment by which we can improve the mechanical properties of PPS.[129] There are two types of curing processes - melt curing and solid state curing. The cure reaction of PPS consists of chain scission, extension and some degrees of cross-linking. When the polymer is cured below T_m, by SSP an increase in the curing temperature results in increases in both cure rate and amount of cure. Either air or oxygen is used as curing atmosphere. Curing rate is higher in oxygen atmosphere. The solid-state

cure behaviour of PPS is also affected by the particle size. As the particle size increases, the rate of cure decreases.

During the curing process of PPS, changes in its properties such as an increase in molecular weight, loss of solubility, increase in melt viscosity, a change in colour from off-white to dark-brown and a decrease in ultimate crystallinity all occur. The resultant cured polymer is much tougher, stronger and easier to process by injection or compression moulding than the virgin polymer. The magnitude of these changes depends on the degree of cure, controlled by variance in the time and temperature of cure.

Due to chemical resistance of PPS resin, elucidation of cure mechanism is difficult. The reactions believed to be involved in high temperature curing[133-135] are: (1) Disproportionation to produce a higher molecular weight moiety and diphenyl sulphide; (2) Heating in air could trigger aryl-ether cross-links between adjacent polymer chains; (3) Thermal curing in the absence of air produces bridges in which connecting species are aryl or sulphur.

When an alkali metal carboxylate is used as polymerisation modifier, higher molecular weight PPS can be obtained. By the incorporation of a small amount of trichloro aromatic compound, we can prepare even higher molecular weight, soluble polymer. Compared to cured resin, a high molecular weight polymer provides higher tensile strength, elongation, flexural strength and impact strength.

PPS finds applications in many areas, including electrical, electronic, mechanical, automotive and coating applications because of its unique combination of properties and wide range of melt viscosities. Most end products are fabricated by injection moulding. For applications involving injection moulding, PPS is compounded with glass fibres and

fillers. Small amount of PPS is used in sintering and compression mouldings. Typical applications include bearings, roller elements and seals, rods, tubes, electrical components, valves, pistons, rings, lighting reflectors, thermostat housings, street light design etc. Exhaust gas emission valve on Toyota automobiles is a specific application of PPS. The polymer can be made conductive by doping and possible applications in the fabrication of printed circuit boards are obvious.

1.9.2. Modification of properties of PPS: PPS Composites and Blends

Reinforcement of PPS with long fibre produces thermoplastic composites exhibiting strength and toughness.[136-140] The PPS thermoplastic composites based on long glass fibres are characterised by high impact strength and flexural moduli. When long carbon fibres are used as reinforcing agent in the PPS composites, an even higher level of mechanical properties can be obtained which are suitable for structural applications. Of particular interest here is the interlamillar fracture toughness. In these, the morphological features of extreme importance are dictated by the processing conditions and fibre characteristics. However, the use of inorganic fibres and fillers in PPS leads to an increase in melt viscosity and lowers the ease of processing.

Composites have been investigated so as to provide an effective means to achieve property balances, processing characteristics, and often to reduce costs. In particular, PPS has been used as a thermoplastic matrix for advanced thermoplastic composites. Blends of PPS with other polymers, glass and carbon fibres have been examined. The other polymers blended with PPS have been poly(ethylene terephthalate),[136,137] polyethylene,[138] poly(ether sulphone)[139] and polyamides.[140] The crystallisation kinetics of PPS with

thermotropic liquid crystalline polymers (TCLPs) are enhanced by the rapidly crystallizing TLCPs,[137] thereby altering the morphological characteristics of PPS.

The crystallisation behaviour and morphology of PPS are found to improve on blending with other thermoplastic polymers.[132-136] Blending of TLCPs with PPS improves properties such as impact resistance, stiffness, heat distortion temperature, chemical resistance and thermal stability.[132] The TLCP phase in these blends has lower viscosity than PPS and results in the formation of molecular composites. In the crystallisation of PPS, TLCP acts as nucleating agent.

1.9.3. PPS-TLCP blends

Several studies have been published on the phase morphology, thermal and crystallisation behaviour, mechanical and rheological properties of the blends of PPS and various commercially available TLCPs such as VECTRA A950, VECTRA B950, HX 4000.

Baird et. al[141] made a preliminary investigation of the morphology, rheology and mechanical properties of PPS blends with three different TLCPs, with the main objective of defining the conditions for the *in-situ* formation of TLCP reinforcing fibrils in the PPS matrix. Stupp and Wu[142] made a NMR investigation on a TLCP containing 5 and 20% PPS, and found that the TLCP induced an orientational order in the PPS dispersed phase.

The properties of the blends are affected by the size, shape and distribution of the TLCPs in the matrix polymer, which in turn are related to the processing conditions such as the blend composition, the extrusion and drawing conditions, the viscosity ratio of the component polymers and the type and grade of the TLCPs and matrix polymers.[143]

1.9.4. Phase behaviour and morphology

The TLCPs are normally immiscible with thermoplastics such as PPS and thus the blends consist of two separate phases. The resultant morphology of the blend largely depends on the interfacial tension, ratio of viscosities of the components and shear rate.[141-156] The TLCP phase appeared in the matrix in the form of small spheres or fibres depending on the TLCP content and orientation during processing.[141-144] There are conflicting reports on the morphology and phase behaviour of PPS/Vectra A950. Subramaniam et. al[144] and Minkova et. al[156] reported that this TLCP reacted with PPS during extrusion. The blends exhibited a foam structure, and no elongation of the TLCP phase was found. They attributed the lack of fibrillation in the PPS/Vectra A950 system to possible chemical reaction between the two components under the prevailing processing conditions. Seppala et. al[145,146] observed skin-core morphology for PPS/Vectra A950 blend. They concluded that properties improved as a result of fibrous blend morphology and that there was no reaction between PPS and TLCP during extrusion.

Gabellini et. al[153] studied the morphology of PPS/HX 4000 (copolyester of terephthalic acid, phenyl hydroquinone and hydroquinone) blend and concluded that the blends were partially miscible. De Gauna et. al[154] reported that PPS/Vectra A blends were immiscible. They observed a clear fibrous morphology that was a consequence of the higher viscosity of the matrix compared with that of Vectra A at the shear strain rate used.

Gomes et. al[155] studied PPS/TLCP blends made by two methods: 1. Mixing and capillary extrusion (sample 1), 2. Injection molding (sample 2). They observed that sample 1 has a morphology composed of fibrils of both polymers, but a matrix made of only one polymer i.e. PPS. Sample 2 had a mainly fibrillar morphology, with no

observable matrix, made of both polymers. Formation of pure TLCP fibrils was observed neither in the extruded blends nor in the injection-molded samples.

Kestenbach et. al[156] used polarised light optical microscopy (PLOM) to investigate the presence of preferred molecular orientation in the TLCP phase of poly(p-phenylene sulphide) (PPS)/TLCP blends after injection molding. Quantitative measurements indicated that the molecular orientation of the TLCP fibrils increased linearly with their length-to-diameter aspect ratios.

1.9.5. Thermal and crystallisation behaviour

The mechanical properties of crystalline PPS are highly dependent on the processing conditions, which govern the crystallisation processes. Much efforts has been made to describe the thermal and crystallisation behaviour of PPS containing TLCP.[150-153] In general, crystallisation proceeds through homogeneous and/or heterogeneous nucleation, followed by growth of the nucleated spherulites. Nucleating agents tested include inorganic additives such as talc, chalk, glass and silica, organic compounds such as polycarboxylic acids and their salts, and polymers such as high-density polyethylene (HDPE) and TLCPs. The crystallisation behaviour of neat PPS,[157] of PPS with solid fillers[158-160] and of PPS blended with thermoplastic polymers[128-131] has already been studied extensively by isothermal methods. Lopez and Wilkes[157] reported non-isothermal study of linear and branched PPS samples. They found that the Avrami exponent, as determined by the Ozawa equation from non-isothermal measurements, was in good agreement with those estimated by isothermal methods. These studies demonstrated that the Ozawa equation holds good not only for PPS but for the blends and composites as

well. The presence of a nucleating polymer has a profound influence on the crystallisation kinetics of crystalline PPS.

Table 1.6: Important published papers on PPS/TLCP blends

Blend components	Studied properties	Ref No.
PPS/(HNA-HBA)	DSC, morphology	126
PPS/(HNA-HBA)	Mechanical properties, morphology, and thermal properties	141
PPS/PET-OB	NMR studies	142
PPS/(HNA-HBA)	Rheology, mechanical properties, morphology	145
PPS/(HNA-TA-AP)	DSC, morphology, mechanical properties	147
PPS/(HNA-HBA)	DSC, morphology	148
PPS/(HNA-HBA)	DSC, mechanical properties	149
PPS/(HNA-TA-AP)	DSC, crystallisation behaviour	150
PPS/(HNA-TA-AP)	DSC, crystallisation behaviour	151
PPS/(HNA-TA-AP)	DSC, crystallisation behaviour	152
PPS/(HNA-TPA-AP)/PSF	DSC, rheology, mechanical properties	153
PPS/(PHQ-TPA-HQ)	DSC, morphology	157

A number of papers have been published on PPS/TLCP blends (Table 1.6). The isothermal crystallisation behaviour of blends of PPS and Vectra A950, Vectra B950 and HX4000 were reported.[149] The isothermal crystallisation of PPS was found to be strongly accelerated by the presence of Vectra B950, as a result of increased nucleation density, whereas no reduction of the degree of crystallinity could be noticed. Minkova et. al[150,151] found that blending PPS with Vectra B950 leads to an increase in the non-isothermal crystallisation temperature without any reduction in the degree of crystallinity. The PPS crystallisation rate coefficient (CRC) was found to increase three times upon addition of 2-50% Vectra B950. The values of the Avrami exponent n were close to 3, as found previously from isothermal analysis, and did not vary appreciably on addition of Vectra

B950. These findings show that the type of nucleation and the geometry of crystal growth do not change **n** in the presence of Vectra B950.

Hong et. al[149] studied isothermal and non-isothermal crystallisation kinetics of PPS/Vectra B950 blends. As the TLCP content was increased, the supercooling required for PPS crystallisation, both half time for crystallisation and size of spherulites, decreased. The PPS containing TLCP exhibited a higher nucleation density than pure PPS, for which three dimensional growth and constant radial growth rate of spherulites are assumed. This study revealed a notable reduction in the Avrami exponent, which indicates that the nucleated process leads to rod shaped growth with thermal nucleation. Gebiliani et. al[153] analysed the isothermal and non-isothermal crystallisation behaviour of PPS/HX4000 blend and observed that rate of crystallisation of PPS increased in presence of HX4000. They also reported that both components had their crystallisation temperature increased and also that the melting temperature of TLCP increased in the blends.[161] Dynamic mechanical thermal analysis showed the blend to be immiscible.

The heat deflection temperature (HDT) and coefficient of linear thermal expansion of PPS improved on blending with TLCPs.[145,146] Thermal stability of PPS was found to increase in presence of TLCP. Han et. al[162] reported that in PPS/TLCP (Vectra A 900) there is no molecular scale mixing or chemical reaction between the components, as evidenced by melting and crystallisation points in the PPS phase.

1.9.6. Mechanical properties

As the polymers are not miscible, the poor adhesion between the two separate phases affects the properties of the blend. Seppala et. al[145,146] reported that the tensile and impact properties of PPS are enhanced on blending with Vectra A950. De Gauna et. al[154]

studied the fracture properties of the as-molded blends, such as ductility and tensile strength, were higher than in annealed blends, as a consequence of the higher deformability of the less crystalline structure**.** Similar results of improvement in the mechanical properties has been reported.[145,146,151,152,155] Shonaike et. al[151,152,163] investigated the effect of TLCP distribution on the mechanical properties. They observed an increase in bending modulus with increasing TLCP content and attributed this to the reinforcing nature of the TLCP fibrils in the skin layer. Shonaike et. al[103] reported the bending test result of PPS/TLCP blends that showed a rapid load drop at the brittle-ductile transition temperature region. A number of patents have been filed on PPS/TLCP blends (Table 1.7).

Table 1.7: Some Important Patents on PPS/TLCP blends

Blend	Advantages/applications	Ref
PPS/(HNA-HBA)	Coating applications	165
PPS/(H.T.I.DODP)	Moulding composition, improved properties	166
PPS/LC Polyester	Fibre reinforced composites	167
PPS/TLCP	Moulding composition, improved properties	168
PPS/(HNA-HBA)	Coating applications	169
PPS/TLCP	Moulding composition, improved mechanical, thermal properties	170
PPS/TLCP	Moulding composition, improved mechanical, thermal properties	171
PPS/TLCP	Moulding composition, improved mechanical, thermal properties	172
PPS/TLCP	Moulding composition, improved mechanical, thermal properties	173
PPS/TLCP	Coating; Moulding; Electronic applications	174
PPS/(HNA-HBA)	Moulding composition, improved mechanical, thermal properties	175
PPS/TLCP	*In-situ* composites, Electronic connectors	176
PPS/LC Polyester	Moulding composition, improved mechanical, thermal properties	177
PPS/LC Polyester	Coating, Moulding improved mechanical, thermal properties	178
PPS/LC Polyester	Fibre reinforcement	179

1.9.7. Rheological properties

The rheology of TLCP blends is a complex but exciting new field of academic interest where many significant questions remain to be answered. There are many reports of reduction in melt viscosity of PPS on addition of TLCP.[144-146] Viscosity drops with TLCP amount, indicating that TLCP plays the role of a processing aid for the PPS phase. Han et. al[164] studied entire composition range of PPS/TLCP (Vectra A900) blends using stress rheometer, capillary rheometer. At low rate, when the TLCP is added to the PPS, the pure melts have similar viscosity: for TLCP and for PPS, but the viscosity of the blends goes through a maximum with concentration that is nearly three times the viscosity of the individual melts. At high rate, a significant depression of the viscosity is observed in the PPS rich composition.

1.10. Polymer-layered silicate nanocomposites

Polymer nanocomposites are composites with inorganic components in which the inorganics are nanosized.

1.10.1. Clays

Clays constitute a large part of the rocks and soil. Smectite or phyllosilicates group of clays are largely used in polymer nanocomposite.

1.10.2. Phyllosilicates-structure

Smectite or phyllosilicates are aluminosilicate which condensates in 2:1 ratio of tetrahedral silicon (Si) sheets with an octahedral aluminium (Al) sheet are called as 2:1 phyllosilicates. In many phyllosilicates either Al^{3+} or Si^{4+} ions are isomorphically substituted partially by lower valency metal cations of similar sizes like magnesium (II) (Mg^{2+}) and ferrous (II) (Fe^{2+}).

1.10.3. Smectite clays

Smectite clays are classified as montmorillonite, saponite, vermiculite and illite. Out of these four clays montmorillonite is the most widely used clay for making polymer nanocomposite.

1.10.4. Montmorillonite

This dioctahedral 2:1 phyllosilicate (Fig. 1.12) has silica tetrahedrons having oxygen and hydroxyl ions tetrahedrally arranged around central silicon atoms. The base of tetrahedron is made up of oxygen atoms while hydroxyl group makes up the tip of the tetrahedron and is fused with the aluminium octahedron. The aluminium octahedral sheet has Al^{3+} ion octahedrally coordinated to the hydroxyl groups.[180,181] Two third of the Al^{3+} ions are substituted by lower valency cations such as Mg^{2+} and Fe^{2+} in octahedral sites.

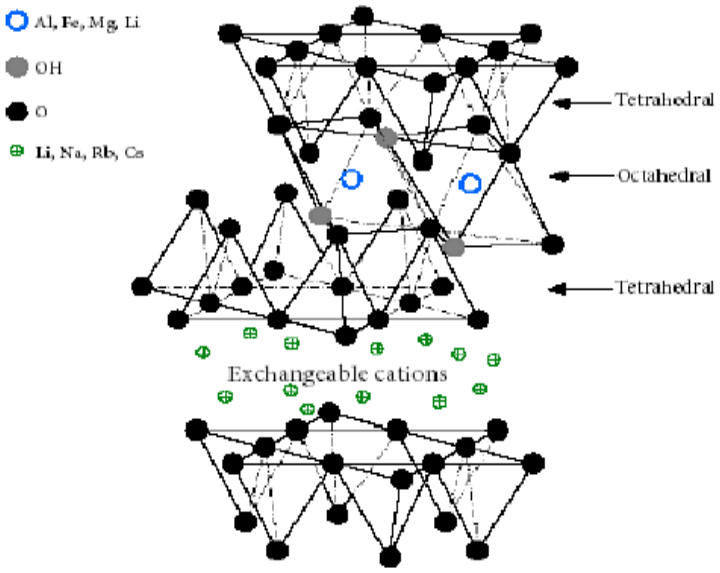

Figure 1.12: Structure of montmorillonite

Montmorillonites have a highly asymmetric structure, in which each two dimensional aluminosilicate platelet or clay layer is about 0.95 - 1.3 nm thick and about 500 - 1000 nm in lateral dimensions. For nanoclays an aspect ratio may be defined as D/t,

where D is the average platelet diameter and t is the thickness of either individual platelet or a stack of platelets [called as tactoids]. For montmorillonite, the aspect ratios are as high as 1000 for individual platelets and 300-500 for tactoids. The clay is white-pale yellow in colour. An interlamellar space or *gallery* of about ~ 1 nm separates these platelets. Consequently montmorillonite has a large surface area of about 700 - 800 m^2/g. It has a high cation exchange capacity (CEC) of 70 - 150 meq/100 g for a comparatively lower isomorphic substitution of ~ 0.25 - 0.6. The successive layers in montmorillonite are more randomly stacked compared to pyrophyllites.[182]

1.10.5. Advantages of layered silicates

Any physical mixture of a polymer and an inorganic material (such as clay) does not form a nanocomposite. Conventional polymer composites that are prepared by reinforcing a polymer matrix with inorganic materials like reinforcing fibres and minerals have poor interaction between the organic and the inorganic components, which leads to separation into discrete phases. Therefore, the inorganic fillers are required to be added in higher concentrations to achieve enhancements in the thermomechanical properties of the polymer.[180-183] In contrast to conventional composites, significant property enhancement is still achieved at much lower filler loading for nanoclays. Importantly, this is achieved with negligible increase in the weight of the part.

The reasons for the greater effectiveness of the nanoclays are two-fold. First, the nanoclays can be dispersed to the level of individual platelets. This nano scale dispersion of silicates provides very high surface area for polymer clay interaction.[180,183] Second, the lamellar surfaces of the nanoclays can be modified through an ion exchange reaction to make them compatible with the polymer matrix. In addition to the above-mentioned

advantages nanoclays offer other interesting features. For instance, polymer nanoclay composites can potentially form optically clear films under certain conditions.[184] Incorporation of nano-clays is believed to increase the barrier properties by creating additional '*tortuous path*' that impedes the diffusion of gas or solvent molecules while passing through the matrix resin.[185,186] To sum up, polymer nanoclay composites exhibit unique thermomechanical, barrier and optical properties not shared by conventional filled composites.

1.10.6. Methods of polymer nanocomposite preparation

The synthesis of polymers such as polystyrene[187,188] and poly(acrylic acid)[189] within the interlayer spacing of montmorillonite has been reported as early as in the 1960's. The technological potential of these materials was realised after the pioneering efforts of the research group in Toyota Motor Co. Polymer nanoclay composites can be synthesised by four methods:

1.10.7. Sol-gel process

The sol-gel process involves hydrolysis and polycondensation of metal alkoxides $\{M(OR)_n\}$ in aqueous acid or base, to form an inorganic gel network in an organic polymer matrix. Most of the efforts in this method have been concentrated on metal organic alkoxides, especially tetraethyl orthosilicate (TEOS) and tetramethyl orthosilicate (TMOS), since they can form an oxide network in an organic matrix.[190] The mild conditions allow for the incorporation of an organic matrix in the inorganic network. Poly(methyl methacrylate) (PMMA) nanocomposites are reported to be synthesised by the sol-gel method.[191-196] However, composites synthesised by this method are found to be very difficult to process, because often the initially soluble polymers phase-separate

once the gelation begins. Also, the choice of suitable solvent-polymer pairs further limits the applicability of this method.[192] Seckin et. al synthesised PMMA nanoclay composite using bentonite clay. FTIR and XRD analysis showed that the polymer was linked to clay via hydrogen bonding.[194] Huang et. al synthesised polymer layered silicate (PLS) nanocomposites by using different functionalised viz., trialkoxysilyl, hydroxyl and unfunctionalised methacrylic polymers by the sol-gel method.[196] The trialkoxysilyl functionalised PMMA was found to be best suited, since it exhibited maximum property improvement.

1.10.8. *In-situ* polymerisation

First, the nano dimensional clay is dispersed in the monomer, which is then polymerised. The monomer may be intercalated with the help of a suitable solvent and then polymerized (Fig. 1.13)**.** Polycaprolactone[197] and nylon[198] nanocomposites are commonly synthesised by intercalation of monomer. *In-situ* polymerisation of monomer very often produces nearly exfoliated nanocomposites. However, commercialisation of this method would require separate production lines or major changes in the existing production facilities to suit the heterogeneous polymerisation of monomer in the presence of clay. Such factors limit the commercialisation of this method.[199]

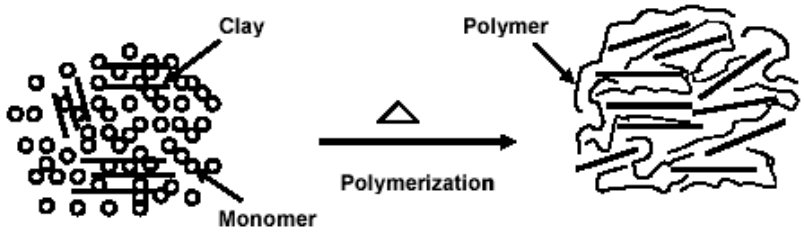

Figure 1.13: Schematic of nanocomposite synthesis by *in-situ* polymerisation

Usuki et. al reported the synthesis of nylon 6-clay hybrid by *in-situ* polymerisation of ε-caprolactam in the interlayer layer space of montmorillonite, the

surface of which was modified by ω-amino acid.[200] The carboxylic acid end group of the amino acid initiated the polymerisation of ε-caprolactam. Transmission electron microscopy (TEM) and X-ray diffraction (XRD) analysis of these hybrids showed an exfoliated microstructure. Polymers like poly(ε-caprolactone) (PCL),[201] polycarbonate (PC)[190,202] epoxy,[203-206] polyethylene (PE),[207-209] polypropylene (PP),[190,208,210] poly(ethylene terephthalate) (PET),[191] poly(dimethyl siloxane) (PDMS),[192] polyamide[197,198,211] and polyimide[185] have also been reported to give exfoliated hybrids by *in-situ* polymerisation of the respective monomers in the interlayer spacing of the clays. Thus it may be inferred that *in-situ* polymerisation often leads to exfoliated nanocomposites.

1.10.9. Solution intercalation

In this method the polymer is dissolved in an appropriate solvent, in which the nano-clay is dispersed. Intercalation of polymer chains into the clay galleries occurs from solution. The operating temperatures are typically low. This method can be useful for few polymers, for which suitable solvents are available. This route is also preferred for polymers that require high processing temperature at which the organoclay may degrade. Nanocomposites of polymers like poly(ethylene oxide)[212] and polylactide[211] have been synthesised by this method. Apart from the limited choice of suitable solvents, factors like the cost and the recovery of the solvents, would further restrict the commercial viability of this method.[201]

Polymer clay hybrids can be synthesised by solution blending (i.e., intercalation of polymer from solution). PLS nanocomposites based on polymers like polycaprolactam (PCL),[213] polylactide (PLA),[214] poly(ethylene oxide) (PEO),[215] syndiotactic-polystyrene

(s-PS),[216] PMMA,[217]and PE[218] have been synthesised by solution blending. Jeon et. al have reported the synthesis of HDPE nanoclay composites by solution blending.[218]

1.10.10. Melt intercalation

This method involves the mixing of polymer with clay above the polymer's glass transition or melt temperature. At higher temperatures polymer chains are sufficiently mobile to diffuse into the galleries of the clay.[185,219-222] Vaia et. al have shown that intercalation can be improved with conventional processing techniques. Twin-screw extrusion has been found to be effective for the dispersion of silicate layers.[185-221] Cho et. al found that an organoclay, if compatible with the polymer, may even exfoliate during extrusion due to shear. The dispersion of clay depends on the parameters like residence time, level of shear, etc.[219]

Melt intercalation is an environmentally friendly technique, as it does not require any solvent. It is also commercially attractive due to its compatibility with existing processing techniques. However, the resulting morphology of the nanocomposite is often an intercalated microstructure rather than the preferred exfoliated state. Apart from the four main techniques listed above, a few other techniques for the preparation of polymer nanocomposites include sonication[223] and miceller intercalation.[193]

Giannelis et. al proposed the more versatile and environmental friendly method for nanocomposite synthesis namely, melt intercalation, which involves melt mixing the polymer and clay.[224] Vaia et. al found improved intercalation through the aid of conventional processing techniques like extrusion.[225-228] Cho et. al have shown twin-screw extrusion to be more effective for exfoliation and dispersion of the clay layers compared to single screw extrusion due to more extensive shear. Furthermore, for

optimally compatibilised polymer-organoclay systems twin-screw extrusion leads to composite properties comparable to those produced by *in-situ* polymerisation.[228] Fornes et. al have suggested that during melt compounding the shear stress dictates the final morphology of the hybrid.[229,230] In the initial stages of extrusion the stress would break up the organoclay particles into smaller tactoids. Further during the extrusion, individual platelets of these tactoids would be peeled apart by combined effect of shear and diffusion of polymer chains in the gallery as illustrated in Figure 1.14.

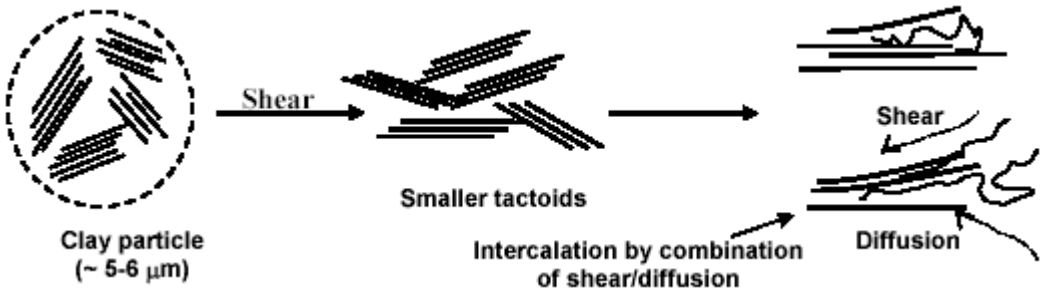

Figure 1.14: Stepwise mechanism of clay exfoliation during the melt mixing of nanocomposites

Dennis et. al have reported on the effects of the melt processing conditions on the exfoliation of PLS nanocomposites.[231] They observed that factors like the residence time in the extruder and the intensity of shear play a crucial role in determining the dispersion of clay in the polymer matrix. They found that the degree of clay dispersion was maximised by the backmixing in a co-rotating twin-screw extruder.[231]

Polymer layered silicate nanocomposites of almost all commercially important polymers like polystyrene,[232] Nylon,[229-231] polyethylene,[233] polypropylene,[234,235] polycaprolactam,[236,237] poly(butylene terephthalate),[238] poly(ethylene-co-vinyl alcohol) (EVOH),[239] and polycarbonate[205] can be manufactured by melt intercalation. Polymer layered silicate nanocomposites of polymers like poly(ethylene oxide),[227,240] poly(methyl methacrylate),[217,232,241,242] polycaprolactam[213,233] and Nylon[197,198,229,230] can be prepared

by more than one method based on the availability of suitable polymer solvent pair and processibility issues.

In the case of many commercially important polymers, the solution intercalation or the *in-situ* polymerisation techniques are difficult to implement on an industrial scale, because a suitable solvent polymer system is not always available and also an additional step of solvent removal is involved.[243,244] Ecofriendly and cost-effective melt intercalation shifts the synthesis of the nanocomposites downstream to the polymer processing industry.

Vaia et. al have shown that the d spacing in PEO/Na^+ montmorillonite hybrids prepared by melt intercalation at 80^oC matches with those of the PEO hybrids prepared by solution intercalation.[227] Thus, under suitably chosen processing conditions the morphology of hybrids obtained by melt intercalation can be comparable with that in hybrids prepared by other synthetic routes.

Organic modifiers play a crucial role in the synthesis of PLS nanocomposites. Layered silicates, montmorillonite in particular, are hydrophilic in the pristine form. The clay surface can be rendered organophilic by exchanging the mobile Na^+ with suitable cationic surfactants. Such organoclays have lower surface energy compared to pristine clay and are more compatible with the polymer matrix.[224,225] Vaia et. al found that PS does not intercalate in pristine Na^+-montmorillonite. However, the intercalation does take place with organosilicates.[225] Usuki et. al. synthesised nylon-6 nanocomposite using the Na^+-montmorillonite modified with various ω-amino acids.[188,189,199-203,206,207,211] XRD results showed that amino acids were stretched with longitudinal axes perpendicular to the silicate layer in the interlayer gallery. Among the different amino acids used, 12-

aminolauric acid was found to be the most appropriate modifier for nylon nanocomposites.

1.10.11. Morphologies of polymer nanocomposites

In general, the microstructures of polymer-layered silicate nanocomposites are classified in two idealised morphologies viz., intercalated and exfoliated.[194,195,199,201]

In an immiscible composite or an unmixed system the polymer does not penetrate inside the galleries between the clay layers and hence the pristine gallery distance is maintained in the composite. In intercalated structures, however, polymer chains penetrate inside the galleries and effectively expand the silicate layers.[195] Such structures consist of ordered, alternating polymer silicate layers with repeat distance of a few nanometers. The equilibrium gallery height is determined by entropic and energetic factors. When the gallery distance, (h) is less than the radius of gyration, (R_0), of the polymer chains, the configurational entropic penalty of polymer chain confinement may be compensated by increased conformational freedom of the tethered surfactant chain. When $h > R_0$, the entropy is change is almost zero.[194]

An ideal exfoliated state refers to a structure where the polymer extensively penetrates in the silicate galleries so as to completely delaminate the layered structure. In the exfoliated state the average gallery height is determined by clay loading. This class of microstructure can be further classified based on the relative change in the separation between platelets with silicate volume fraction. Low silicate loadings result in disordered exfoliated nanocomposites in which single clay platelets are randomly suspended in the polymer matrix and are typically separated by an average distance of > 10 nm. Above a critical clay loading, the platelets start arranging in an ordered fashion and this is called

the *ordered exfoliated nanocomposites,* as shown in Fig. 1.15.[195] The state of dispersion of clay in polymer is in general dictated by the polymer-silicate interactions, aspect ratio of silicate, method of manufacturing (melt, solution, *in-situ* polymerisation) and possible orientation of layers during processing.

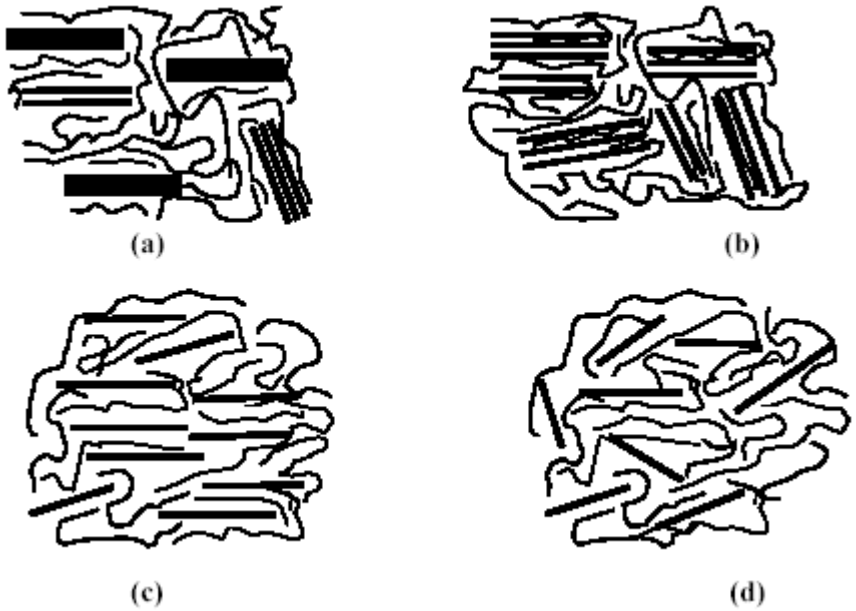

Figure 1.15: Schematic of various morphologies of composites: (a) immiscible composite, (b) intercalated nanocomposite, (c) ordered exfoliated and (d) disordered exfoliated nanocomposite.

1.10.12. Characterisation and properties of PLS nanocomposites

The state of dispersion of clay in PLS nanocomposites may be classified in two idealised class of morphologies: (1) *Intercalated,* in which the polymer expands the interlayer distance resulting in an ordered, alternating multilayered polymer clay layer structure, and (2) E*xfoliated*, where the polymer chains completely delaminate the layered clay structure. However, real nanocomposites exhibit morphologies that are combinations of these two idealised cases as discussed in several researches.[245-247] Transmission electron microscopy (TEM), scanning electron microscopy (SEM) and x-ray diffraction (XRD) techniques are often used to directly quantify the structure of PLS

nanocomposites.[180] XRD, the most obvious technique to study the periodic structure of clays in case of intercalated PLS nanocomposites, has also been extensively used to study polymorphism in PLS nanocomposites, and the effect of clay on polymorphism.[248-252] It has been reported that clay induces the γ phase of nylon-6 in nylon-6/PLS nanocomposites.[250,251] Similarly, for nylon-66 PLS nanocomposites, the γ phase of nylon-66 is favoured and the crystalline phase transition was lowered by 20^{o}C.[248-49] Tseng et. al reported that in s-PS nanocomposites the presence of clay facilitated the formation of â phase of s-PS.[252] Spectroscopic techniques like fourier transform infrared spectroscopy (FTIR)[253] and nuclear magnetic resonance (NMR)[254-256] are also being employed to probe the interlayer structure of the clay.

Analytical techniques like differential scanning calorimetry (DSC), dynamical mechanical analysis (DMA) and thermogravimetric analysis (TGA) can provide indirect but useful evidence of structural attributes. For instance, Vaia et. al have used DSC to study the kinetics of PEO/clay hybrid formation.[227] Pristine PEO is a crystalline material. At time t = 0 hr, it showed a distinct endotherm corresponding to the crystalline PEO. Vaia et. al have shown that the DSC thermograms of pristine PS, physical mixture of PS organoclay and intercalated PS organoclay are qualitatively different.[226] Both the pristine polymer and the physical mixture of PS with organoclay exhibited characteristic glass transition at 96^{o}C, while the intercalated hybrid did not show any such transition. These results complimented the results obtained by high temperature x-ray analysis, which showed that with annealing time the clay peak shifted to higher d spacing.

PLS Nanocomposites exhibit improved thermo-mechanical properties, reduced gas permeability and improved solvent resistance.[180] Kojima et. al showed that modulus

of nylon-6 PLS nanocomposite increased by 100%, impact strength by 25%, flexural modulus by 100% and heat distortion temperature (HDT) increased by 125%. These improvements in properties were achieved by the addition of just 4.5 wt% of clay.[212] Usuki et. al tested mechanical properties of nylon-6 clay hybrid using four different types of clays viz., montmorillonite, aconite and synthetic clays like limonite and mica. These clays were modified using 12-aminolauric acid.[211] They found that mechanical properties for hybrid synthesised by using montmorillonite were superior to other clay hybrids. Using NMR measurements they attributed this property enhancement to greater ion bonding between the montmorillonite and nylon-6, as compared to that in the other the types of clays.[207,254] Lan et. al have shown that exfoliated epoxy clay nanocomposites have higher modulus than the intercalated epoxy clay composites.[257]

The mechanical property enhancement was found to be dependent on many factors such as the concentration and aspect ratio of the silicate layers,[198] interactions between clay and polymer,[258] and orientation of clay and polymer.[259-261] Yano et. al have shown that incorporation of nano-clays in polyimide matrix increases the barrier properties by creating additional '*tortuous path*' that impedes the diffusion of gas or solvent molecules while passing through the matrix resin.[186] Interestingly, Merkel et. al have shown that dispersion of nanoparticles of fumed silica increases the permeability of glassy amorphous poly(4-methyl-2-pentyne) membranes due to disruption of chain packing and a subsequent increase in the free volume.[261]

1.10.13. Applications of polymer-nanocomposites

Polymer-nanoclay composites caught the attention of the technologist after nylon nanocomposite made a market debut in Toyota Motor Company's car model in the late

1980's. Since then nanocomposites are gradually gaining acceptance in mainstream polymer industry, finding applications in automotive to packaging sectors.[181-183,262] Polymer-nanoclay composites have huge potential as they can achieve the same properties, e.g., increased tensile strength, improved heat deflection temperature and impact strength, with typically 3–5 wt% of the filler compared to 30-wt% for conventional composites, as shown in Table 1.8. Such improvements in the thermo-mechanical properties make nanocomposites a potential candidate for many automotive products such as mirror housings, door handles, engine covers and timing belt covers. General industrial applications currently being considered include usage as impellers and blades for vacuum cleaners, power tool housings, etc.[183]

Nanocomposites offer 25% weight reduction over conventional composites and as much as 80% over steel. Reduced weight helps to increase fuel efficiency. Further, such improvements can be achieved with very little increase in fabrication cost and material cost. General Motors and Montell have jointly developed olefin (TPO) clay nanocomposite for an exterior step assist for the 2002 Astra and Safari vans. Mitsubishi used a nanocomposite in the engine cover for its GDI engines.[183] A recent study in UBE Industries revealed significant reductions in diffusive fuel loss through polyamide–6/66 polymers by using nanoclay as filler. This is due to the enhanced barrier properties of polymer-nanoclay composites. As a result, considerable interest is now being shown in these materials as both fuel tank and fuel line components for cars.[263]

Honeywell Inc. claims that incorporation of just 2% nanoclays improves the oxygen barrier (OTR) three times than that of pristine nylon 6 films.[263] Owing to the

excellent barrier properties, nanocomposite films can be used in food packaging like pet foods, boil-in bags and vacuum packs.

Table 1.8: List of nanocomposite suppliers and targeted applications

Supplier, Trade Name	Matrix Resin	Target Application
Bayer AG (Durethan LPDU)	Nylon 6	Barrier films
Clariant	PP	Packaging
Creanova (Vestamid)	Nylon 12	Electrically conductive
GE Plastics (Noryl GTX)	PPO/Nylon	Automotive painted parts
Honeywell (Aegis)	Nylon 6, Barrier Nylon	Multi-purpose bottles and film
Hyperion	PETG, PBT, PPS, PC, PP	Electrically conductive
Kabelwerk Eupen of Belgium	EVA	Wire & cable
Nanocor (Imperm)	Nylon 6, PP Nylon MDX6	Multi-purpose molding PET beer bottles
Polymeric Supply	Unsaturated polyester	Marine, transportation
RTP	Nylon 6, PP	Multi-purpose, electrically conductive
Showa Denko (Systemer)	Nylon 6, Acetal	Flame retardance, Multi-purpose
Ube (Ecobesta)	Nylon 6, 12, Nylon 6, 66	Multi-purpose Auto fuel systems
Unitika	Nylon 6 Multi-	purpose
Yantai Haili Ind., Commerce of China	UHMWPE	Earthquake-resistant pipe

Source: Bins & Associates, Sheyboygan, U.S.A.

Bayer and Nanocor are aiming nylon 6 nanocomposites cast film for multi-layer packaging, protective films for medical and corrosion-prone items. Kabelwerk Eupen of Belgium claims to be on the way to commercialise ethyl vinyl acetate (EVA) nanocomposites for wire and cable compounds.[263] Calorimeter tests for these materials

show decline in heat release at relatively low (3-5 wt%) loadings. Nano EVAs also exhibit superior mechanical properties, chemical resistance and thermal stability. Showa Denko commercialised nylon 66 nanocomposites of improved flame retardancy and rigidity.[263] Table 1.8 lists commercially available polymer-nanoclay composites. Various industries and academic groups are investigating nanocomposites of polycarbonate, biodegradable poly(lactic acid) (PLA) and polyaniline.

1.10.14. Thermodynamics of polymer layered silicate nanocomposites

Vaia et. al proposed a mean-field, lattice-based model of polymer melt intercalation in organically modified layered silicates (OLS). In general, interplay of entropic and energetic factors determines the outcome of polymer intercalation. The entropic penalty of polymer chain confinement is compensated by the increased conformational freedom of the surfactant, when the layers are separated. When the total entropy change is small, small changes in the internal energy of the system will determine whether the intercalation is thermodynamically possible. However, exfoliation requires complete layer separation [i.e., interlayer distance (h) > radius of gyration of polymer chain].

This requires very favourable polymer OLS interactions to overcome the polymer-polymer and clay - clay interaction.[264,265] Thus, the dispersion of OLS in polymer matrix requires sufficiently favourable enthalpic contribution to overcome any entropic penalties. Favourable enthalpy of mixing is achieved when the polymer OLS interactions are more compared to surfactant OLS interactions.[263-268] For polar polymers like nylons and TLCPs, an alkylammonium surfactant (most commonly used organic modifier) is sufficient to offer the excess enthalpy, required for the formation of PLS nanocomposite.

1.11. Scope and objectives of the present work

The present work is an interdisciplinary research. It involves synthesis of polymer, coupling agent, physico-chemical characterisation, processing, property evaluation to examine some critical issues relating to PPS/TLCP, PSU/TLCP blends and polymer-clay nanocomposites such as:

i. To blend poly(phenylene sulphide) with aliphatic aromatic thermotropic liquid crystalline polymer;

ii. To blend polysulphone with aliphatic aromatic thermotropic liquid crystalline polymers;

iii. To synthesise and characterise 2,2'-bis(2-oxazoline), a chain coupling agent;

iv. To synthesise and characterise block copolymer from dicarboxyl terminated poly(phenylene sulphide) and dicarboxyl terminated poly(ethyleneterephthalate-co-oxybenzoate);

v. To synthesise and characterise block copolymer from dicarboxyl terminated polysulphone and dicarboxyl terminated poly(ethyleneterephthalate-co-oxybenzoate);

vi. Evaluation of the block copolymers as compatibilising agent for the poly(phenylene sulphide)-semi aromatic thermotropic liquid crystalline polymer blends;

vii. Evaluation of the block copolymers as compatibilising agents for the polysulphone-semi aromatic thermotropic liquid crystalline polymer blends;

viii. To synthesise and characterise semiaromatic thermotropic liquid crystalline polymer-clay nanocomposite;

1.12. References

1 Paul D. R., Newman S., *Polymer Blends, Vol. 1 and 2*, Academic Press, San Diego, 1978.

2 Utracki L. A., *Polymer Alloys and Blends: Thermodynamics and Rheology,* Carl Hanser Publications, Munich, 1990.

3 Olabisi O., Shaw M. T., Robeson L. M., *Polymer-Polymer Miscibility*, Academic Press, New York, 1979.

4 Platzer N. A. J., Gould R. F., Eds., *Copolymers, Polyblends and Composites*, ACS, Washington DC, 1975.

5 Folkes M. J., Hope P. S., Eds., *Polymer Blends and Alloys*, Blackie Academic and Professional, London, 1993.

6 Manson J. A., Sperling L. H., *Polymer Blends and Composites*, Plenum Press, New York, 1976.

7 Walsh D. J, Higgins J. S., Maconnachie A., Eds., *Polymer Blends and Mixtures*, Applied Sciences Martinus Nijhoff, Dordrecht, The Netherlands, 1985.

8 Paul D. R., Barlow J. W., in Solc K., Ed., *Polymer Compatibility and Incompatibility: Principles and Practice*, MMI Press Symposium Series, Vol. 2, Harwood Academic Publishers, New York, 1982.

9 Klempner D., Frisch K. L., Bailey W. J., Berry J. P., Hoeve C. A. J., Eds., *Polymer Alloys: Blends, Blocks, Grafts and Interpenetrating Networks*, Plenum Publishing Corporation, New York, 1977.

10 Martuscelli E., Palumbo, R., Kryszewski M., Eds., *Polymer Blends: Processing, Morphology and Properties*, Plenum Publishing Corporation, New York, 1980.

11 Giles H. F., *Alloys and Blends, Modern Plastic Encyclopedia*, 105, 1986.

12 Utracki L. A., Weiss R. A., Eds., *Multiphase Polymers: Blends and Ionomers*, ACS Symposium Series 395, ACS, Washington DC, 1989.

13 Bonner J. G., Hope P. S., *Compatibilisation and Reactive Blending,* in Folkes M. J., Hope P. S., Eds., Polymer *Blends and Alloys*, Blackie Academic and Professional, London, 1993.

14 Barentsen W. M., Heikens D., Piet P., *Polymer*, **15**, 119, 1974.

15 Fayt R., Jerome R., Teyssie Ph., *J. Poly. Sci*. *Poly. Lett.,* **24**, 25, 1974; Harrats C., Fayt R., Jerome R., Blacher S., *J. Poly. Sci. Poly. Phys.,* **41**, 202, 2002.

16 Paul D. R., in Paul D. R., and Newman S., Eds., *Polymer Blends*, Vol. 2, Academic Press, London.

17 Gaylord N. G., *Copolymers, Polyblends and Composites*, in Platzer N. A. J., Gould R. F., Eds., *Copolymers, Polyblends and Composites*, ACS, Washington DC, 1975.

18 Fayt R., Jerome R., Teyssie Ph., *J. Poly. Sci. Poly. Phys*., **27**, 775, 1989.

19 Robeson L. M., *J. Appl. Poly. Sci*., **30**, 4081, 1985.

20 Sjoerdsma S. D., *Polymer Commun.*, **30**, 106, 1989.

21 Brown S. B., Chapter 8, in Xanthos M., Biesenberger J. A., Eds., *Reactive Extrusion: Principles and Practices*, Hanser Publishers, Munich, 1992.

22 Martuscelli E., Pracella M., Avella M., Greco R., Ragosta G., Felice A., in Martuscelli E., Palumbo R., Kryszewski M., Eds., *Polymer Blends: Processing,*

Morphology and Properties, Plenum Publishing Corporation, New York, 1980.
23 Vanoene H., *J. Col. Int. Sci.,* **40**, 448, 1972.
24 Acierno D., Nobile M. R., Nicolais L., Incarnato L., in Collyer A. A., Utracki L. A., Eds., *Polymer Rheology and Processing*, Elsevier Applied Science Publishers, Barking, England, 1990.
25 Martuscelli E., Silvertre C., Greco R., Ragosta G., *in* Martuscelli E., Palumbo R., Kryszewski M., Eds., *Polymer Blends: Processing, Morphology and Properties*, Plenum Publishing Corporation, New York, 1980.
26 Chin H. B., Han C. D., *J. Rheol*., **23**, 557, 1979.
27 Serhatkulu T., Erman B., Bahar I., Fakirov S., Evstatiev M., Sapundjieva D, *Polymer,* **36**, 2371, 1995.
28 Fakirov S., Evstatiev M., Petrovich S., *Macromolecules*, **26**, 5219, 1993.
29 Evstatiev M., Fakirov S., *Polymer*, **33**, 877, 1992.
30 de Gennes P. G., *The Physics of Liquid Crystals*, Clarenden Press, Oxford, 1971.
31 Onsagar L., *The Effect of Shapes on the interaction of Colloidal Particles*, *Ann. N.Y. Acad. Sci.,* **51**, 627, 1949.
32 Flory P. J., *Phase Equilibria in Solutions of Rod-like Particles*, Proc. R. Soc., *London,* **A234**: 73, 1956.
33 Blumstein A., Ed., *Liquid Crystalline Order in Polymers*, Academic Press, New York, 1978.
34 Zeng H., He G., Yang G., *Angew. Makromol. Chem*., **143**, 25, 1986.
35 Brown C. S., Alder P. T., *Blends Containing Liquid Crystal Polymers;* in Folkes M. J., Pope P. S., Eds., *Polymer Blends and Alloys*, Blackie Academic and Professional, London, 1993.
36 Steadman S. C., *Fibre Forming Blends and in situ Fibre Compsites;* in Folkes M. J., Pope P. S., Eds., *Polymer Blends and Alloys*, Blackie Academic and Professional, London, 1993.
37 La Mantia F. P., Ed., *Thermotropic Liquid Crystal Polymer Blends*, Technomic Publishing Co., USA, 1993.
38 Aceimo D., La Mantia F. P., Eds., *Processing and Properties of Liquid Crystalline Polymers and LCP Based Blends*, ChemTech Publishing, Canada, 1993.
39 Baird D. G., *Thermotropic-Liquid Crystal Polymer Plends; Advanced Composites Bulletin*, 6, 1989.
40 Magagnini P., *Molecular Design of Thermotropic, Main-Chain Liquid Crystalline Polymers*; *in* La Mantia F.P., Ed., *Thermotropic Liquid Crystal Polymer Blends,* Technomic Publishing Co., Lancaster, Pennsylvania, 1993.
41 Volegova I. A., Godovskii Y. K., Aksenov A. N., Storozhuk I. P., Korshak V. V., *Vysokomol. Soedin., **Ser. B.*** **25**, 792, 1983.
42 Xie H., Chen X., Guo J., *Angew. Macromol. Chem.,* **200**, 49, 1992.

43 Inata H., Matsumura S., *J. Appl. Poly. Sci.,* **32**, 4581, 1986.

44 Inata H., Matsumura S., *J. Appl. Poly. Sci.,* **30**, 3325, 1985.

45 Inata H., Matsumura S., *J. Appl. Poly. Sci.,* **32**, 5193, 1986.

46 Inata H., Matsumura S., *J. Appl. Poly. Sci.,* **33**, 3069, 1987.

47 Cardi N., Po R., Giannotta G., Occhiello, E., Garbassi, F., Messina G., *J. Appl. Poly. Sci.,* **50**, 1501, 1993.

48 Douhi A., Fradet A., *J. Poly. Sci. Poly. Chem.,* **33**, 691, 1995.

49 Loontjens T., Belt W., Stanssens D., Weerts P., *Makromol. Chem., Makromol Symp.,* **75**, 211, 1993.

50 Inata H., Matsumura S., *J. Appl. Poly. Sci.,* **34**, 2609, 1987.

51 Ueda M., Kino K., Yamaki K., Imai Y., *J. Poly. Sci. Poly. Chem.,* **16**, 155, 1978.

52 Rasmussen J. K., Heilmann S. M., Krepski L. R., Smith H. K. II, Katritzky A. R., Sakizadeh K., *J. Poly. Sci. Poly. Chem.,* **24**, 2739, 1986.

53 Acevedo M., Fradet A., *J. Poly. Sci. Poly. Chem.,* **31**, 1579, 1993.

54 Douhi A., Fradet A., Judas D., European Patent *EP 581642A1*, assigned to Elf Atochem S.A., France, 2 Feb., 1994.

55 Collyer A. A., Ed., *Liquid Crystal Polymers: From Structures to Applications*, Elsevier Science Publications Ltd., London, 1992.

56 Carfagna C., Ed., *Liquid Crystalline Polymers*, Elsevier Science Publications Ltd., London, 1994.

57 Chapoy L. L., Ed., *Recent Advances in Liquid Crystalline Polymers*, Elsevier Applied Science Publishers, London, 1985.

58 Blumstein A., Ed., *Polymeric Liquid Crystals*, Plenum Press, New York, 1985.

59 Kohli A., Chung N., Weiss R. A., *Poly. Eng. Sci*., **29**, 573. 1989.

60 Blizard K. G., Baird D. G., *Poly. Eng. Sci.,* **27**, 653, 1987.

61 Min K., White J. L., Fellers J. F., *Poly. Eng. Sci.,* **24**, 1327, 1984.

62 Kiss G., *Poly. Eng. Sci*., **27**, 410, 1987.

63 Isayev A. I., Modic M., *Polymer Composites*, **8**, 158, 1987.

64 Blizard K. G., Federici C., Federico O., Chapoy L. L., *Poly. Eng. Sci*., **30**, 1442, 1990.

65 Xue, Y., Zhang J., Zheng X., He J., *J. Appl. Poly. Sci*., **89**, 1493, 2003.

66 Joseph E., Wilkes G. L., Baird D. G., *Polymer Preprints*, **25**(2), 94, 1984.

67 Amano M., Nakagawa K., *Polymer,* **28**, 263, 1987.

68 Brostow W., Dziemianowicz T. S., Romanski J., Werber W., *Poly. Eng. Sci*., **28**, 785, 1988.

69 Zhuang P., Kyu T., White J. L., *Poly. Eng. Sci*., **28**, 1095, 1988; Sukhadia A. M.,

Done D., Baird D. G., *Poly. Eng. Sci*., **30**, 519, 1990.

70 Weiss R. A., Huh W., Nicolais L., *Poly. Eng. Sci*., **27**, 684, 1987.

71 Kimura M., Porter R. S., *J. Poly. Sci. Poly. Phys*., **22**, 1697, 1984.

72 Blizard K. G., Baird D. G., *SPE ANTEC-86*, 44, 311, 1986.

73 Ramanathan R., Blizard K. G., Baird D. G., *SPE ANTEC-87,* **45**, 1399, 1987; Ramanathan R., Baird D. G., *Contemporary Topics in Polymer Science*, Vol. **6**, 73, 1989.

74 Cogswell F. N., Griffin B. P., Rose J. B., *European Patent EP 30417*, assigned to ICI, London, 17 June, 1981.

75 Nobile M. R., Acierno D., Incarnato L., Amendola E., Nicolais L., Carfagna C., *J. Appl. Poly. Sci*., **41**, 2723, 1990.

76 Liang Y. C., Isayev, A. I., *Poly. Eng. Sci.,* **42**, 994, 2002.

77 Lee B. L., *Poly. Eng. Sci*., **28**, 1107, 1988.

78 Son Y., Weiss R. A., *Poly. Eng. Sci.,* **41**, 329, 2001; **42**, 1322, 2002.

79 Isayev A. I., Viswanathan R., *Polymer*, **36**, 1585, 1995.

80 Viswanathan R., Isayev A. I., *J. Appl. Poly. Sci*., **55**, 1117, 1995.

81 Han M., Park J., Cheen S. W., Kim S. H., Kim W. N., *Poly. Bulletin,* **45**, 151, 2000.

82 Johnson, R. N., Farnham, A. G., U.S. Patent *US 4108837,* assigned to Union Carbide Corp., New York, 22 Aug., 1978.

83 Johnson R. N., Farnham A. G., Clendinning R. A., Hale W. F., Merriam C. N., *J. Poly. Sci., A-1* **5**, 2375, 1967.

84 Farnham A. G., Johnson R. N., U.S. Patent *US 3332909,* assigned to Union Carbide Corp., New York, 25 July, 1967.

85 Savariar S., U.S. Patent *US 5239043,* assigned to Amoco Corp., Chicago, 24 Aug., 1993.

86 Savariar S., U.S. Patent *US 5235019,* assigned to Amoco Corp., Chicago, 10 Aug., 1993.

87 Barr D. A., Rose J. B., UK Patent *GB 1153035*, assigned to ICI, London, 12 Sept., 1966; Jones M. E. B., U.S. Patent *US 4008203*, assigned to ICI, London, 15 Feb., 1977; Freeman J. L., U.S. Patent *US 4105635*, assigned to ICI, London, 28 June, 1977.

88 Rose J. B., *Chem. Ind*., 461, 1968; Vogel H. A., *J. Poly. Sci., A-1* **8**, 2035, 1970.

89 Rose J. B., *Polymer,* **15**, 465, 1974.

90 Percec V., Nava H., *J. Poly. Sci. Poly. Chem.,* **26**, 783, 1988.

91 Arzak A., Eguiazabal J. I., Nazabal J., *J. Appl. Poly. Sci*., **65**, 1503, 1997.

92 Jung H. C., Lee H. S., Chun Y. S., Kim S. B., Kim W. N., *Poly. Bull*., **41**, 387,

1998.

93 He J., Liu J., *J. Appl. Poly. Sci*., **67**, 2141 1998.

94 Li W., Jin X., Li G., Jiang B., *Eur. Poly. J.,* **30**, 325, 1994.

95 Hong S. M., Kim B. C., Kim K. U., Chung I. J., *Poly. J.,* **23**, 1347, 1991.

96 Golovoy A., Kozlowski M., Narkis M., *Poly. Eng. Sci.,* **32**, 854, 1992.

97 He J. S., Zhang H. Z., Yuan Q., Xie P., Zhang G. Y., Xu X. Q., *Prog. Nat. Sci.,* **4**, 373, 1994.

98 Shi F., *Int. J. Polym. Mater.,* **23,** 207, 1994.

99 Wang H., Yi X., Hinrichsen G., *Poly. J.,* **29**, 881, 1997.

100 Garcia M., Eguiazabal JI., Nazabal J., *Poly. Int.,* **53**, 272, 2004.

101 Xu J., Xian W., Zeng H., *Polym. Commun.,* **32**, 336, 1991.

102 Skovby M. H. B., Kops J., Weiss R. A., *Poly. Eng. Sci.,* **31**, 954, 1991.

103 Cohen-Addad S., Stein R. S., Esnault P., *Polymer*, **32**, 2319, 1991.

104 He J., Bu W., Zhang H., *Poly. Eng. Sci.,* **35**, 1695, 1995.

105 James S. G., Donald A. M., Miles I. S., Macdonald, W. A., *High Perform. Polym.,* **4**, 3, 1992.

106 Zheng J. Q., Kyu T., *Poly. Eng. Sci*., **32**, 1004, 1992.

107 Wiff D. R., Weinert R. J., *Polymer,* **39**, 5069, 1998.

108 Li G., Yin J., Li B., Zhuang G., Yang Y., Nicolais L., *Poly. Eng. Sci.,* **35**, 658, 1995.

109 Engberg K., Stromberg O., Martinsson J., Gedde U. W., *Poly. Eng. Sci.,* **34**, 1336, 1994**.**

110 He J., Bu W., *Polymer,* **35**, 5061, 1994.

111 Yang Y., Yin J., Li B., Zhuang G., Li G., *J. Appl. Poly. Sci.,* **52**, 1365, 1994.

112 Kim B. C., Hong S. M., *Mol. Cryst. Liq. Cryst. Sci. Technol*., *Sect. A,* **254**, 251, 1994.

113 Magagnini P. L., Paci M., La Mantia F. P., Surkova I. N., Vasnev V. A.*, J. Appl. Poly. Sci*., **55**, 461, 1995.

114 La Mantia F. P., Paci, M., Magagnini P. L., *Rheol. Acta*, **36**, 152, 1997.

115 Kulichikhin V. G., Vasil'eva, O. V., Litvinov I. A., Antipov E. M., Parsamyan I. L., Plate N. A., *J. Appl. Poly. Sci.,* **42**, 363, 1991.

116 Tanaka A., *Macromol. Chem*., **2**, 268, 1991; *Chemical Abstracts*, 116:60288.

117 Kulichikhin V., Plotnikova, E., Subbotin A., Plate N., *Rheol. Acta,* **40**, 49, 2001.

118 Machiels A. G. C., Busser R. J., Van Dam J., De Boer A. P., *Poly. Eng. Sci.,* **38**, 1536, 1998.

119 Machiels A. G. C., Van Dam J., De Boer A. P., Norder B., *Poly. Eng. Sci.,* **37**, 1512, 1997.

120 Yi X. S., Zhao G., Shi F., *Polym. Int*., **39**, 11, 1996.

121 Shi F., Yi X., *Int. J. Polym. Mater.,* **28**, 227, 1995; Yazaki F., Kohara R., Yosomiya R., *Poly. Eng. Sci.,* **34**, 1129, 1994.

122 Zhang Q., Xie G., Yan H., *Polym.-Plast. Tech. Eng.,* **42**, 311, 2003.

123 Pospiech D., Haubler L., Meyer E., Janke A., Vogel R., *J. Appl. Poly. Sci.,* **64**, 619, 1997.

124 Haubler L., Pospiech D., Eckstein K., Janke A., Vogel R., *J. Appl. Poly. Sci.,* **66**, 2293, 1997.

125 Yang H., Wu X., Li S., *Poly. Eng. Sci.,* **36**, 2781, 1996.

126 Kim B. C., Hong S. M., Hwang S. S., Kim K. U., *Poly. Eng. Sci.,* **36**, 574, 1996.

127 Yazaki F., Kohara A., Yosomiya R., *Poly. Eng. Sci.,* **34**, 1129**,** 1994**.**

128 Genvresse P., *Bull. Soc.Chim*. *Fr.,* **17**, 599, 1898.

129 Friedeland C., Crafts J. M., *Ann. Chem. Phys.,* **14**, 433, 1888.

130 Lenz R. W., Carrington W. K., *J. Poly. Sci*., **41**, 333, 1959.

131 Edmonds J. T. Jr., Hill H. W. Jr., *U.S. Patent US 3354129*, assigned to Phillips Petroleum Company, Delaware, 27 Nov., 1967.

132 Chance R. R., Shacklette L. W., Miller G. G., Ivory D. M., Sowa J. M., Elsenbaumer R. L., Baughman R. H., *J. Chem. Soc., Chem. Commun.,* **348**, 1980; Rabolt J. F., Clarke T. C., Kanazawa K. K., Reynolds J. R., Street G. B., *J. Chem. Soc., Chem. Commun.,* **347**, 1980; Frommer J. E., Elsenbaumer R. L., Eckhardt H., Chance R. R., *J. Poly. Sci. Poly. Letts.,* **21**, 39, 1983.

133 Hawkins R. T., *Macromolecules*, **9**, 189, 1976.

134 Seymour R. S., Krishenbaum G. S., Eds.,*"High Performance Polymers: Their Origin and Development*", Elsevier Science Publishers, Amsterdam, 1986.

135 Akhtar S., White J. L., *J. Appl. Poly. Sci*., **31**, 84, 1991.

136 Ravindranath K., Jog J. P., *J. Appl. Poly. Sci.*, **49**, 1395, 1993.

137 Jog J. P., Shingankuli V. L., Nadkarni V. M., *Polymer,* **34**, 1966, 1993.

138 Nadkarni V. M., Shingankuli V. L., Jog J. P., *Int. Polym. Process*, **2**, 55, 1987.

139 Radhakrishnan S., Joshi S. G., *Eur. Poly. J*., **23**, 819, 1987.

140 Nadkarni V. M., Jog J. P., *J. Appl. Poly. Sci*., **32**, 5817, 1986.

141 Baird D. G., Sun T., Done D. S., Ramanathan R., *Polymer Preprints, **30(2)**, 546, 1989.*

142 Stupp S. I., Wu J., *Polym. Mater. Sci. Eng.,* **58**, 714, 1988.

143 Ramanathan R., Blizard K., Baird D. G., *SPE ANTEC*, **45**, 1399, 1987.

144 Subramaniam P. R., Isayev A. I., *Polymer*, **32**, 1961, 1991.

145 Seppala J., Heino M., Kapanen C., *J. Appl. Poly. Sci*., **44**, 1051, 1992.

146 Heino M. T., Seppala J. V., *J. Appl. Poly. Sci*., **44**, 2185, 1992.

147 Shonaike G. O., Hamada H., Yamaguchi S., Nakamichi M., Makawa Z., *J. Appl. Poly. Sci*., **54**, 881, 1994.

148 Shonaike G. O., Yamaguchi S., Ohta M., Hamada H., Maekawa Z., Nakamichi M., Kosaka W., *Eur. Poly. J.,* **30**, 413, 1994.

149 Hong S. M., Kim B. C., Kim K. U., Chung. I. J., *Poly. J.*, **24**, 727, 1992.

150 Minkova L. I., Paci M., Pracella M., Magagnini P., *Poly. Eng. Sci*., **32**, 57, 1992.

151 Minkova L. I., Magagnini P. L., *Polymer*, **36**, 2059, 1995.

152 Shonaike G. O., Yamaguchi S., Ohta M., Hamada H., Maekawa Z., Nakamichi M., Kosaka W., Toi K., *Poly. Eng. Sci*., **35**, 240, 1995.

153 Gabellini G., De Moraes M. B., Bretas R. E. S., *J. Appl. Poly. Sci*., **60**, 21, 1996.

154 Ruiz De Gauna B. E., Gaztelumendi M., Nazabal J., *Polymer Composites*, **21**, 72, 2000.

155 Gomes M., Scuccuglia M., Bretas R. E. S., *J. Mater. Sci.,* **34**, 1407, 1999.

156 Kestenbach H. J., Rogausch K. D., *Materials Research,* **6**, 75, 2003.

157 Lopez L. C., Wilkes G. L., *Polymer*, **29**, 106, 1988.

158 Desio G. P., Rebenfeld L., *J. Appl. Poly. Sci.,* **39**, 39, 1990.

159 Song S. S., White J. L., Cakmak M., *Poly. Eng. Sci*., **30**, 944, 1990.

160 Jog J. P., Nadkarni V. M., *J. Appl. Poly. Sci*., **30**, 997, 1985.

161 Gabellini G., Bretas R. E. S., *J. Appl. Poly. Sci.,* **61**, 1803, 1996.

162 Han M., Kim W. N., Giles D. W., *Poly. Eng. Sci.,* **41**, 1506, 2001.

163 Shonaike G. O., Hamada H., Maekawa, Z., Yamaguchi S., Toi K., *J. Macromol. Sci., Phys.,* **B34**, 177, 1995.

164 Shonaike G. O., Hamada H., Maekawa Z., Yamaguchi, S., Nakamichi M., Kosaka W., *J. Mater. Sci.,* **30**, 473, 1995.

165 Fukuoka T., Kamisaka T., Japanese Patent, *JP 1074265*, assigned to Sekisui Chemical Co. Ltd., Japan, 20 March, 1989.

166 Tsuruta A., Kawaguchi H., Ishikawa T., Kondo Y., European Patent *EP 321236*, assigned to Tosoh Corp., Japan, 21 June, 1989.

167 Ferdinand U., Ludwig B., German Patent *DE 3813919*, assigned to Siemens AG, Germany, 2 Nov., 1989.

168 Kayaba K., Okamoto M., Inoue S., Japanese Patent *JP 1292058*, assigned to Toray Industries Inc., Japan, 24 Nov., 1989.

169 Umezawa M., Kodera Y., Japanese Patent *JP 3021639*, assigned to Toray Industries Inc., Japan, 30 Jan., 1991.

170 Okamoto M., Inoue S., Japanese Patent *JP 2206644*, assigned to Toray Industries Inc., Japan, 16 Aug., 1990.

171 Yamanaka T., Okamoto M., Inoue S., Japanese Patent *JP 3095261*, assigned to Toray Industries Inc., Japan, 19 April, 1991.

172 Yamanaka T., Inoue S., Tsunashima K., Okamoto T., Japanese Patent *JP 3047861*, assigned to Toray Industries Inc., Japan, 28 Feb., 1991.

173 Okamoto M., Ichikawa Y., Inoue S., Yamanaka T., Japanese Patent *JP 3179051*, assigned to Toray Industries Inc., Japan, 5 Aug., 1991.

174 Yamanaka T., Okamoto M., Inoue S., Japanese Patent *JP 4225054*, assigned to Toray Industries Inc., Japan, 14 Aug., 1992.

175 Chen P., Sullivan V., Dolce T., Jaffe M., US Patent *US 5182334*, assigned to Hoechst Celanese, Somerville, NJ, April 3, 1991.

176 Yamada S., Japanese Patent *JP 5112716*, assigned to Tosoh Corp., Japan, 7 May, 1993.

177 Akiyama F., Watanabe A., Yamanaka T., Japanese Patent *JP 5086266*, assigned to Toray Industries Inc., Japan, 6 April, 1993.

178 Okamoto M., Kitajima N., Inoue S., Japanese Patent *JP 4311758*, assigned to Toray Industries Inc., Japan, 4 Nov., 1992.

179 Kim K. U., Kim B. C., Hong S. M., US Patent *US 5276107*, assigned to Korea Institute Science and Technology, 1 April, 1994.

180 Giannelis E. P., Krishnamoorti R., Manias E., *Adv. Poly. Sci.,* **138**, 107, 1999.

181 Giannelis E. P., *Adv. Mater.,* **8,** 29, 1996.

182 LeBaron P. C., Wang Z., Pinnavaia T. J., *Appl. Clay Sci.,* **15,** 11, 1999.

183 Garces J. M., Moll D. J., Bicerano J., Fibiger, R., McLeod, D. G., *Adv. Mater.,* **12,** 1835, 2000.

184 Dietsche F., Thomann, Y., Thomann R., Mulhaupt R., *J. Appl. Poly. Sci.,* **75**, 396, 2000.

185 Yano K., Usuki A., Okada, A., Kurauchi T., Kamigaito O., *J. Poly. Sci. Poly. Chem.,* **31**, 2493, 1993.

186 Yano K., Usuki A., Okada A., *J. Poly. Sci. Poly. Chem.,* **35**, 2289, 1997.

187 Blumstein A., *J. Poly. Sci., A,* **3**, 2653, 1965.

188 Friedlander H. Z., Frink C. R., *J. Poly. Sci. B,* **2**, 475, 1964.

189 Solomon D. H., Loft B. C., *J. Appl. Poly. Sci.,* **12**, 1253, 1968.

190 Ma J., Qi Z., Hu Y., *J. Appl. Poly. Sci.,* **82**, 3611, 2001.

191 Ke Y., Long C., Qi Z., *J. Appl. Poly. Sci.,* **71**, 1139, 1999.

192 Burnside S. D., Giannelis E. P., *Chem. Mater.,* **7**, 1597, 1995.

193 Lemmon J. P., Wu J., Lerner M. M., in Mark J. E., Lee C. C-Y., Bianconi P. A., Eds., *Hybrid Organic-Inorganic Composites,* ACS Symposium Series, 585, ACS, Washington D.C., 1995.

194 Seckin T., Gultek A., Onal Y., Yatinci E., Aksoy I., *J. Mater. Chem.,* **7**, 265, 1997.

195 Ellsworth M. W., Novak B. M., *J. Am. Chem. Soc.,* **113**, 2756, 1991.

196 Huang Z. H., Qiu K. Y., *Polymer,* **38**, 521, 1997.

197 Yang F., Ou Y., Yu Z., *J. Appl. Poly. Sci.,* **69**, 355, 1998.

198 Kojima Y., Usuki A., Kawasumi M., Okada A., Kurauchi T., Kamigaito O., *J. Poly. Sci. Poly. Chem.,* **31,** 1755, 1993.

199 Huang X., Lewis S., Brittain, W. J., Vaia, R. A., *Macromolecules,* **33**, 2000, 2000.

200 Usuki A., Kojima Y., Kawasumi M., Okada A., Fukushima Y., Kurauchi T., Kamigaito O., *J. Mater. Res.,* **8**, 1179, 1993.

201 Messersmith, P. B.; Giannelis, E. P., *Chem. Mater.,* **5,** 1064, 1993.

202 Huang X., Lewis, S., Brittain W. J., Vaia R. A., *Polymer Preprints,* **41**(1), 589, 2000.

203 Lan T., Pinnavaia T. J., *Chem. Mater.,* **6**, 2216, 1994.

204 Kornmann X., Lindberg H., Berglund L. A., *Polymer,* **42**, 4493, 2001; Chin I. J., Thurn-Albrecht T., Kim H. C., Russel T. P., Wang J., *Polymer,* **42**, 5947, 2001; Becker O., Varley R., Simon G., *Polymer,* **43**, 4365, 2002.

205 Lan T., Kaviratna P. D., Pinnavaia T. J., *Polym. Mater. Sci. Eng.,* **71**, 527, 1994.

206 Lan T., Wang Z., Shi H., Pinnavaia T. J., *Polym. Mater. Sci. Eng.,* **73**, 296, 1995.

207 Heinemann J., Reichert P., Thomann R., Mulhaupt R., *Macromol. Rapid Commun.,* **20**, 423, 1999.

208 Tudor J., Willington L., O'Hare D., Royan B., *Chem. Commun.,* **17**, 2031, 1996.

209 Rong J., Li, H.; Jing Z., Hong X., Sheng M., *J. Appl. Poly. Sci.,* **82**, 1829, 2001.

210 Weiss K., Wirth-Pfeifer C., Hofmann M., Botzenhardt S., Lang H., Bruning K., Meichel E., *J. Mol. Cat. A: Chemical,* **182**, 143, 2002.

211 Usuki A., Kawasumi M., Kojima Y., Okada A., Kurauchi T., Kamigaito O., *J. Mater. Res.,* **8**, 1174, 1993.

212 Kojima Y., Usuki A., Kawasumi M., Okada A., Kurauchi T., Kamigaito O., *J. Poly. Sci. Poly. Chem.,* **31**, 983, 1993.

213 Jimenez G., Ogata N., Kawai H., Ogihara T., *J. Appl. Poly. Sci.,* **64**, 2211, 1997.

214 Ogata N., Kawakage S., Ogihara T., *Polymer,* **38**, 5115, 1997.

215 Ogata N., Jimenez G., Kawai H., Ogihara T., *J. Poly. Sci. Poly. Phys.,* **35**, 389,

1997.

216 Tseng C. R., Wu J. Y., Lee H. Y., Chang F. C., *Polymer,* **42**, 10063, 2001.

217 Tabtiang A., Lumlong S., Venables R. A., *Polym.-Plast. Technol. Eng.,* **39**, 293, 2000.

218 Jeon H. G., Jung H. T., Lee S. W., Hudson S. D., *Poly. Bull.,* **41**, 107, 1998.

219 Liu C., Tang T., Zhao Z., Huang B., *J. Poly. Sci. Poly. Chem.,* **40**, 1892, 2002.

220 Weimer M. W., Chen H., Giannelis E. P., Sogah, D. Y., *J. Am. Chem. Soc.,* **121**, 1615, 1999.

221 Jin Y. H., Park H. J., Im S. S., Kwak S. Y., Kwak S., *Macromol. Rapid Commun.,* **23**, 135, 2002.

222 Rong J., Jing Z., Li H., Sheng M., *Macromol. Rapid Commun.,* **22**, 329, 2001.

223 Bergman J. S., Chen H., Giannelis E. P., Thomas M. G., Coates, G. W., *Chem. Commun.,* **21**, 2179, 1999.

224 Giannelis E. P., *Applied Organometallic Chemistry,* 12, 675 1999.

225 Vaia R. A., Jandt K. D., Kramer E. J., Giannelis E. P., *Chem. Mater.,* **8**, 2628, 1996.

226 Vaia R. A., Jandt K. D., Kramer E. J., Giannelis E. P., *Macromolecules,* **28**, 8080, 1995.

227 Vaia R. A., Vasudevan S., Krawiec W., Scanlon L. G., Giannelis E. P., *Adv. Mater.,* **7**, 154, 1995.

228 Cho J. W., Paul D. R., *Polymer,* **42**, 1083, 2000.

229 Fornes T. D., Yoon P. J., Keskkula H., Paul D. R., *Polymer,* **42**, 9929, 2001.

230 Fornes T. D., Yoon P. J., Paul D. R., *Polym. Mater. Sci. Eng.,* **87**, 104, 2002; *Chemical Abstracts,* 137:248338.

231 Dennis H. R., Hunter D. L., Chang D., Kim S., White J. L., Cho J. W., Paul D. R., *Polymer,* **42**, 9513, 2001.

232 Huang X., Brittain W. J., *Macromolecules,* **34**, 3255, 2001.

233 Koo C. M., Ham H. T., Kim S. O., Wang K. H., Chung I. J., Kim D. C., Zin W. C., *Macromolecules,* **35**, 5116, 2002.

234 Kawasumi M., Hasegawa N., Kato M., Usuki A., Okada A., *Macromolecules*, **30**, 6333, 1997.

235 Kurokawa Y., Yasuda H., Oya A. J., *Mater. Sci. Lett.,* **15**, 1481, 1996.

236 Di Y., Iannace S., Di Maio E., Nicolais L., *J. Poly. Sci. Poly. Phy.,* **41**, 670, 2003.

237 Lepoittevin B., Devalckenaere M., Pantoustier N., Alexandre M., Kubies D., Calberg C., Jerome R., Dubois P., *Polymer,* **43**, 4017, 2002.

238 Chisholm B. J., Moore R. B., Barber G., Khouri F., Hempstead A., Larsen M.,

Olson E., Kelley J., Balch G., Caraher J., *Macromolecules,* **35**, 5508, 2002.

239 Artzi N., Nir Y., Wang D., Narkis M., Siegmann A., *Polym. Comp.,* **22**, 710, 2001.

240 Wu J., Lerner M. M., *Chem. Mater.,* **5**, 835, 1993.

241 Huang X., Brittain W. J., *Polymer Preprints,* **41**(1), 521, 2000.

242 Choi Y. S., Choi M. H., Wang K. H., Kim S. O., Kim Y. K., Chung I. J., *Macromolecules,* **34**, 8978, 2001.

243 Zeng C., Lee L. J., *Macromolecules,* **34**, 4098, 2001.

244 Wang D., Zhu J., Yao Q., Wilkie C. A., *Chem. Mat.,* **14**, 3837, 2002.

245 Lincoln D. M., Vaia R. A., Wang Z. G., Hsiao B. S., Krishnamoorti R., *Polymer,* **42**, 9975, 2001.

246 Lincoln D. M., Vaia R. A., Wang Z. G., Hsiao B. S., *Polymer,* **42**, 1621, 2001.

247 Vaia R. A., Lincoln D., Wang Z. G., Hsiao B. S., *Polym. Mater. Sci. Eng.,* **82**, 257, 2000; *Chemical Abstracts,* 132:309335.

248 Liu X., Wu Q., Berglund L. A., *Polymer,* **43**, 4967, 2002.

249 Liu X., Wu Q., *Macromol. Mater. Eng.,* **287**, 180, 2002.

250 Liu X., Wu Q., *Eur. Poly. J.,* **38**, 1383, 2002.

251 Kojima Y., Matsuoka T., Takahashi H., Kurauchi T., *J. Mater. Sci. Lett.,* **12**, 1714, 1993.

252 Tseng C. R., Lee H. Y., Chang F. C., *J. Poly. Sci. Poly. Phy.,* **39**, 2097, 2001.

253 Vaia R. A., Teukolsky R. K., Giannelis E. P., *Chem. Mater.,* **6**, 1017, 1994.

254 Usuki A., Kojima Y., Kawasumi M., Okada A., Kurauchi T., Kamigaito O., *Polymer Preprints,* **31**(2), 651, 1990.

255 Krishnamoorti R., Vaia R. A., Giannelis E. P., *Chem. Mater.,* **8**, 1728, 1996.

256 VanderHart D. L., Asano A., Gilman J. W., *Chem. Mater.,* **13**, 3796, 2001.

257 Lan T., Kaviratna P. D., Pinnavaia T. J., *Chem. Mater.,* **7**, 2144, 1995.

258 Worley D. C., Akkapeddi M. K., Socci E. P., "*Deformation and Orientation of Polyamide 6 Nanocomposite*", ANTEC 2001 Conference Proceedings, p. 5.

259 Kojima Y., Usuki A., Kawasumi M., Okada A., Kurauchi T., Kamigaito O., Kaji K., *J. Poly. Sci. Poly. Phys.,* **32**, 625, 1994.

260 Varlot K., Reynaud E., Kloppfer M. H., Vigier G., Varlet J**.,** *J. Poly. Sci. Poly. Phy.,* **39,** 1360, 2001.

261 Merkel T. C., Freeman B. D., Spontak R. J., He. Z., Pinnau I., Meakin P., Hill A. J., *Science,* **296**(5567), 519, 2002.

262 Dagani R., *Chem. Eng. News,* **77**(23), 25, 1999.

263 DeGaspari J., *Prospecting Paydirt*, Mechanical Engineering, 2001;

http://www.memagazine.org/ backissues/april01/features/prospect/prospect.html
264 Vaia R. A., Giannelis E. P., *Macromolecules,* **30**, 7990, 1997.
265 Vaia R. A., Giannelis E. P., *Macromolecules,* **30**, 8000, 1997.
266 Ginzburg V. V., Balazs A. C., *Macromolecules,* **32**, 5681, 1999.
267 Balazs A. C., Singh C., Zhulina E., Lyatskaya Y., *Acc. Chem. Res.,* **32**, 651, 1999.
268 Lyatskaya Y., Balazs A. C., *Macromolecules,* **31**, 6676, 1998.

CHAPTER-2

Poly(ethylene terephthalate-co-oxybenzoate)-block-poly(phenylene sulphide) and polysulphone

Rajkumar Patel

Chapter 2. Poly(ethylene terephthalate-co-oxybenzoate)-*block*-poly(phenylene sulphide) and polysulphone

Abstract

In this chapter the syntheses of telechelic dicarboxyl terminated poly(phenylene sulphide), polysulphone and poly(ethylene terephthalate-co-oxybenzoate) are reported. 2,2'-Bis(2-oxazoline), a chain coupler, was synthesised and characterised. poly(phenylene sulphide)-block-poly(ethylene terephthalate-co-oxybenzoate) (BCP-1) was synthesised by coupling dicarboxyl terminated poly(phenylene sulphide) and dicarboxyl terminated poly(ethylene terephthalate-co-oxybenzoate) with 2,2'-bis(2-oxazoline). This block copolymer was used as a compatibiliser for compatibilisation of PPS/TLCP blend system. Similarly, polysulphone-block-poly(ethylene terephthalate-co-oxybenzoate) (BCP-2) was synthesised by coupling dicarboxyl terminated polysulphone and dicarboxyl terminated poly(ethylene terephthalate-co-oxybenzoate) with 2,2'-bis(2-oxazoline). This block copolymer was used as a compatibiliser for compatibilisation of PSU/TLCP blend system.

2.1. Introduction

Block copolymers can be synthesised by coupling two telechelic homopolymers either with or without chain coupling agents. Daccord and Sillion[1] reported the synthesis of block copolymer of poly(phenylene sulphide) (PPS). Heitz et. al[2,3] reported block copolymer of carboxyl terminated telechelic PPS with polyamides and polyester. Pospiech et. al[4] prepared copolymer of polysulphone (PSU) and thermotropic liquid crystalline polymer by transesterification. Gopakumar et. al[5] studied block copolymer of PPS and thermotropic liquid crystalline polymer (TLCP).

Douhi et. al[6] synthesised bisoxazoline thereby using it as coupling agent to couple functionalised homopolymer to synthesise different block copolymers. It has several advantages over normal polycondensation reaction. Here, block copolymer can be made with small quantity

of coupling agents, at lower temperature and short duration of time without the worry of side product formation due to other inter-chain transfer reactions.

In this chapter synthesis and physico-chemical characterisation of two block copolymers is described. These are: (i) copolymer of dicarboxyl terminated poly(phenylene sulphide) (DCTPPS) and dicarboxyl terminated poly(ethylene terephthalate-co-oxybenzoate) DCTPET/OB and (ii) copolymer of dicarboxyl terminated polysulphone (DCTPSU) and DCTPET/OB. Thermal properties as well as crystallisation were studied using differential scanning calorimetry (DSC). The chain coupler used was 2,2'-bis(2-oxazoline).

2.2. Experimental

2.2.1. Materials and synthesis

Sodium sulphide, 1,4-dichlorobenzene, ethanolamine, diethyl oxalate, acetic anhydride, zinc acetate, sodium carbonate, terephthalic acid, 2,2'-bis(4-hydroxyphenyl) propane (bisphenol-A (BPA)), 4-hydroxy benzoic acid (HBA), dimethylsulphoxide (DMSO) and toluene were procured from SD Fine Chemicals, India. 4-Chlorobenzoic acid and N-methyl-2-pyrrolidone (NMP) were obtained from Thomas Baker Chemicals, India. 4,4'-Dichlorodiphenyl sulphone (DCDPS) was procured from Fluka, Germany.

Dicarboxyl terminated poly(ethylene terephthalate-co-oxybenzoate) (DCTPET-OB), an aliphatic-aromatic thermotropic liquid crystalline polymer (TLCP), with 30, 45 and 60 mole percent oxybenzoate were synthesised as described in Section 2.2.1.1. Dicarboxyl terminated poly(phenylene sulphide) (DCTPPS) of varying chain length (n≈6, 9 and 12), dicarboxyl terminated polysulphone (DCTPSU) with chain lengths (n≈4, 6 and 8) and 2,2'-bis(2-oxazoline), a chain coupling agent were synthesised as described in Sections 2.2.1.2, 2.2.1.3 and 2.2.1.4. Block copolymers of: (i) DCTPET-OB and DCTPPS as well as (ii) DCTPET-OB and DCTPSU (equimolar %) were synthesised by polyaddition reaction for 20 minutes with equimolar amount

of 2,2'-bis(2-oxazoline) at 300^{o}C under nitrogen atmosphere, as described in Sections 2.2.1.5 and 2.2.1.6.

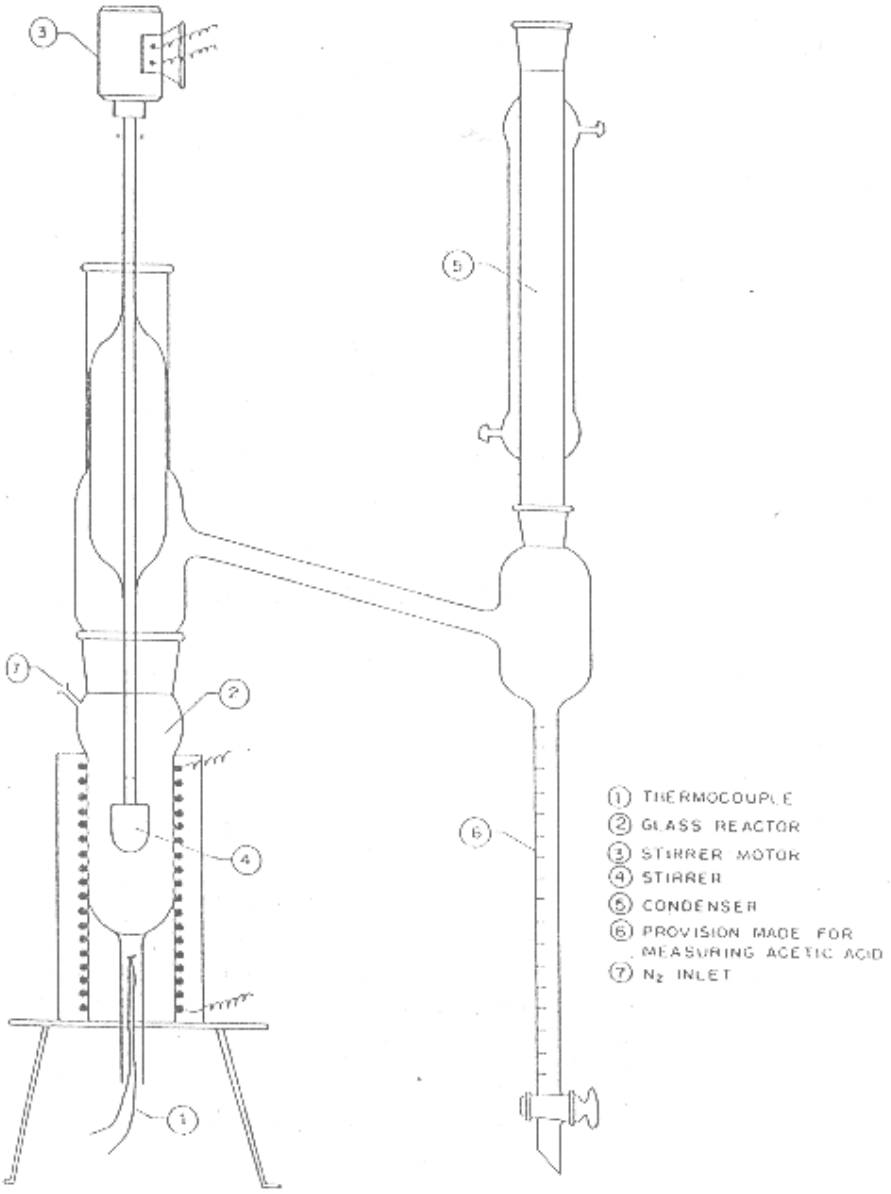

Figure 2.1: Laboratory scale reaction set-up for the synthesis of poly(phenylene sulphide)-*block*-poly(ethylene terephthalate-co-oxybenzoate)

2.2.1.1. Dicarboxyl terminated poly(ethylene terephthalate-co-oxybenzoate)

Virgin fibre grade poly(ethylene terephthalate) (PET) of intrinsic viscosity 0.60 dL/g (M/S Century Enka Pvt. Ltd., Pune, India) was used as received. 4-Acetoxy benzoic acid (ABA)

was synthesised by dissolving 138.2 g 4-hydroxy benzoic acid in 2 L cold alkaline solution prepared by dissolution 60 g sodium hydroxide (Figure 2.1). Acetic anhydride (150 mL) was added drop-wise to the solution under constant stirring. A white precipitate was formed. 2 N hydrochloric acid was added to acidify the precipitate. Subsequently, the precipitate was washed with distilled water to free it from the acid. The precipitate was boiled in distilled water and filtered to remove any sodium salt. It was recrystallised from distilled methanol and dried in vacuum oven at 70^{o}C.

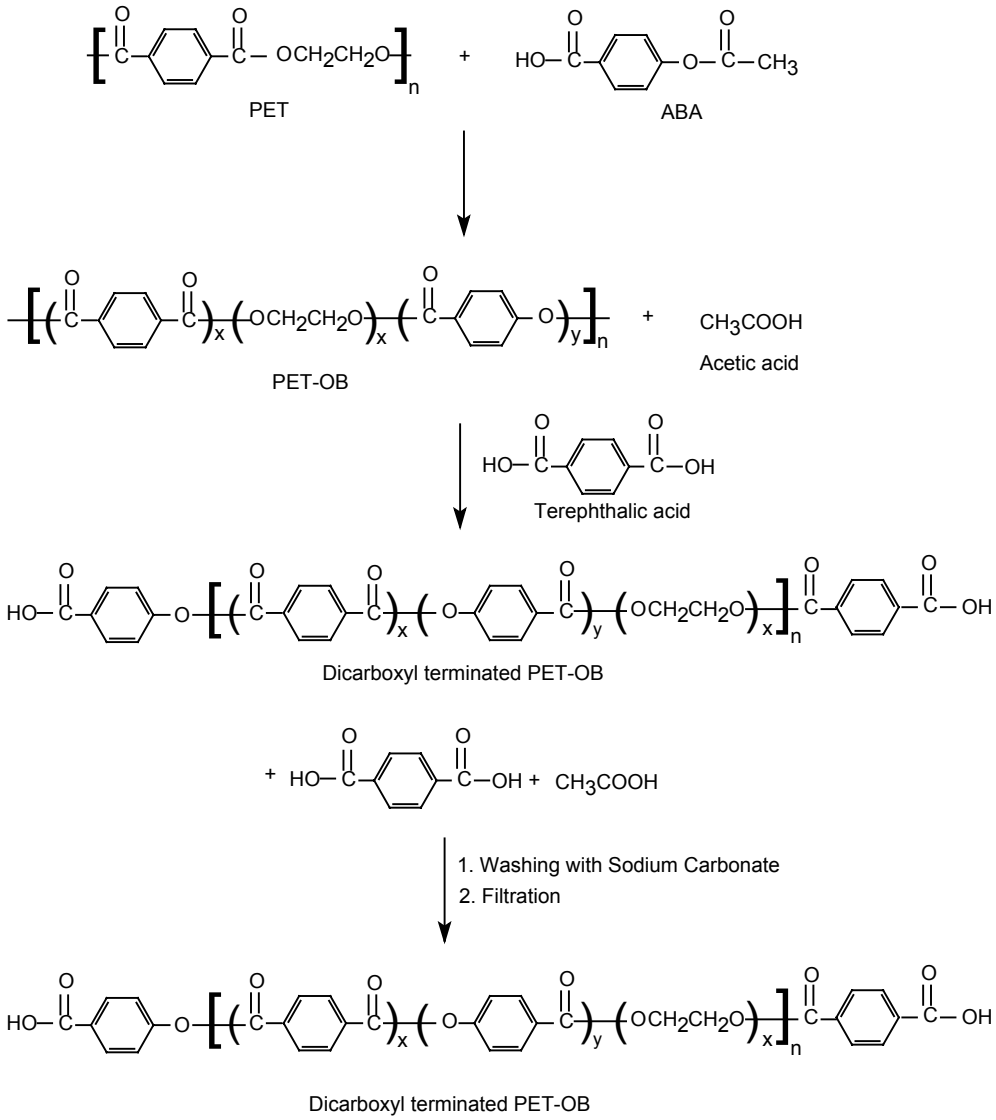

Scheme 2.1: Synthesis of dicarboxyl terminated poly(ethylene terephthalate-co-oxybenzoate) (DCTPET-OB)

Thermotropic liquid crystalline poly(ethylene terephthalate-co-oxybenzoate) PET/OB was synthesised from PET, 4-acetoxy benzoic acid (ABA) and zinc acetate as catalyst. Three random copolymers of PET:OB molar ratio 70:30, 55:45 and 40:60 were synthesised. A 500 mL of glass lined electrically heated reactor was charged with PET, ABA and zinc acetate (1 mol % of ABA) and stirred at 275^{o}C under nitrogen atmosphere for 45 minutes. Acetic acid generated in the reaction was collected in the side arm. Vacuum was applied to remove final traces of acetic acid. Terephthalic acid (TPA) was added to the reaction mixture and stirred for further 20 minutes to obtain dicarboxyl terminated PET-OB, as shown in *Scheme 2.1.*

Mole ratio of PET-OB:TPA was 1:1 and 1:2 as shown in Table 2.1. The product was washed with 5 % sodium carbonate solution to remove unreacted terephthalic acid (TPA).

Table 2.1: Synthesis of dicarboxyl terminated poly(ethylene terephthalate-co-oxybenzoate)

DCTPET-OB	PET-OB: TPA	PET	4-Acetoxy benzoic acid	Terephthalic acid
		g	g	g
DCTPET/OB (70/30)	1:1	46.54	18.70	34.73
DCTPET/OB (70/30)	1:2	34.52	13.87	51.57
DCTPET/OB (55/45)	1:1	46.54	18.70	34.73
DCTPET/OB (55/45)	1:2	34.52	13.87	51.57
DCTPET/OB (40/60)	1:1	46.54	18.70	34.73
DCTPET/OB (40/60)	1:2	34.52	13.87	51.57

*PET-OB=poly(ethylene terephthalate-co-oxybenzoate; PET=poly(ethylene terephthalate); 4-ABA=4-acetoxy-benzoic acid**;** DCTPET/OB (70/30)=dicarboxyl terminated poly(ethylene terephthalate-co-oxybenzoate) with PET=70 mol% and OB=30 mol%.*

2.2.1.2. Dicarboxyl terminated poly(phenylene sulphide) (DCTPPS)

DCTPPS of varied statistically average degree of polymerisation were synthesised by reacting 4-chloro benzoic acid, 1,4-dichloro benzene and sodium sulphide (Na_2S) in N-methyl-2-pyrrolidone (NMP) at 230^{o}C in a Parr reactor,[2,3] as shown in *Scheme 2.2.*

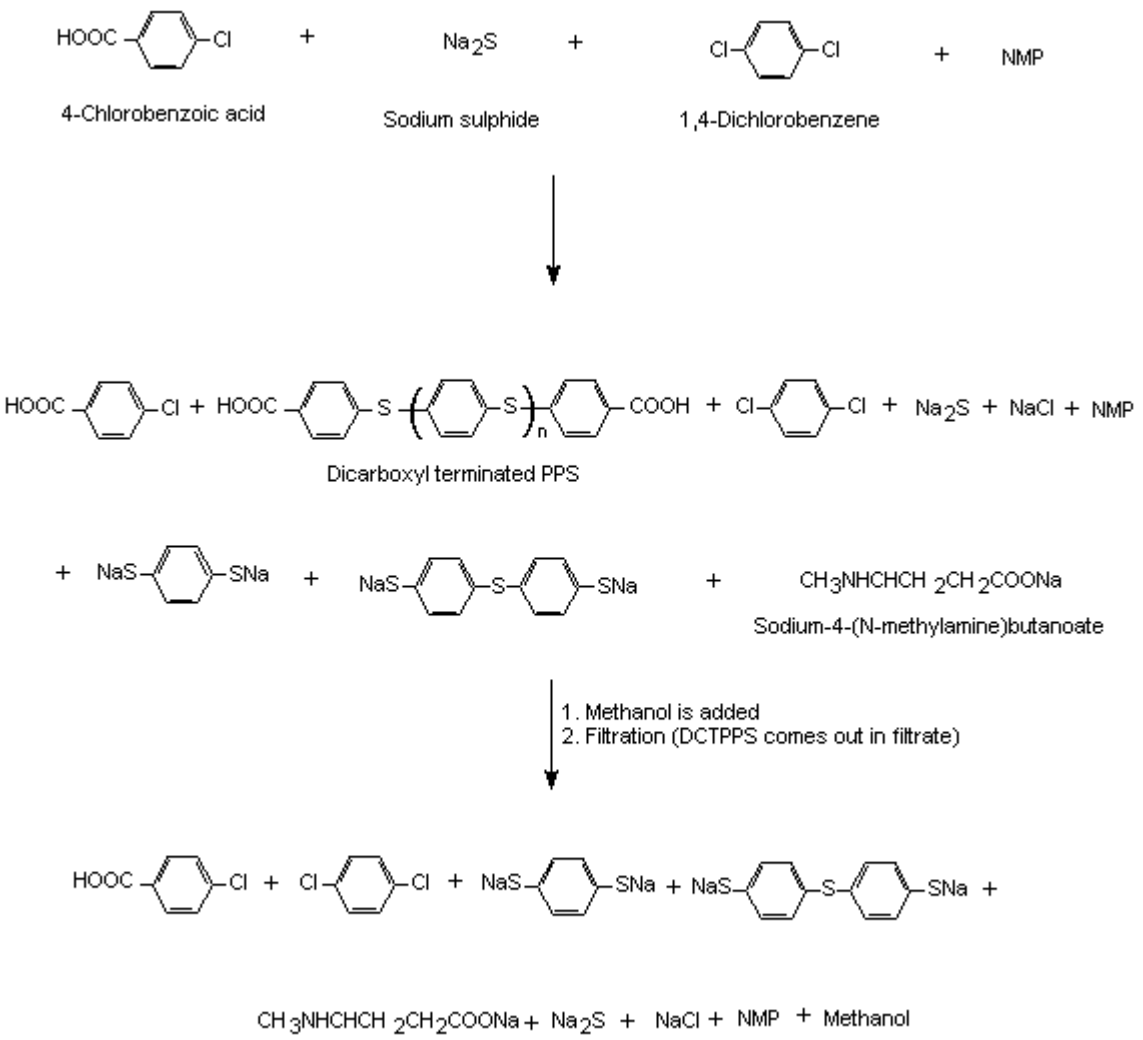

Scheme 2.2: Synthesis of dicarboxyl terminated poly(phenylene sulphide)

The mole ratio of 4-chloro benzoic acid:1,4-dichloro benzene was varied to prepare dicarboxyl terminated PPS telechelics of varied chain length (n≈6, 9, 12), as presented in Table 2.2.

Table 2.2: Synthesis of DCTPPS of different chain length (n ≈ 6, 9 and 12)

DCTPPS	4-chlorobenzoic acid mole ratio	1,4-dichlorobenzene mole ratio	sodium sulphide mole ratio
DCTPPS-6	2	6	7
DCTPPS-9	2	9	10
DCTPPS-12	2	12	13

2.2.1.3. Dicarboxyl terminated polysulphone

Dicarboxyl terminated polysulphone (DCTPSU) of different chain length (n ≈ 4, 6 and 8) were synthesised by reaction of 4,4'-dichlorodiphenyl sulphone with 2,2'-bis(4-hydroxyphenyl) propane and 4-hydroxy benzoic acid (Scheme 2.3). The reaction was carried out in a mixture of dimethyl sulphoxide (DMSO), a dipolar aprotic solvent, and toluene to remove the water formed during the reaction by azeotropic distillation. Potassium carbonate was dried and used as a base to generate phenoxide ion of BPA and HBA *in situ* that later on reacted with DCDPS at higher temperature. Compositions are presented in Table *2.3*.

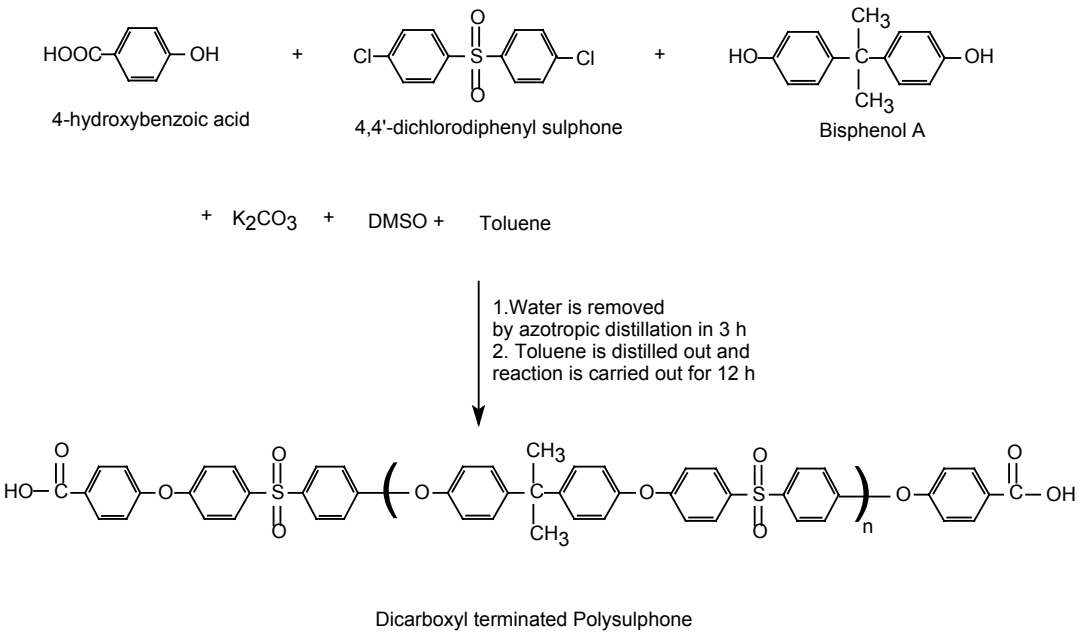

Scheme 2.3: Synthesis of dicarboxyl terminated polysulphone

Table 2.3: Synthesis of dicarboxyl terminated polysulphone

Polysulphone	HBA	Bisphenol A	DCDPS	Potassium Carbonate	DMSO/ Toluene	Reaction time
	mol	mol	mol	g	mL	h
DCTPSU-4	0.015	0.0225	0.03	12	100/50	15
DCTPSU-6	0.010	0.025	0.03	12	100/50	15
DCTPSU-8	0.0075	0.0262	0.03	12	100/50	15

The reaction mixture was refluxed with stirring at 160^{o}C under the nitrogen flow until all water formed in the reaction was removed completely by azeotropic distillation (three hours). Toluene was removed by distillation and the reaction was continued for twelve hours at 175^{o}C, as in S*cheme 2.3*. After cooling, the inorganic salt was filtered off and filtrate was poured into water. It was acidified to pH 4 by adding 5% hydrochloric acid. White precipitate formed was filtered and washed repeatedly with water. The product was dried dissolved in chloroform and precipitated into ethanol.

2.2.1.4. 2,2'-Bis(2-oxazoline)

2,2-Bis(2-oxazoline) was synthesised in three steps. In first step a solution of ethanolamine (48.8 g; 0.8 mol) in 200 mL absolute ethanol was slowly dropped into a stirred solution of diethyl oxalate (58.4 g; 0.4 mol) in 200 mL absolute ethanol. An exothermic reaction occurred and N,N'-bis(2-hydroxyethyl)oxamide (A) precipitated. Absolute ethanol (1 L) was added, the mixture was heated to reflux until complete dissolution and cooled to room temperature. White crystals of N,N'-bis(2-hydroxyethyl)oxamide formed were filtered, washed with cold ethanol and dried under vacuum. Melting point noted was 171.3^{o}C (lit. 168^{o}C).

In second step a stirred mixture of N,N'-bis(2-hydroxyethyl)oxamide (20 g; 0.1 mol), thionyl chloride (20 mL; 0.24 mol) and 100 mL dry toluene was heated to 60^{o}C for 30 minutes, raised to 100^{o}C and maintained for 90 minutes. N,N'-Bis(2-hydroxyethyl)oxamide did not dissolve but the medium turned into a thick paste. After cooling the product, N,N'-bis(2-chloroethyl)oxamide (B), was filtered, washed sequentially with ethanol, water and ethanol. It was dried in vacuum oven at 60^{o}C. Melting point noted was 204.5^{o}C (lit. 203^{o}C).

In the third step, a solution of N,N'-bis(2-chloroethyl)oxamide (5 g; 0.0235 mol) in 47 mL 1 N potassium hydroxide/methanol was heated to reflux for 1 h. After cooling potassium chloride was filtered off and the filtrate was evaporated to dryness. A white product formed,

2,2'-bis(2-oxazoline), was dried under vacuum at 60°C. Melting point noted was 214.8°C (lit. 213°C).[6]

2.2.1.5. Poly(phenylene sulphide)-*block*-poly(ethylene terephthalate-co-oxybenzoate)

Dicarboxyl terminated poly(phenylene sulphide) (DCTPPS) of statistically averaged chain length 12 was taken in a glass reactor. dicarboxyl terminated poly(ethylene terephthalate-co-oxybenzoate) (DCTPET-OB) (55/45) (M_n = 1760 g/mol) was chosen as the liquid crystalline segment. DCTPPS and DCTPET-OB (55/45) were mixed in 1:1 mole ratio in the glass reactor and the temperature was raised to 300°C. Equimolar concentration of 2,2'-bis(2-oxazoline) was added and stirred at 200 rpm under nitrogen atmosphere. Block copolymer formed, poly(phenylene sulphide)-*block*-poly(ethylene terephthalate-co-oxybenzoate) (BCP-1), was removed from reactor in molten form after 20 minutes. Three block copolymers (BCP-1A, BCP-1B and BCP-1C) were synthesised from DCTPPS of differing molecular weights (Scheme 2.4).

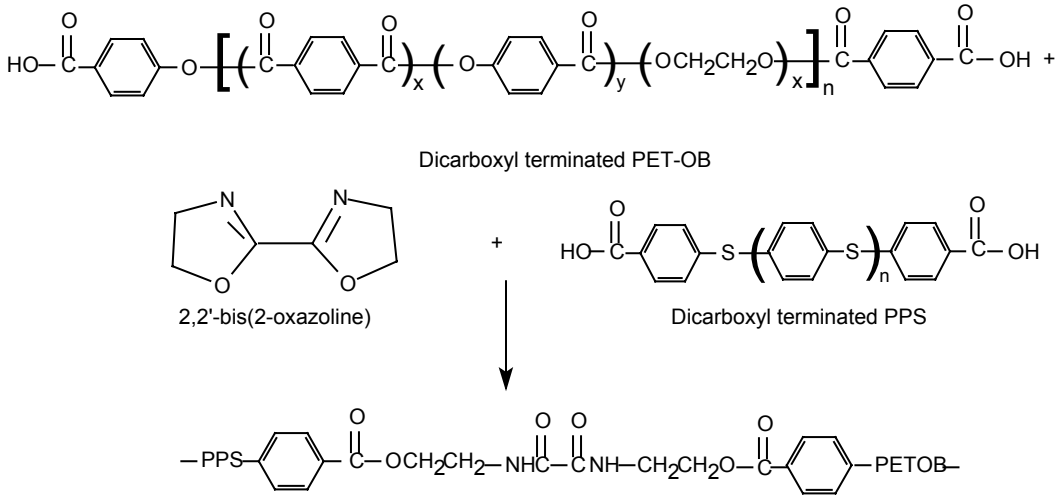

Scheme 2.4: Poly(phenylene sulphide)-*block*-poly(ethylene terephthalate-co-oxybenzoate)

2.2.1.6. Polysulphone-*block*-poly(ethylene terephthalate-co-oxybenzoate)

Three different dicarboxyl terminated polysulphone (DCTPSU) of approximate chain length (n≈ 4, 6, and 8) were chosen for the synthesis. DCTPET-OB (55/45) (M_n = 1760 g/mol)

was chosen as the liquid crystalline polymer. The block copolymers of: (i) DCTPSU-4 and DCTPET-OB; (ii) DCTPSU-6 and DCTPET/OB and (iii) DCTPSU-8 and DCTPET/OB were synthesised. DCTPSU and DCTPET/OB (55/45) were mixed in 1:1 mole ratio in the glass reactor and the temperature was raised to 260^{o}C. Equimolar concentration of 2,2'-bis(2-oxazoline) was added and stirred at 200 rpm for under nitrogen atmosphere. Block copolymer, polysulphone-*block*-poly(ethylene terephthalate-co-oxybenzoate), (BCP-2A, BCP-2B and BCP-2C) were removed from the reactor in melt condition after 20 minutes (Scheme 2.5).

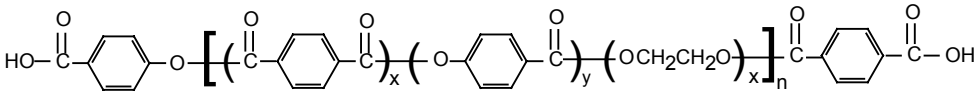

Dicarboxyl terminated PET-OB

+

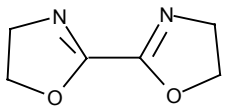

2,2'-bis(2-oxazoline)

+

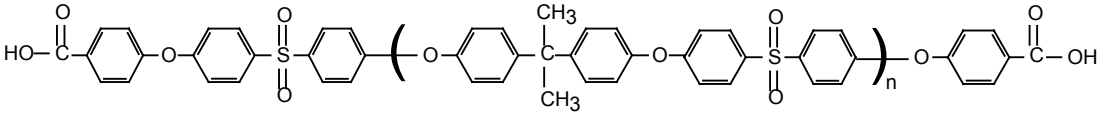

Dicarboxyl terminated Polysulfone

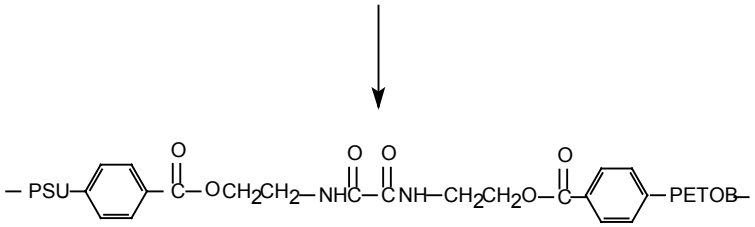

Scheme 2.5: Synthesis of polysulphone-*block*-poly(ethylene terephthalate-co-oxybenzoate)

2.2.2. Characterisation

The synthesised telechelic homopolymers, the chain coupled block copolymers were characterised by molecular weight determination, spectroscopy, thermal analysis and morphology.

2.2.2.1. Thermal analysis

Thermal properties were measured by a *Mettler TA 4000* series DSC. The apparatus was calibrated with Indium at different scanning rates. The lag between sample and pan holder temperature was also taken into account and computed through Indium crystallisation test as described by Elder-Wolchowicz.[8] The weight of samples were kept constant (6±0.1 mg) throughout the analysis so that the effect of weight change on the enthalpy change could be minimised. The heat of fusion and heat of crystallization were determined from the peak area of the DSC thermograms. Thermogravimetric analysis (TGA) measurements were carried out on a *Perkin Elmer TGA-7*. Samples were heated from 50^{o}C to 900°C at different heating rates under nitrogen atmosphere.

2.2.2.2. X-Ray diffraction (XRD)

The X-ray diffraction (XRD) patterns were recorded on a *Rigaku diffractometer* using CuK_{α} radiation at 50 kV and 120mA. The experiments were performed with a scan speed of 1° per minute.

2.2.2.3. Size exclusion chromatography (SEC)

Molecular weight and molecular weight distribution of the end-functional DCTPSU were determined from size exclusion chromatography (SEC) (*THERMO SEPARATION PRODUCTS*) equipped with spectra series UV 100 and Spectra system RI 150 detectors while Spectra series P100 pump was used with auto sampler: Spectra series AS 300. Linear polystyrene standards (*Polymer Laboratories*, M_p 685 g/mol to 8,27,000 g/mol., M_w/M_n = 1.02 – 1.09) were used for column calibration. Two 60 cm PSS SDV-gel columns 1 × linear (10^2 – 10^5 Å) and: 1 × 100Å with 10μ at 25^{o}C. The sample concentration was 2 g /L and the injection volume was 50 μL. HPLC grade THF was used as eluent at room temperature, with a flow rate of 1 mL / min.

2.3. Results and discussion

2.3.1. Dicarboxyl terminated poly(ethylene terephthalate-co-oxybenzoate)

The molecular weight was characterised by end group titration. Dicarboxyl terminated poly(ethylene terephthalate-co-oxybenzoate) (DCTPET-OB) was dissolved in the 20 mL of solvent (*o*-cresol/chloroform (70/30 v/v)) and titrated against butanolic potassium hydroxide solution. The number average molecular weight was calculated from the volume of potassium hydroxide consumed, as indicated in Table 2.4. IR spectra of DCTPET-OB showed characteristic peak for -OH group at 3390 cm^{-1} and C=O stretching at 1720 cm^{-1}.

Table 2.4: Titration of dicarboxyl terminated poly(ethylene terephthalate-co-oxybenzoate)

Polymer	Polymer, TPA (1,1)	Potassium hydroxide A mL	Potassium hydroxide B mL	Potassium hydroxide A-B mL	M_n g/mol
DCTPET/OB (70/30)	1,1	6.3	0.1	6.2	1839
DCTPET/OB (55/45)	1,1	6.6	0.1	6.5	1754
DCTPET/OB (40/60)	1,1	6.1	0.1	6.0	1900
DCTPET/OB (70/30)	1,2	7.5	0.1	7.4	1540
DCTPET/OB (55/45)	1,2	7.3	0.1	7.2	1583
DCTPET/OB (40/60)	1,2	6.5	0.1	6.4	1781

TPA=terephthalic acid; A=0.0877 N butanolic potassium hydroxide consumed by 0.5 g polymer in 20 mL of solvent (o-cresol/chloroform (70/30 v/v)); B=potassium hydroxide consumed by 20 ml of solvent; A-B=potassium hydroxide consumed by 0.5 g polymer.

2.3.2. Dicarboxyl terminated poly(phenylene sulphide)

There are a number of disadvantages in this methodology followed for the synthesis of dicarboxyl terminated poly(phenylene sulphide) (DCTPPS):

1. Sodium sulphide is not soluble in NMP[9]. Therefore, the reaction mixture was not homogenous.

2. Reactivities of 4-chlorobenzoic acid and 1,4-dichlorobenzene with sodium sulphide are not similar. It was therefore difficult to get a monodisperse product.

3. The polymer formed comes out of phase, which further increases the polydispersity.

2.3.2.1. Reaction mechanism

PPS is insoluble in all common organic solvents below about 200^{o}C[10] and hence it is extraordinarily difficult to characterise it. As a result, molecular weight and end groups are reliably related to the reaction parameters. The severity of the polymerisation conditions poses additional experimental difficulties for mechanistic study. The polymerisation does not exhibit classic condensation polymerisation behaviour. Thus, a polymer of high molecular weight than that predicted by the Carother's equation is produced at low conversion and even at unique 1,4-dichlorobenzene to sodium sulphide ratio.[9]

Lenz, Handlovits and Smith studied the self-condensation of sodium 4-chlorobenzothiolate as a possible route to synthesise PPS.[11] On the basis of model compound studies, they concluded that mechanism follows aromatic nucleophilic substitution reaction (S_NAr). Subsequent publications by Brady,[12] Sergeev and Nedelkin[13] also suggest the S_NAr mechanism.

N-methyl pyrrolidone has the duel role of catalyst as well as reactant. It transforms sodium sulphide into a soluble nucleophile $Na_2S.NMP.H_2O$. Sodium 4-(N-methylamino) butanoate (SMAB) results from this hydrolysis of NMP.[14]

Mechanism involves two steps: (i) A preliminary step where a mixture of water, NMP and alkaline sulphide is dehydrated at 150-190^{o}C. (ii) The addition of halogenated monomer followed by polymerisation at 200-240^{o}C under pressure.

2.3.2.2. End group analysis

Dicarboxyl terminated PPS of different molecular weights (about 0.5 g each) were kept with an excess of 20 mL methanolic standard potassium hydroxide for 7 days in stoppered Erlenmeyer flask with nitrogen overlay. It was titrated with standard hydrogen chloride to know

the volume of remaining potassium hydroxide. So we can calculate the amount of potassium hydroxide consumed by carboxyl terminated PPS. Molecular weight determined by this method is given in the Table 2.5. Titrimetry can be used for end group analysis of dicarboxyl terminated PPS either if it is completely soluble or the terminal carboxyl groups are present at the surface. It has always a chance of error. Hence, the supernatant was also analysed for carboxyl groups.

Table 2.5: Titration of dicarboxyl terminated poly(phenylene sulphide)

DCTPPS	Potassium hydroxide (mL)	Hydrogen chloride (mL)	Potassium hydroxide (mL)	M_n g/mol
DCTPPS-6	20	13.7	9.6	1104
DCTPPS-9	20	14.3	10.0	1066
DCTPPS-12	20	12.3	8.6	1233

0.1019 N hydrogen chloride; 0.0943 N potassium hydroxide

2.3.2.3. Titration of supernatant

Reactants 4-chloro benzoic acid (4.05 g), 2,4-dichloro benzene, (22.82 g), and sodium sulphide (13.12 g) with 100 mL NMP were charged in the *Parr reactor* and allowed to react for six hours at 230^{o}C under stirring. After the reaction was over the product, dicarboxyl terminated PPS, was filtered off and washed with methanol. The supernatant along with washing was taken in 250 mL volumetric flask and made up to the mark with methanol. The amount of unreacted 4-chlorobenzoic acid in the supernatant was analysed by titration. 20 mL of supernatant was titrated pH metrically against 0.0884 N potassium hydroxide. Volume of 0.0884 N potassium hydroxide consumed is 0.4 mL. So the strength of the supernatant is 0.0017 N. This implies that the 250 mL supernatant contains 0.07 g of 4-chlorobenzoic acid. Thus, of 4.05 g of 4-chlorobenzoic acid 0.07 g remained unreacted.

2.3.2.4. Infrared spectra

IR spectrum of DCTPPS depicts characteristics peaks of carboxyl and carbonyl groups at 3350 and 1637 cm^{-1}. The presence of sulphide linkage (-S-) is confirmed (817 cm^{-1}).

2.3.3. 2,2'-Bis(2-oxazoline)

2,2'-Bis(2-oxazoline) shows ^{1}H NMR peaks at (200 MHz, DMSO-d_6, ref TMS) 3.98 (t, 2H, N-CH_2) and 4.35 (t, 2H, O-CH_2) ppm. ^{13}C-NMR peaks are observed at (MHz, DMSO-d_6, ref TMS): 54.74, 67.94 and 155.09 ppm. IR shows one peak at 2295 cm^{-1} for νCH_2 stretching and the 1620 cm^{-1} for $\nu C{=}N$ stretching.

2.3.4. Dicarboxyl terminated polysulphone (DCTPSU)

DCTPSU, of differing chain lengths, were dissolved in 20 mL of dimethyl formamide (DMF) and titrated against standard tetrabutyl ammonium hydroxide, as shown in Table 2.6. The calculated number average molecular weights are less then the experimental number average molecular weight.

Table 2.6: Titration of dicarboxyl terminated polysulphone

DCTPSU	TBAH (A) mL	TBAH (B) mL	TBAH (A – B) mL	M_n (Expt.) g/mol	M_n (Cal) g/mol
DCTPSU-4	2.6	0.1	2.5	2,960	2,258
DCTPSU-6	2.0	0.1	1.9	3,895	3,142
DCTPSU-8	1.6	0.1	1.5	4,934	4,026

A=0.1351N methanolic tetrabutyl ammonium hydroxide (TABH); B=TBAH consumed by 20 mL. of DM; A-B=TBAH consumed by DCTPSU in 20 mL. of DMF; M_n (Cal)=theoretical number average molecular weight; Mn (Expt.)=Experimental number average molecular weight.

2.3.4.1. Size exclusion chromatography of dicarboxyl terminated polysulphone

Table 2.7 shows the molecular weight of dicarboxyl terminated polysulphone having different chain length determined by size exclusion chromatography. Polydispersity index (PDI) is more than 2 as expected for condensation polymer. Number average molecular weight (M_n) by

SEC is less then the calculated M_n and this difference goes on increasing with increase in molecular weight. Table 2.8 shows molecular weight determined by three different ways. M_n determined by end group titration method is closer to the calculated M_n.

Table 2.7: SEC analysis of dicarboxyl terminated polysulphone (DCTPSU)

Sample	M_n g/mol	M_w g/mol	PDI	M_n (Cal) g/mol
DCTPSU-4	1,372	3,056	2.23	2,258
DCTPSU-6	1,904	5,157	2.70	3,142
DCTPSU-8	2,493	7,110	2.85	4,026

Table 2.8: Comparison of the molecular weight of DCTPSU by different methods

Sample	M_n[a] g/mol	M_n[b] g/mol	M_n[c] g/mol
DCTPSU-4	2,960	1,372	2,258
DCTPSU-6	3,895	1,904	3,142
DCTPSU-8	4,934	2,493	4,026

a=molecular weight determined by end group titration; b=molecular weight determined by SEC; c=calculated molecular weight.

2.3.4.2. X-ray diffraction analysis (XRD)

Polysulphones show broad peak and 2θ values are similar for both. (*Figure 2.2)*.

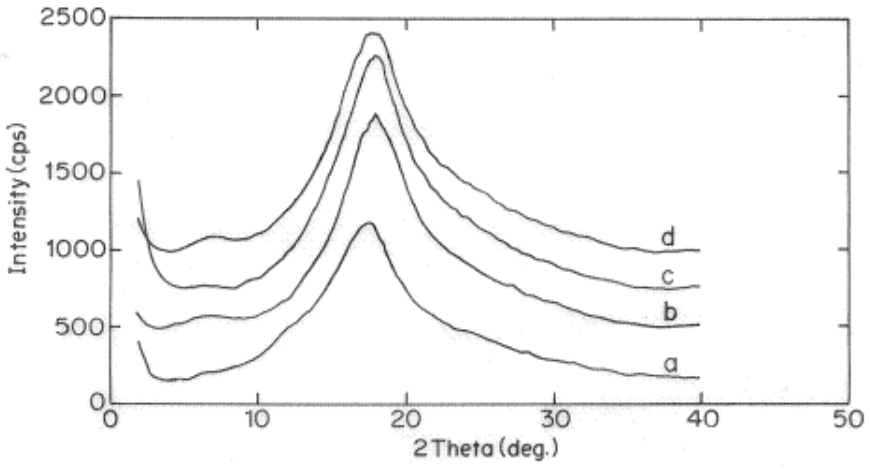

Figure 2.2: X-ray diffraction overlap of polysulphone, DCTPSU-4, DCTPSU-6 and DCTPSU-8

2.3.4.3. Infrared spectroscopy

Hydroxyl of carboxyl group in DCTPSU gives characteristics signal at 3470 cm^{-1} and the carbonyl group at around 1700 cm^{-1} (Table 2.9). The asymmetric and symmetric SO_2 stretching bands appear around 1330 cm^{-1} and 1150 cm^{-1} respectively.

Table 2.9: IR data of dicarboxyl terminated polysulphone

Functional Groups	DCTPSU-4	DCTPSU-6	DCTPSU-8
N_{OH}	3385	3390	3385
N_{CH3}	2970	2970	2970
$\nu_{C=O}$	1700	1700	1695
ν_{CH3}	1585	1585	1585
$\nu_{as\ O=S=O}$	1323/1289	1323/1289	1322/1288
$\nu_{as\ C-O-C}$	1237	1237	1249
$N_{O=S=O}$	1153	1150	1150

2.3.5. Poly(phenylene sulphide)-*block*-poly(ethylene terephthalate-co-oxybenzoate) (BCP-1)

Poly(phenylene sulphide)-*block*-poly(ethylene terephthalate-co-oxybenzoate) termed BCP-1 (A, B and C) were synthesised as described in Section 2.2.1.5. These were characterised by DSC, IR and XRD.

2.3.5.1. Thermal analysis

DSC was run on the poly(phenylene sulphide)-block-poly(ethylene terephthalate-co-oxybenzoate) (BCP-1) and its homopolymers at two different rates. The heat of melting was reduced in block copolymer drastically as shown in Table 2.10 and the overlapped figures are presented in Figures 2.3 and 2.4.

The crystallisation temperature (T_c) of dicarboxyl terminated poly(phenylene sulphide) (DCTPPS), dicarboxyl terminated poly(ethylene terephthalate-co-oxybenzoate)

(DCTPET-OB) correspond to the to exotherm peak maxima and are corrected as desired by Elder and Wolchowich.[8] The crystallisation temperature and heat of crystallisation (ΔH_c) of DCTPPS decrease after the formation of block copolymer, as shown in Table 2.10. This might be due to the inhibition of crystallisation by the TLCP part due to the formation of block copolymer. Figures 2.5 and 2.6 represent the overlap of DSC thermogram as presented in the Table 2.10.

Table 2.10: Thermal calorimetric measurement

System	Heating rate 10°C/min					Heating rate 20°C/min				
	T_m °C	ΔH_m J/g	T_c °C	ΔH_c J/g	α	T_m °C	ΔH_m J/g	T_c °C	ΔH_c J/g	α
DCTPPS	267.5	58.8	230.6	64.9	0.40	275.8	49.0	224.2	55.5	0.33
BCP-1	279.5	18.9	217.4	24.8	0.13	279.1	24.1	209.5	25.5	0.16
DCTLCP	-	-	146.1	10.1	-	-	-	140.9	9.3	-

***T_m**: Melting peak temperature; **ΔH_m**: Heat of fusion; **ΔH_c**: Heat of Crystallization; **BCP-1**: Poly(phenylene sulphide)-block-poly(ethylene terephthalate-co-oxybenzoate); **T_c**: Crystallization Temperature; α: Degree of crystallinity.*

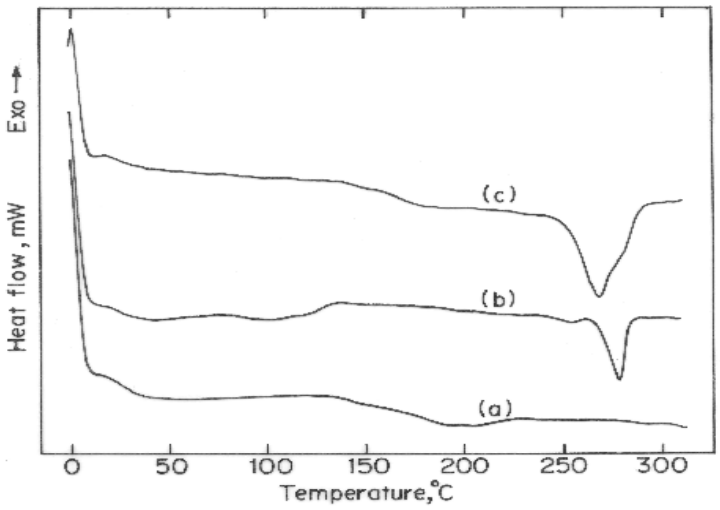

Figure 2.3: DSC thermogram of a) DCTLCP; b) poly(phenylene sulphide)-*block*-poly(ethylene terephthalate-co-oxybenzoate) and c) DCTPPS) at 10°C/min

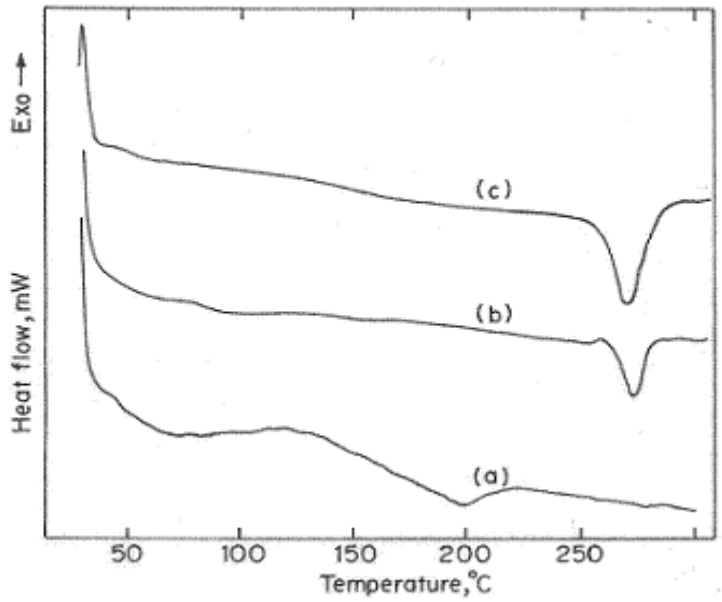

Figure 2.4: DSC thermogram of a) DCTLCP; b) poly(phenylene sulphide)-*block*-poly(ethylene terephthalate-co-oxybenzoate) and c) DCTPPS) at 20°C/min

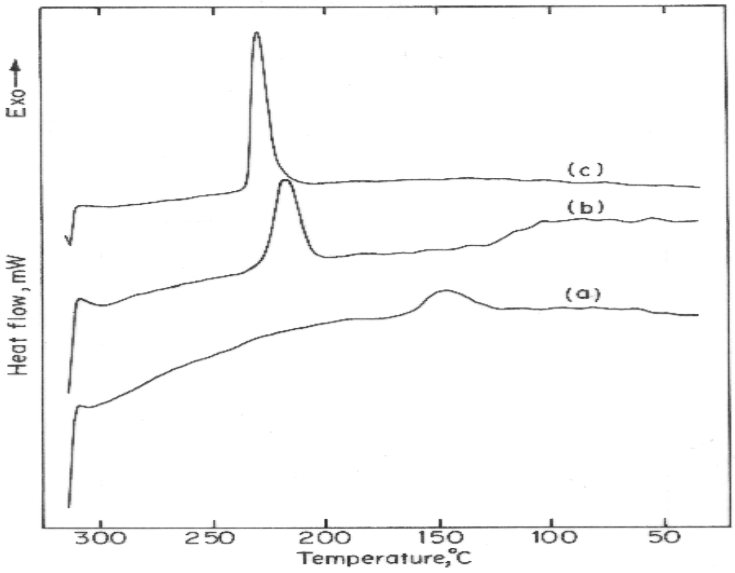

Figure 2.5: DSC thermogram corresponding to second cooling of a) DCTLCP; b) poly(phenylene sulphide)-*block*-poly(ethylene terephthalate-co-oxybenzoate) and c) DCTPPS) at 10°C/min

Degree of crystallinity (α) of the DCTPPS phase is presented in Table 2.10. The heat of crystallisation (ΔH_c) of the TLCP is less than that of DCTPPS. Therefore, degree of crystallinity has been calculated from the enthalpy of fusion normalised to the PPS

content, assuming that the contribution of PET-OB phase is negligible. A value of 146.2 J/g was estimated by Maeumura et. al[15] for enthalpy of fusion of 100% crystalline PPS.

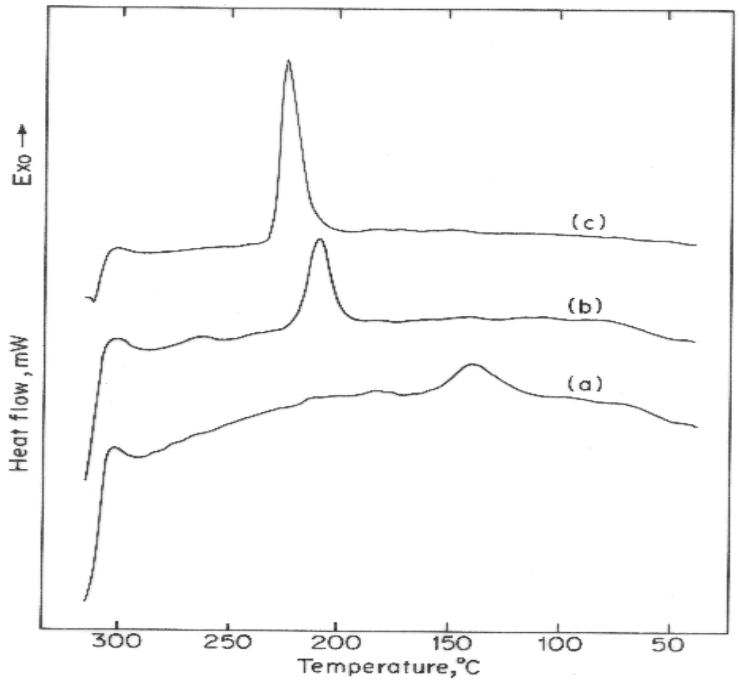

Figure 2.6: DSC thermogram corresponding to second cooling of a) DCTLCP; b) poly(phenylene sulphide)-*block*-poly(ethylene terephthalate-co-oxybenzoate) and c) DCTPPS) at 20°C/min

2.3.5.1.1. Thermogravimetric analysis

Table 2.11: Thermogravimetric analysis of poly(phenylene sulphide)-*block*-poly(ethylene terephthalate-co-oxybenzoate)

System	$T_{5\%}$ °C	T_{max} °C	T°C at Wt.% loss			Wt.loss % at 800°C
			20	40	60	
DCTPPS	392.126	513.42	497.22	516.35	546.09	68.645
BCP-1	312.99	537.66	375.28	417.475	517.66	77.718
DCTLCP	295.41	442.68	337.99	420.88	442.85	86.45

T_{max} - Temperature of maximum rate of weight loss; $T_{5\%}$ - Temperature at which 5% weight loss takes place; $T_{10\%}$ - Temperature at which 10% weight loss takes place; *BCP-1–Poly(phenylene sulphide)-block-poly(ethylene terephthalate-co-oxybenzoate); Rate of heating 10°C/min*

Table 2.11 represents weight loss at various temperatures. The temperature at which 5% weight loss takes place is $T_{5\%}$. The $T_{5\%}$ of block copolymer (BCP-1) is higher than that for DCTLCP but lower than the temperature for DCTPPS. This indicates that block copolymer is more stable than DCTLCP but DCTPPS is of higher stability than its block copolymer.

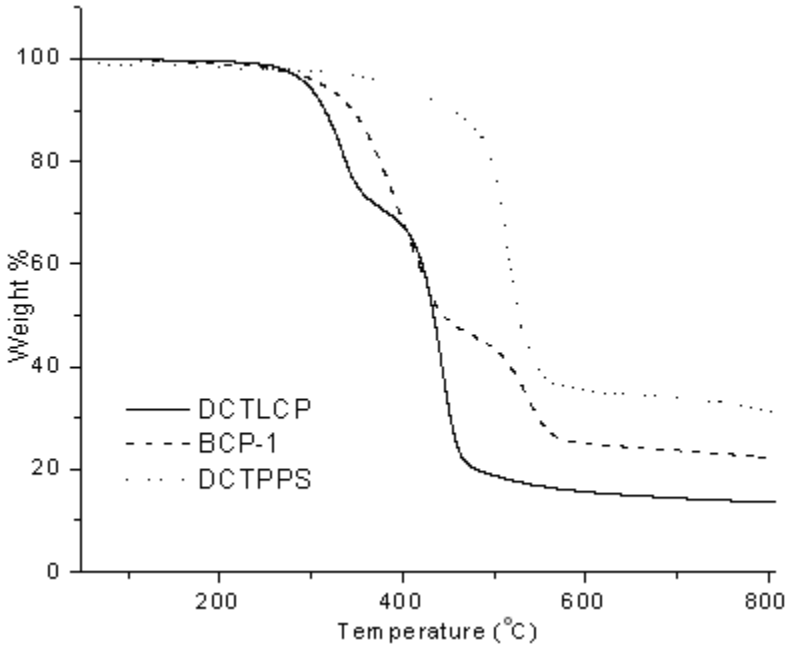

Figure 2.7: TGA of DCTLCP, BCP-1 and DCTPPS in nitrogen at 10°C/min

Figure 2.7 shows the weight loss of poly(phenylene sulphide)-*block*-poly(ethylene terephthalate-co-oxybenzoate) measured by thermogravimetric analysis (TGA) under nitrogen atmosphere. The thermal stability of the block copolymer is in between the stability of dicarboxyl terminated poly(phenylene sulphide) and dicarboxyl terminated poly(ethylene terephthalate-co-oxybenzoate).

2.3.5.2. Infrared spectroscopy

Poly(phenylene sulphide)-*block*-poly(ethylene terephthalate-co-oxybenzoate) was characterised by infrared spectroscopy (Figure 2.8). Bisoxazolines react with carboxyl group of the polymer (broad band between 3400 cm^{-1} and 3150 cm^{-1}) forming oxamide

group shown as NH peak at 3370 cm^{-1}. Carbonyl stretching vibration (Amide I) was observed at 1690 cm^{-1}. NH bending vibration (Amide II) was observed at 1527 cm^{-1}. Weaker band at 1258 cm^{-1} shows interaction between NH bending and CN stretching vibration. -S- stretching vibration was observed at 817 cm^{-1}.

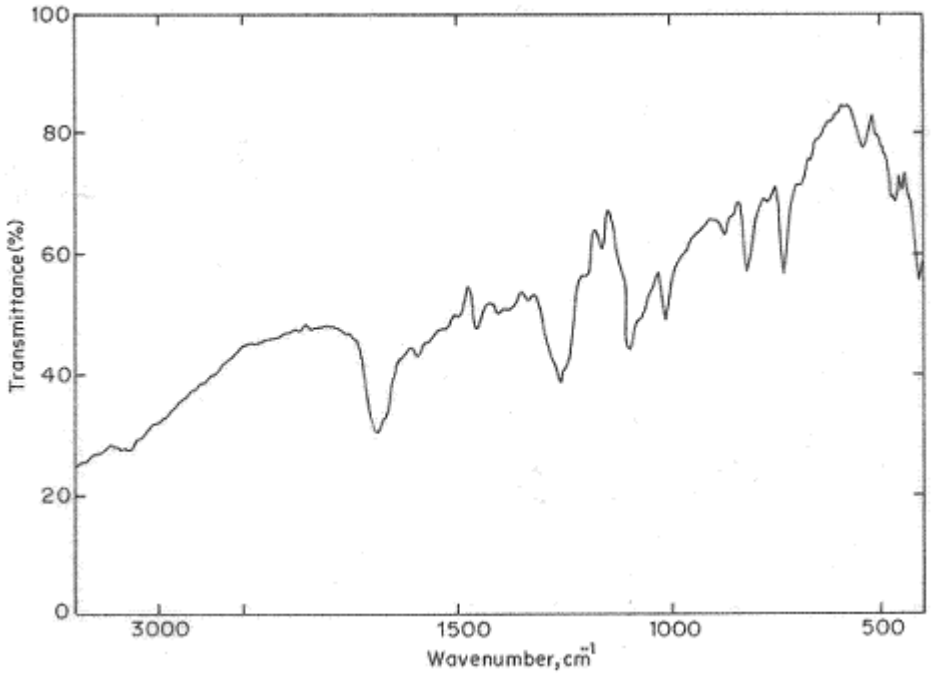

Figure 2.8: IR spectra of poly(phenylene sulphide)-*block*-poly(ethylene terephthalate-co-oxybenzoate)

2.3.5.3. X-ray diffraction analysis

X-ray diffraction of the block copolymer and the individual homopolymers were compared. Figure 2.9 shows the overlap of block copolymer (BCP-1) with the individual blocks of DCTPPS and DCTLCP. The crystal structure of dicarboxyl terminated PET-OB is not reflected in the block copolymer. The crystallinity of dicarboxyl terminated poly(phenylene sulphide) is dominated in the final block copolymer.

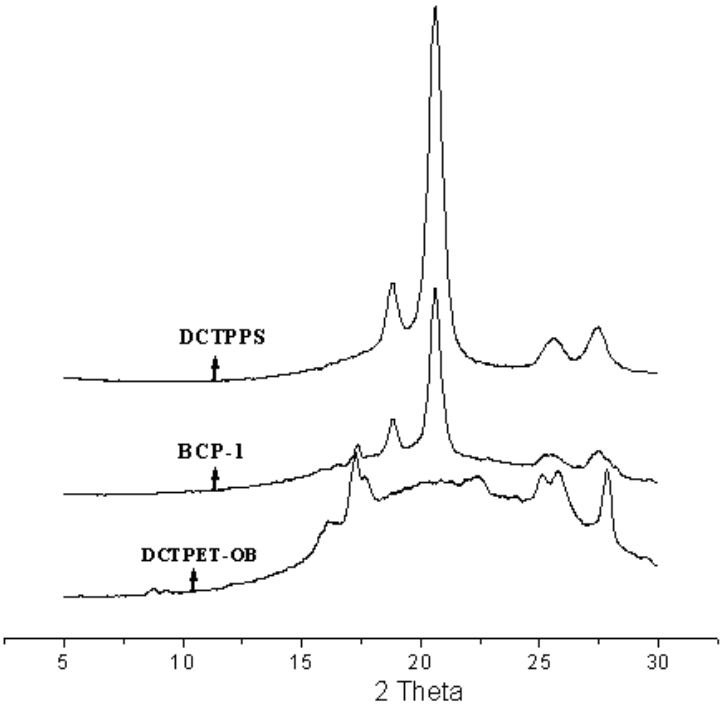

Figure 2.9: XRD overlap of DCTPPS, BCP-1 and DCTPET-OB.

2.3.6. Polysulphone-*block*-poly(ethylene terephthalate-co-oxybenzoate)

Synthesis of polysulphone-*block*-poly(ethylene terephthalate-co-oxybenzoate) (BCP-2) of differing segment lengths: (i) DCTPSU-4 and DCTPET/OB, (ii) DCTPSU-6 and DCTPET/OB and (iii) DCTPSU-8 and DCTPET/OB were presented in Section 2.2.1.6. These copolymers were characterised by ^{1}H NMR, ^{13}C NMR, DSC, IR and XRD.

2.3.6.1. Spectroscopy analysis

^{1}H NMR of telechelic polymer and block copolymer in DMSO-d_6 were taken at room temperature and recorded on 200 MHz and 300 MHz Bruker spectrophotometers.

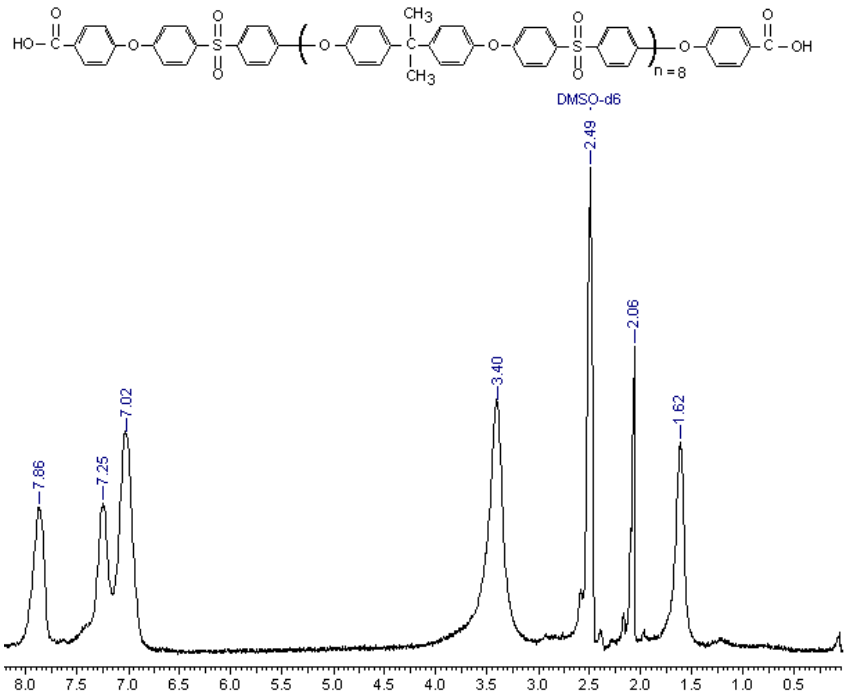

Figure 2.10: ^{1}H NMR of dicarboxyl terminated polysulphone (DCTPSU-8, n≈8)

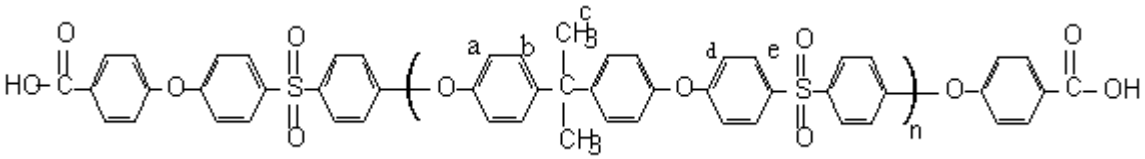

Figure 2.11: Dicarboxyl terminated polysulphone (DCTPSU)

In case of dicarboxyl terminated polysulphone (DCTPSU-8) in Figure 2.10 the aromatic region is shown by peaks around 7 to 8 ppm. The 7.9 ppm peak is shown by d,e protons depicted in Figure 2.11 due to the deshielding effect of neighbouring electron withdrawing sulphone group. Similarly, the peak 7.25 ppm is assigned for proton a. The end group protons are less intense than the protons of repeating unit. Proton b is assigned value of 7.03 ppm due to the shielding effect of isopropylidene group. Aliphatic region peaks of 1.63 ppm and 2.06 ppm are for the six isopropylidene protons. Similar spectra were observed for DCTPSU-4 (n≈4) and DCTPSU-6 (n≈6).

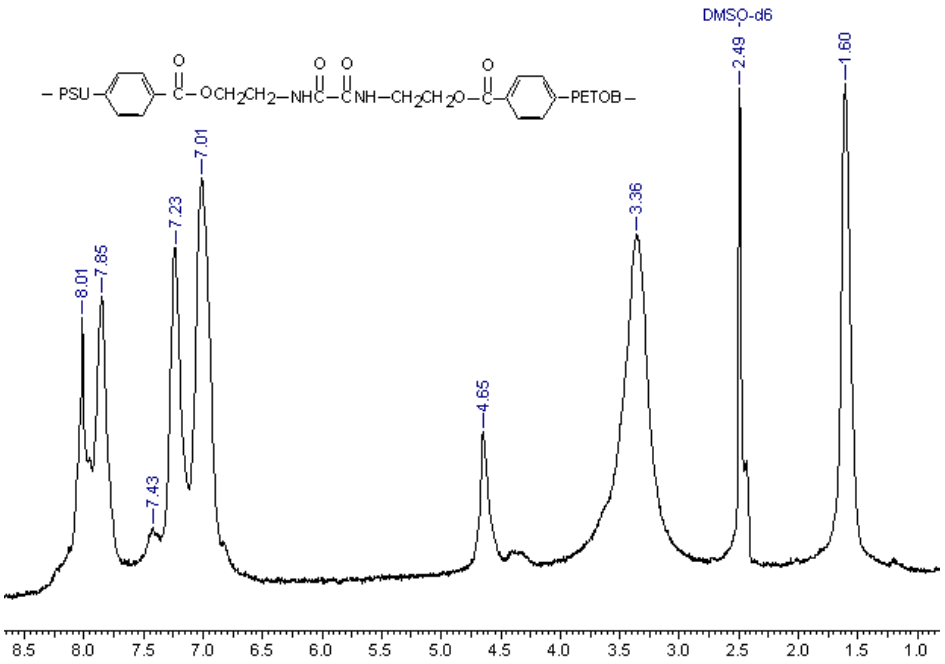

Figure 2.12: ^{13}C NMR of polysulphone (n≈8)-*block*-poly(ethylene terephthalate-co-oxybenzoate) (BCP-2C)

The spectra of block copolymer recorded in 300 MHz Bruker spectrophotometer in Figure 2.12 shows additional two peaks. The aromatic region value of 8.02 ppm corresponds to the aromatic proton of terephthalate group. The other peak at 4.65 ppm is assigned to the -O-CH_2CH_2 protons. The peak at 3.36 ppm is due to the presence of moisture in the solvent. Similar spectra were observed for BCP-2A and BCP-2B.

^{13}C NMR spectra of dicarboxyl terminated polysulphone (DCTPSU-8) and polysulphone-*block*-poly(ethylene terephthalate-co-oxybenzoate) in DMSO-d6 was taken at room temperature and recorded on a 200 MHz Bruker spectrophotometer. To assign the class of carbon atom DEPT (Distortionless Enhancement by Polarisation Transfer) sequence was used.

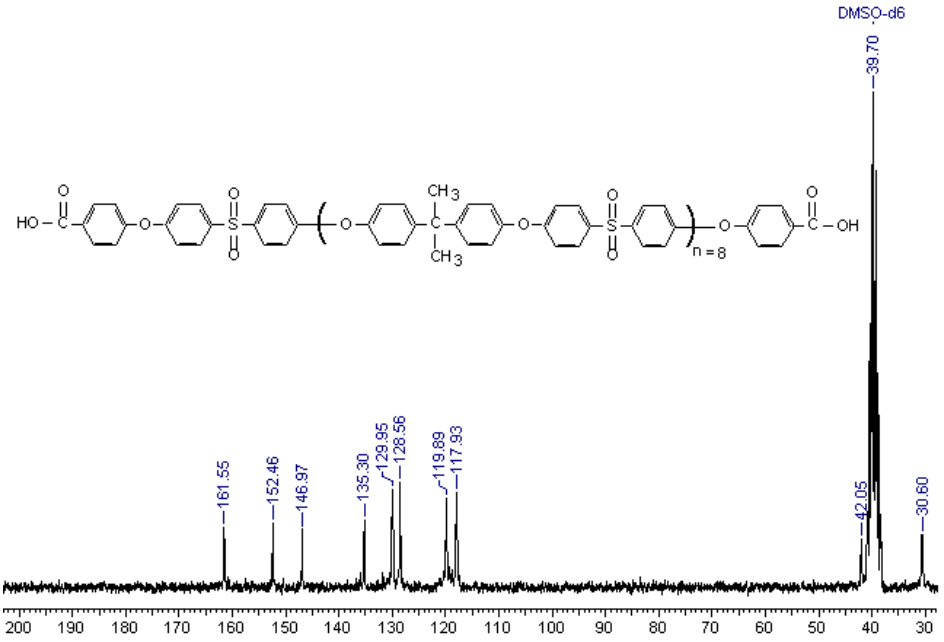

Figure 2.13: ^{13}C NMR of dicarboxyl terminated polysulphone (DCTPSU-8, n≈8)

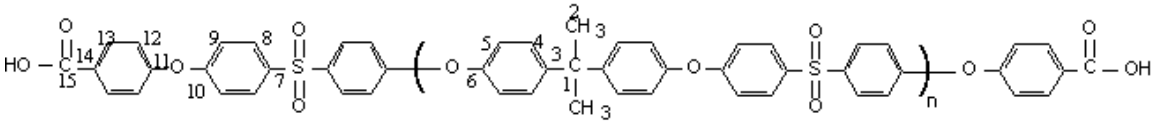

Figure 2.14: Dicarboxyl terminated polysulphone (DCTPSU)

^{13}C spectra of dicarboxyl terminated polysulphone (DCTPSU-8) is presented in Figure 2.13. C_1 the quaternary carbon (Figure 2.14) corresponds to peak at 42.09 ppm and C_2 (methyl) corresponds to 30.65 ppm. Peak at 117.95 ppm is due to C_5, C_9 and C_{12}. 119.92 ppm is due to C_{14}, 128.59 ppm is due to C_4, 129.99 ppm is from C_8 and 135.31 ppm is from C_{13}. C_3 and C_7 show at 146.99 ppm. C_6 and C_{10} show at 152.47 ppm. C_{11} and C_{15} show at 161.58 ppm. Similar spectra were observed for DCTPSU-4 and DCTPSU-6.

Coupling agent, 2,2'-bis(2-oxazoline), gives ^{13}C peaks at 54.74 ppm, 67.94 ppm, 155.09 ppm. Dicarboxyl terminated poly(ethylene terephthalate-co-oxybenzoate) has oxybenzoate, terephthalate and ethylene oxide groups. In this case terephthalate carbonyl

carbon peak was observed at 165 ppm. The phenyl carbon peak of terephthalate was observed at 135.31 ppm.

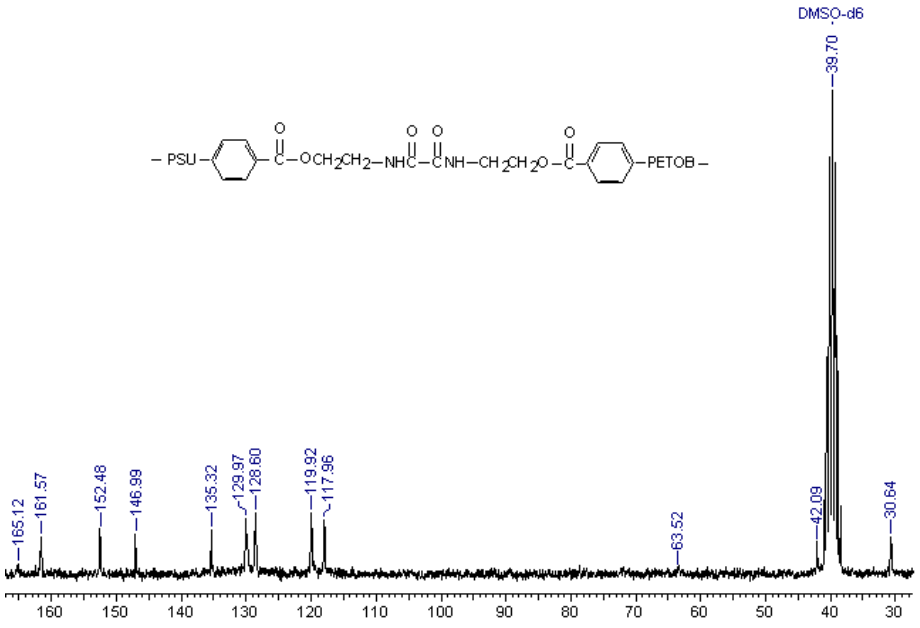

Figure 2.15: ^{13}C NMR of polysulphone (n≈8)-*block*-poly(ethylene terephthalate-co-oxybenzoate) (BCP-2C)

The spectra of block copolymer (BCP-2C) in Figure 2.15 shows additional peak at 165.11 ppm due to the carbonyl carbon of terephthalate. Another peak at 63.06 ppm is due to the -$\underline{C}H_2$NH carbon and –O$\underline{C}$H2 carbon of 2,2-bis(2-oxazoline). The –$\underline{C}$ONH carbon of 2,2-bis(2-oxazoline) appears at 161.5 ppm along with carbonyl carbon of carboxylic group. Similar spectra were observed for BCP-2A and BCP-2B.

2.3.6.2. Thermal analysis

Polysulphone is highly amorphous and the melting transition temperature (T_m) observed is due to solvent induced crystallisation in not prominent. Glass transition temperature (T_g) is noted for block copolymer and its homopolymers (Table 2.12).

Table 2.13 represents weight loss at various temperatures. $T_{5\%}$ of block copolymers (BCP-2A, BCP-2B, BCP-2C) is higher than DCTLCP but lower than that of DCTPSU. This indicates that block copolymer is more stable than DCTLCP but

DCTPSU is more stable than block copolymer. In case of $T_{5\%}$ of DCTPSU block copolymers, their stabilities are more than DCTLCP but less than that of DCTPSU block.

Table 2.12: Thermal characterisation of polysulphone-*block*-poly(ethylene terephthalate-co-oxybenzoate)

Polymer	T_g ^oC	T_c ^oC	ΔH_c J/g
DCTPSU-4	152.6	-	-
DCTPSU-6	155.9	-	-
DCTPSU-8	164.2	-	-
BCP2A	124.8	124.7	4.7
BCP2B	131.0	139.5	2.9
BCP2C	135.4	142.1	2.9

Rate of heating is 10^oC/min

Table 2.13: Thermogravimetric analysis of polysulphone-*block*-poly(ethylene terephthalate-co-oxybenzoate)

System	$T_{5\%}$ ^oC	T_{max} ^oC	T^oC at Wt % loss			Wt loss % at 800^oC
			20	40	60	
DCTLCP	295.41	442.68	337.99	420.88	442.85	86.45
BCP-2A	303.95	508.67	465.00	495.05	-	75.6
DCTPSU-4	398.30	493.23	469.20	499.04	671.47	66.34
BCP-2B	300.96	504.45	404.87	481.90	515.12	74.30
DCTPSU-6	414.90	524.78	504.6	528.36	666.33	62.31
BCP-2C	309.34	508.00	429.86	494.15	524.9	71.75
DCTPSU-8	404.21	475.85	470.23	504.5	766.8	61.56

T_{max} - Temperature of maximum rate of weight loss; $T_{5\%}$ - Temperature at which 5% weight loss takes place; $T_{10\%}$ - Temperature at which 10% weight loss takes place; *BCP-2A – Polysulphone (n≈4)-block-poly(ethylene terephthalate-co-oxybenzoate); BCP-2B – Polysulphone (n≈6)-block-poly(ethylene terephthalate-co-oxybenzoate); BCP-2C – Polysulphone (n≈8)-block-poly(ethylene terephthalate-co-oxybenzoate); Rate of heating is 10^oC/min;*

T_{max} is the temperature at which maximum degradation takes place. This temperature is higher for block copolymer than the individual homopolymers. This indicates the stability of block copolymers is more then the individual blocks. This is quite interesting to note that the stability of block copolymer is good at higher temperature than at lower temperature.

Similarly, the temperature at which 20%, 40% and 60% weight loss take place were noted. Block copolymer degradation temperature is in between that of the individual blocks, implying that it is more stable than the dicarboxyl terminated polysulphone but less stable than dicarboxyl terminated poly(ethylene terephthalate-co-oxybenzoate).

Thermal stabilities of BCP-2A, BCP-2B and BCP-2C are shown in Figures 2.16, 2.17 and 2.18.

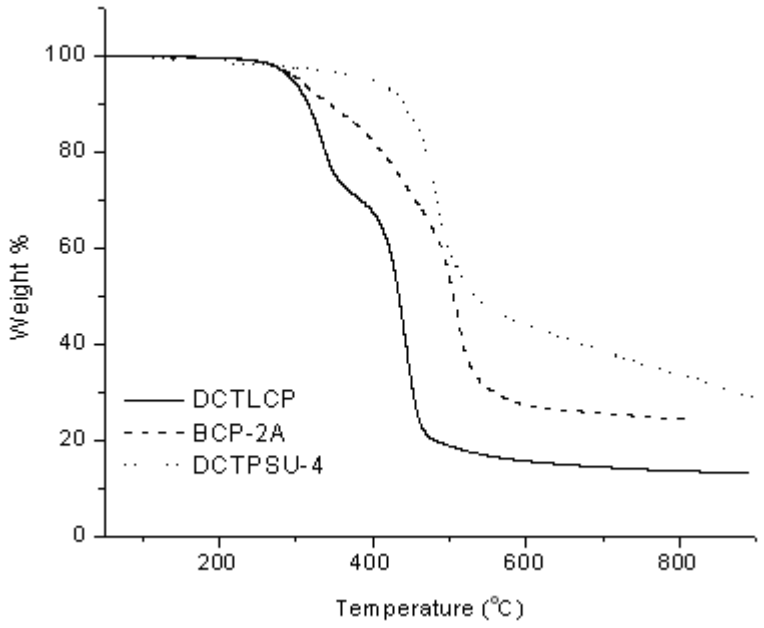

Figure 2.16: TGA of DCTLCP, BCP-2A and DCTPSU-4.

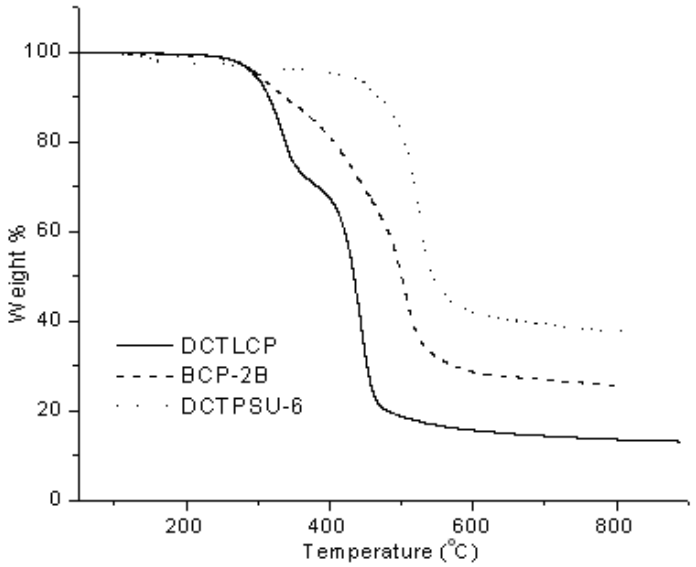

Figure 2.17: TGA of DCTLCP, BCP-2B and DCTPSU-6.

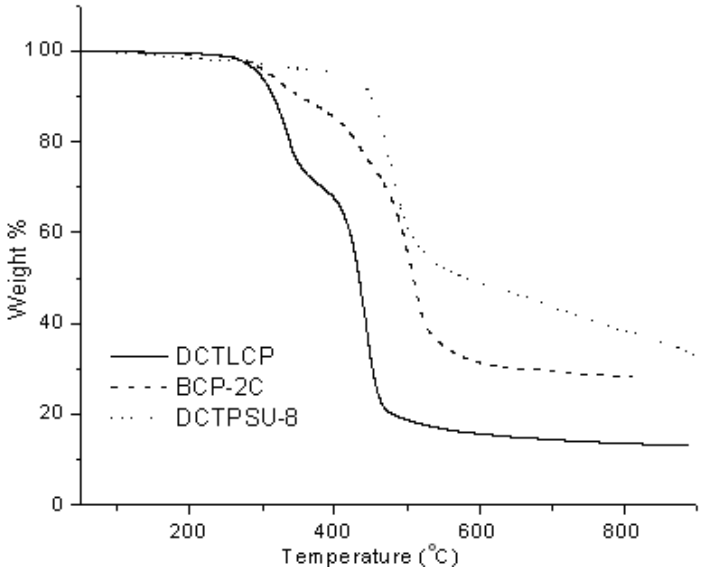

Figure 2.18: TGA of DCTLCP, BCP-2C and DCTPSU-8.

2.3.6.3. Infrared spectroscopy

Polysulphone (n≈8)-*block*-poly(ethylene terephthalate-co-oxybenzoate) (BCP-2C) was characterised by infrared spectroscopy. As indicated earlier, bisoxazolines react with carboxyl group of the polymer (broad band between 3400 cm^{-1} and 3150 cm^{-1}) forming

oxamide group shown as NH peak at 3380 cm^{-1}. Carbonyl stretching vibration (Amide I) was observed at 1685 cm^{-1}. NH bending vibration (Amide II) was observed at 1500 cm^{-1}.

The asymmetric and symmetric SO_2 stretching bands appears at around 1330 cm^{-1} and 1150 cm^{-1}, respectively, as shown in Table 2.14.

Table 2.14: IR of polysulphone-*block*-poly(ethylene terephthalate-co-oxybenzoate)

Functional group	BCP-2A	BCP-2B	BCP-2C
	cm^{-1}	cm^{-1}	cm^{-1}
ν_{NH}	3370	3370	3380
ν_{CH3}	2955	2955	2950
$\nu_{C=O}$	1700	1695	1685
ν_{NH}	1499	1503	1495
ν_{CH3}	1573	1573	1575
$\nu_{as\ O=S=O}$	1359/1285	1359/1286	1311/1288
$\nu_{as\ C-O-C}$	1233	1242	1241
$N_{O=S=O}$	1143	1150	1158

Similarly, polysulphone (n≈4)-*block*-poly(ethylene terephthalate-co-oxybenzoate) (BCP-2A) and polysulphone (n≈6)-*block*-poly(ethylene terephthalate-co-oxybenzoate) (BCP-2B) were also characterised by IR.

2.3.6.4. X-ray diffraction analysis

Figure 2.19 shows that the dicarboxyl terminated polysulphone is highly amorphous. This amorphous nature of the polysulphone is dominated in the block copolymer. PET-OB is semicrystalline and its semicrystalline nature is suppressed in the block copolymer (BCP-2A).

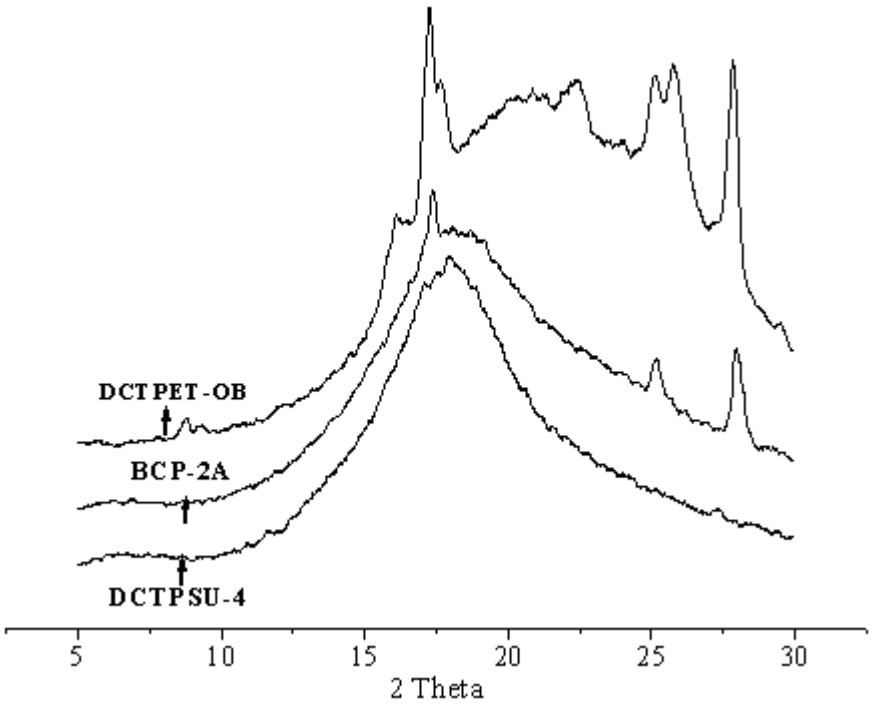

Figure 2.19: XRD of DCTPSU-4, BCP-2A and DCTPET-OB

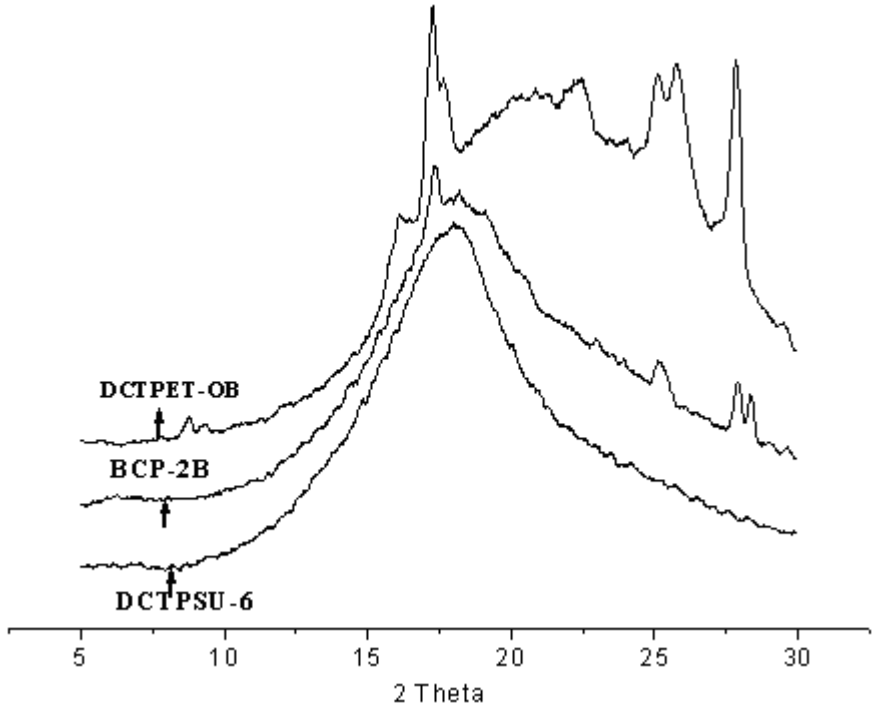

Figure 2.20: XRD of DCTPSU-6, BCP-2B and DCTPET-OB

Figures 2.20 and 2.21 also show a similar trend as with BCP-2A. Block copolymer (BCP-2B) structure is dominated by the amorphous nature of dicarboxyl terminated polysulphone.

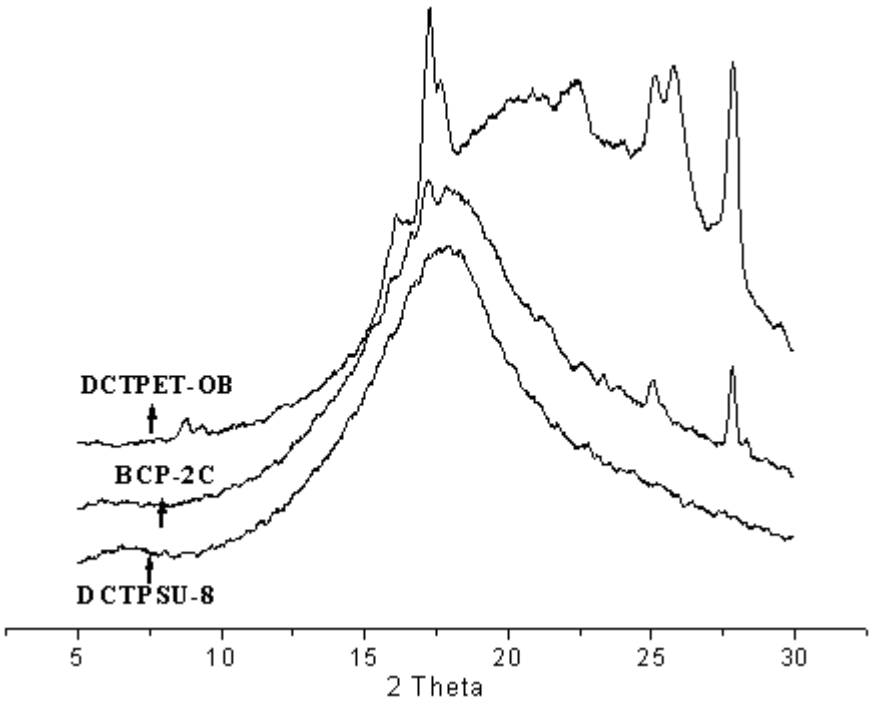

Figure 2.21: XRD of DCTPSU-8, BCP-2C and DCTPET-OB

2.4. Conclusion

Three poly(phenylene sulphide)-*block*-poly(ethylene terephthalate-co-oxybenzoate) (BCP-1) and three polysulphone-*block*-poly(ethylene terephthalate-co-oxybenzoate) (BCP-2) were synthesised from dicarboxyl terminated poly(phenylene sulphide), dicarboxyl terminated polysulphone and dicarboxyl terminated poly(ethylene terephthalate-co-oxybenzoate) by coupling with chain coupler 2,2'-bis(2-oxazoline). IR, thermal analysis and structural analysis indicated the formation of block copolymer (BCP-1). Similarly, NMR, IR, thermal analysis and structural analysis show the

formation of block copolymer (BCP-2). These two block copolymers were further used as compatibiliser for PPS/TLCP and PSU/TLCP blends.

2.5. References

1 Daccord G., Sillion B., *Polymer Bull.,* **6**, 477, 1982.

2. Heitz W., *Makromol. Chem. Symp.,* **26**, 1, 1987.

3. Heitz W., Freund L., *Makromol. Chem.,* **191**, 815, 1990.

4 Pospiech D., Haubler L., Komber H., Voigt D., Jehnichen D., Janke A., Baier A., Ekstein K., Bohme F., *J. Appl. Polym. Sci.,* **62**, 1819, 1996.

5 Gopakumar T. G., Ponrathnam S., Rajan C. R., Fradet A., *J. Polym. Sci. Polym. Chem.,* **36**, 2707, 1998.

6 Douhi A., Fradet A., *J. Polym. Sci. Polym. Chem*., **33**, 691, 1995.

7 Mathew J., Ghadage R. S., Ponrathnam S., and Prasad S. D., *Macromolecules*, **27**, 4021, 1994.

8 Elder M., Wlochowicz A., *Polymer*, **24**, 1593, 1983.

9 Rajan, C. R, Ponrathnam, S., Nadkarni, V. M., *J. Appl. Polym. Sci*., **32**, 4479, 1986.

10 Hedhli L., Fradet A., Marechal E., *Polym. Prepr*., **36**, 731, 1995.

11 Lenz R. W., Handlovits C. E., Smih H .A., *J. Polym. Sci.,* **58,** 351, 1962.

12 Brady D. G., *J. Appl. Polym. Sci., Appl. Polym. Symp.,* **36**, 231, 1981.

13 Fahey D. R., Hensley H. D., Ash C. E., Senn D. R*., Polym. Mater. Sci. Eng***.,* 67**, 468, 1992.

14. Acevedo M., Fradet A., *Polym. Prepr., Am. Chem. Soc. Div. Polym. Chem*., **34**, 457, 1993.

15 Maemura E., Cakmak M., White L. J., *Intern. Polym. Proc.*, **3**, 79, 1990.

CHAPTER-3

Compatibilisation of PPS/PET-OB blends

Rajkumar Patel

National Chemical Laboratory

Chapter 3. Compatibilisation of PPS/PET-OB blends

Abstract

Poly(phenylene sulphide)-block-poly(ethylene terephthalate-co-oxybenzoate) (BCP-1), synthesised from dicarboxyl terminated poly(phenylene sulphide) (n≈12) and dicarboxyl terminated poly(ethylene terephthalate-co-oxybenzoate), was evaluated as compatibiliser for PPS/PET-OB blend system. Four compositions of PPS/TLCP were chosen. Two different loading (5 wt.% and 10 wt.%) of poly(phenylene sulphide)-block-poly(ethylene terephthalate-co-oxybenzoate) were chosen. Compatibilised and uncompatibilised blends were characterised for thermal, mechanical and morphological properties. Differential scanning calorimetry studies indicate that maximum compatibilisation was achieved using 5 wt.% poly(phenylene sulphide)-block-poly(ethylene terephthalate-co-oxybenzoate). Mechanical properties show only marginal increase on compatibilisation with 5 wt.% of BCP-1. The compatibilised blend with PPS/PET-OB/BCP-1 80/20/5 showed better morphology then the uncompatibilised PPS/PET-OB 80/20 blend.

3.1. Experimental

3.1.1. Materials

Poly(phenylene sulphide) (PPS) (unfilled grade Fortron 0220 A1), PET/OB (55/45 mol%) and dicarboxyl terminated PET/OB a semi-aromatic thermotropic liquid crystalline polymer were prepared. Dicarboxyl terminated poly(phenylene sulphide)s (DCTPPS) of varying statistically average block length (n ≈ 6, 9, 12) were prepared as described in Section 2.2.1.2. The synthesis of block copolymer poly(phenylene sulphide)-*block*-poly(ethylene terephthalate-co-oxybenzoate) (BCP-1) with PPS block length (n≈12) was described in Section 2.2.1.5.

3.1.2. Methods

Pellets of PPS and PET/OB were manually mixed in the ratio 95/5, 90/10, 85/15, 80/20 (wt./wt.%) and dried in an air oven dryer at 150^{o}C. Poly(phenylene sulphide)-*block*-poly(ethylene terephthalate-co-oxybenzoate) (BCP-1) was taken at two different ratio i.e. 5 wt.% and 10 wt.%.

The melt blending of PPS, PET/OB and BCP were done with *DSM microcompounder*. The cylinder temperature of the microcompounder was maintained at 300^{o}C and the screw speed was 100 rpm. Uncompatibilised PPS/PET-OB blends with PET-OB content 5, 10, 15 and 20 (wt./wt.%) were prepared under identical conditions for comparative study.

3.1.3. Processing

Injection moulding was performed with a *DSM micro-injection mould.* The parent polymers were processed under conditions recommended by the manufacturers. The condition chosen for the processing of blends was a suitable compromise between those used for the respective homopolymers. The moulded specimen consisted of standard test bars for tensile and impact tests.

3.1.4. Testing and Analysis

Thermal properties of extruded PPS/TLCP blend samples were measured by *Mettler TA4000* series differential scanning calorimeter. The apparatus was calibrated with Indium at different scanning rates. The lag between sample and pan holder temperature was also taken into account, and computed through Indium crystallisation tests as described by Elder and Wlochowicz.[1] The sample mass were kept constant (6.0±0.1 mg) through out the analysis so as to minimise the effect of mass change on the enthalpy change. The heats of fusion and crystallisation were determined from the peak

area in the DSC thermogram. The melting transition temperature (T_m) and crystallisation temperature (T_c) were calculated from the peak maxima of the thermograms of samples in the second heating and cooling scan, respectively. Thermogravimetric analysis (TGA) was carried out on a Perkin Elmer TGA 7 under nitrogen atmosphere.

Tensile properties of mini tensile bars were measured using an *Instron testing machine* (4204). The strain rate was 50 mm/minute for tensile strength and elongation measurements. The morphology of the fractured surfaces of the injection moulded tensile specimens was observed by *Leica Stereoscan 440* scanning electron microscope.

3.2. Results and Discussion

3.2.1. Thermal analysis

3.2.1.1. Melting behaviour

The degree of interaction between two polymers is described by ΔG, comprising of ΔH and ΔS contributions. For a blend to be single phase, ΔG< 0, since ΔS is negligible for polymers, ΔH dominates in the free energy of mixing in the polymer blend. The introduction of interacting groups by chemical modification of a polymer or by copolymerisation can result in a negative contribution to the enthalpy of mixing. The enthalpy of mixing (ΔH_{mixing}) of rigid rod like liquid crystalline segment with a flexible coil polymer is mostly positive. The enthalpy of mixing (ΔH_{mixing}) of PPS/PET-OB blend (Table 3.1) decreased, indicating a favourable interaction between PPS and PET-OB chain on compatibilisation brought forth by use of block copolymer of PPS and PET-OB.

3.2.1.2. Crystallisation behaviour

The crystallisation temperature (T_c) of PPS, PET-OB, uncompatibilised and compatibilised with 5 and 10 wt.% of poly(phenylene sulphide)-*block*-poly(ethylene terephthalate-co-oxybenzoate) (BCP-1), shown in Table 3.1, correspond to the exotherm

peak maxima and are corrected as desired by Elder and Wolchowich.[1] The crystallisation temperature (T_c) and heat of crystallisation (ΔH_c) of PPS phase decreases on compatibilisation, as seen in Table 3.1, indicating that compatibilisation retards the crystallisation process of PPS. The crystallisation peak of PPS phase in 80/20 wt./wt.% PPS/PET-OB compatibilised by 5 wt.% of BCP-1 was at 238^{o}C but for uncompatibilised blend it was at 246^{o}C. Similarly, for compatibilised blend of PPS/PET-OB by 10 wt.% BCP-1, the crystallisation temperature was at 236^{o}C. When the amount of block copolymer was increased from 5 to 10 wt.% there is only a marginal decrease in the crystallisation temperature.

The decrease in crystallisation temperature indicates that compatibilisation marginally slows down the crystallisation rate of PPS phase. This leads to an increase in the degree of supercooling (T_m-T_c = ΔT) of PPS phase in compatibilised PPS/PET-OB blends. By increasing the block copolymer amount from 5 to 10 wt.%, there is not much change in degree of supercooling. This implies that 5 wt.% of block copolymer is best suitable for compatibilisation.

Similar effect of compatibilisation on crystallisation rate of blend components have been reported earlier.[2-6] Chang et. al reported that the crystallisation behaviour of components of Noryl [blends of poly(phenylene oxide) and polystyrene]/ PET-OB is seriously affected by *in situ* compatibilisation by the addition of reactive components such as styrene-glycidyl methacrylate (SG). Ahn and coworkers[4-6] recently investigated the efficacy of polyacrylate (PAr)-b-polyamide-6 (PA-6) copolymer for compatibilising PAr/PA-6 blends. They observed a depression in crystallisation temperature and degree of crystallinity on compatibilisation.

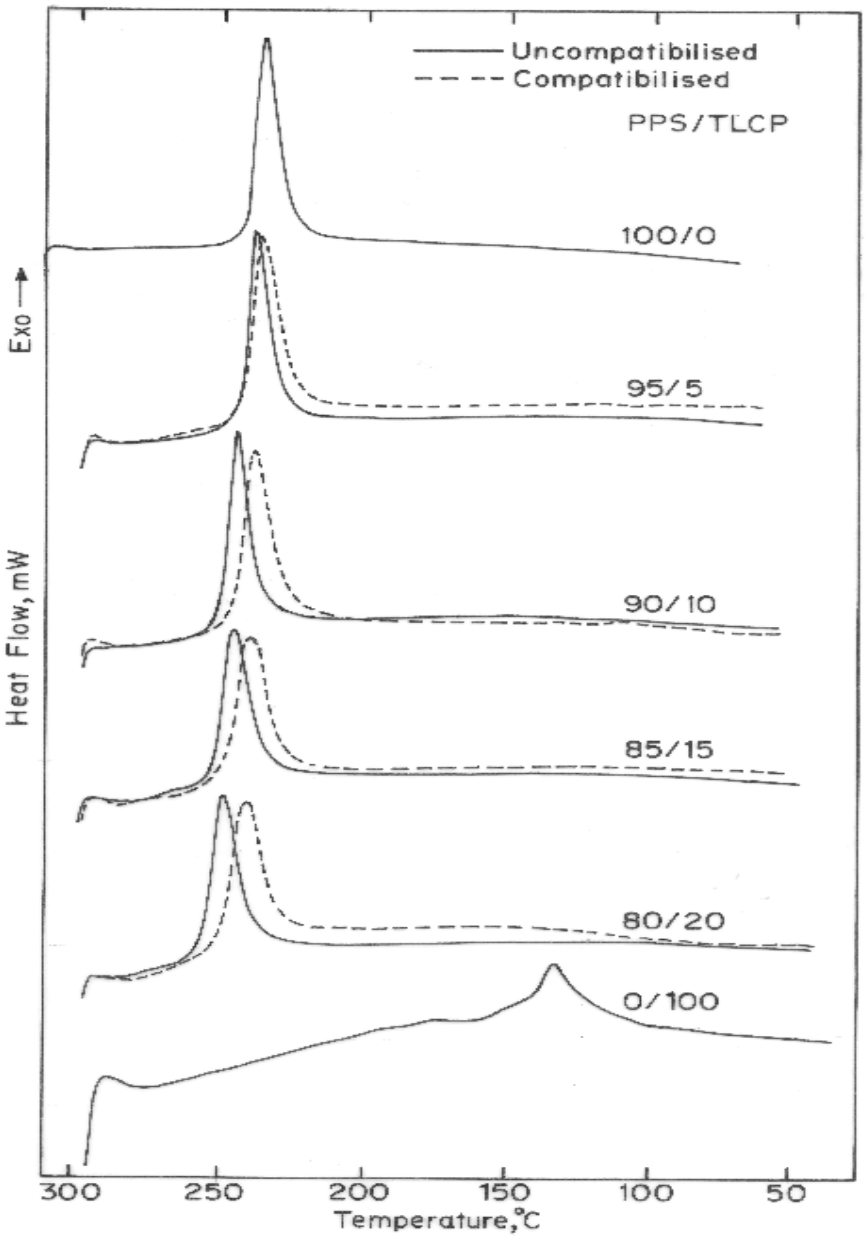

Figure 3.1: DSC exotherms (second cooling) of uncompatibilised and compatibilised PPS/PET-OB blends at a heating rate 10°C/minute.

3.2.1.3. Degree of crystallinity

The degree of crystallinity (α) of the PPS phase in both uncompatibilised and compatibilised blends, tabulated in Tables 3.1 and 3.2, were obtained from DSC thermograms (Figure 3.1). The ΔH_m of PET-OB is small as compared to that of PPS (33.7 J/g). Therefore, the degree of crystallinity (α) has been

Table 3.1: Thermal Calorimetric properties of PPS/TLCP blends at 10°C/min heating and cooling rates

PPS/ TLCP	Compatibiliser (BCP-1) (0% Wt.)						Compatibiliser (BCP-1) (5% Wt.)						Compatibiliser (BCP-1) (10% Wt.)					
	T_m °C	ΔH_m J/g	T_c °C	ΔH_c J/g	ΔT °C	α	T_m °C	ΔH_m J/g	T_c °C	ΔH_c J/g	ΔT °C	α	T_m °C	ΔH_m J/g	T_c °C	ΔH_c J/g	ΔT °C	α
100/0	282	33.7	230	42.8	52.0	0.23	-	-	-	-	-	-	-	-	-	-	-	-
95/5	281	33.2	236	42.5	45.0	0.23	282	33.0	233	37.3	49.0	0.23	282	28.2	232	30.1	50.0	0.19
90/10	281	32.8	240	33.9	41.0	0.22	282	31.3	235	32.1	47.0	0.21	282	25.5	234	28.3	48.0	0.17
85/15	280	30.0	242	32.4	38.0	0.20	282	29.0	236	30.2	46.0	0.20	282	25.0	235	26.7	47.0	0.17
80/20	281	25.3	246	30.1	35.0	0.17	281	24.0	238	27.4	43.0	0.16	282	22.3	236	24.7	46.0	0.15
0/100	-	-	139	11.7	-	-	-	-	-	-	-	-	-	-	-	-	-	-

***T_m**: Melting peak temperature; **ΔH_m**: Heat of fusion; **ΔH_c**: Heat of Crystallisation; **BCP-1**:Poly(phenylene sulphide)-block-poly(ethylene terephthalate-co-oxybenzoate); T_m-T_c = **ΔT:** Degree of super cooling; **T_c**: Crystallisation Temperature; **α**: Degree of crystallinity.*

Table 3.2: Thermal Calorimetric properties of PPS/TLCP blends at 20°C/min heating and cooling rates

PPS/ TLCP	Compatibiliser (BCP-1) (0% Wt.)						Compatibiliser (BCP-1) (5% Wt.)						Compatibiliser (BCP-1) (10% Wt.)					
	T_m °C	ΔH_m J/g	T_c °C	ΔH_c J/g	ΔT °C	α	T_m °C	ΔH_m J/g	T_c °C	ΔH_c J/g	ΔT °C	α	T_m °C	ΔH_m J/g	T_c °C	ΔH_c J/g	ΔT °C	α
100/0	282	31.7	228	43.3	54	0.22	-	-	-	-	-	-	-	-	-	-	-	-
95/5	281	28.6	231	40.6	50	0.20	281	27.1	226	37.1	55	0.19	280	26.6	223	33.0	57	0.18
90/10	280	25.0	233	37.7	47	0.17	281	21.6	228	31.8	53	0.15	281	20.8	225	31.8	56	0.14
85/15	279	22.9	237	34.3	42	0.16	280	21.1	230	30.4	50	0.14	281	19.5	228	26.2	53	0.14
80/20	279	20.4	240	30.9	39	0.14	280	19.0	235	29.4	45	0.13	281	17.2	233	22.8	48	0.12
0/100	-	-	131	17.4	-	-	-	-	-	-	-	-	-	-	-	-	-	-

T_m: Melting peak temperature; ΔH_m: Heat of fusion; ΔH_c: Heat of Crystallisation; ***BCP-1****:Poly(phenylene sulphide)-block-poly(ethylene terephthalate-co-oxybenzoate); T_m-T_c =* ***ΔT:*** *Degree of super cooling; T_c: Crystallisation Temperature;* **α**: *Degree of crystallinity.*

Table 3.3: Thermogravimetric analysis of PPS/TLCP system under nitrogen atmosphere

PPS/ TLCP	Compatibiliser (BCP-1) (0% Wt.)						Compatibiliser (BCP-1) (5% Wt.)						Compatibiliser (BCP-1) (10% Wt.)					
	$T_{5\%}$ ^oC	T_{max} ^oC	T^oC at Wt % loss			Wt loss % at 800 ^oC	$T_{5\%}$ ^oC	T_{max} ^oC	T^oC at Wt % loss			Wt loss % at 800 ^oC	$T_{5\%}$ ^oC	T_{max} ^oC	T^oC at Wt % loss			Wt loss % at 800 ^oC
			20	40	60				20	40	60				20	40	60	
100/0	502.4	549.9	535.4	571.9	-	48.9	-	-	-	-	-	-	-	-	-	-	-	-
95/5	454.0	520.8	522.4	556.9	-	53.9	421.6	522.6	512.8	545.1	838.8	58.5	413.5	544.6	519.8	555.6	-	54.5
90/10	433.3	555.5	522.5	561.9	-	56.3	410.3	537.6	494.1	540.1	765.4	61.5	402.7	545.1	508.3	551.4	895.4	57.1
85/15	418.2	537.0	521.0	556.0	873.2	58.0	407.5	559.2	504.5	553.5	893.3	56.6	399.7	547.2	500.8	551.2	898.8	57.5
80/20	413.7	553.1	499.2	555.2	893.3	57.3	406.5	549.5	491.3	548.5	807.3	59.8	393.8	546.9	456.1	542.8	750.9	61.3
0/100	343.8	443.4	443.1	462.3	478.0	84.7	-	-	-	-	-	-	-	-	-	-	-	-

$T_{5\%}$: Temperature at 5 % wt. Loss;Rate of heating: 10^{o}C/min; BCP-1: Poly(phenylene sulphide)-block-poly(ethylene terephthalate-co-oxybenzoate)

Table 3.4: Mechanical properties of PPS/TLCP blends

PPS/ TLCP	Compatibiliser (BCP-1) (0% Wt.)				Compatibiliser (BCP-1) (5% Wt.)			
	Elongation	Toughness MPa	Modulus MPa	Tensile Strength MPa	Elongation	Toughness MPa	Modulus MPa	Tensile Strength MPa
100/0	79.750	34.75	1650	35.28	-	-	-	-
95/5	49.50	29.47	2263	41.79	52.1	30.03	2274	43.22
90/10	2.14	1.417	2421	53.71	2.43	1.56	2459	55.94
85/15	2.11	0.851	2491	57.40	2.22	0.88	2526	58.25
80/20	1.81	0.71	2500	61.08	1.93	0.765	2568	62.46

BCP-1: Poly(phenylene sulphide)-block--poly(ethylene terephthalate-co-oxybenzoate); *Strain rate: 50 mm/min.*

calculated from the enthalpy of fusion normalised to the PPS content, assuming that the contribution of the PET-OB phase is negligible. A value of 146.2 J/g was estimated by Maemura et. al for enthalpy of fusion of 100 % crystalline PPS.[7] The heat of melting and hence the crystallinity of the compatibilised blend by 10 wt.% block copolymer, rather than by 5 wt.% BCP-1, decreased significantly as compared to the uncompatibilised blend of similar compositions seen in Table 3.1. Compatibilisation by addition of block copolymer results in favourable interaction between the blends components. This interaction leads to a negative contribution to the enthalpy of mixing and this affects crystallisation of blend components. The crystallisation temperature (T_c) and degree of crystallinity (α) of PPS phase in PET-OB blends are decreased on addition of copolymer consisting of PPS and PET-OB blocks.

Chang and coworkers[3,6] observed a reduction in the degree of crystallinity of PP in PP/Vectra A 950 blends in the presence of ethylene-glycidyl methacrylate (EGMA) copolymer. They concluded that EGMA undergoes interchange reaction with Vectra A 950 resulting in EGMA-g-Vectra A 950 block copolymer, which interferes with the crystallisation of PP. As indicated earlier, Ahn and coworkers[4,6] reported a reduction in the crystallinity of PAr/PA-6 blends in the presence of PAr-b-PA-6 copolymer. An effective compatibilisation increases the mutual solubility of the various components, which causes a reduction in the crystallinity of thermoplastic matrix in thermoplastic (TP)/thermotropic liquid crystalline polymer (TLCP) blends. The DSC results lead us to conclude that the increased interaction between the phases modified the crystallisation behaviour of the blend components.

3.2.1.4. Thermogravimetric analysis

The TGA thermographs are depicted in Figures 3.2 and 3.3. The analysis is shown in Table 3.3. The 5% decomposition temperature (5% DT) goes on decreasing with increase in the TLCP percentage in the composition. This trend is followed in both compatibilised and uncompatibilised systems. This 5% DT is minimum in PPS/TLCP/BCP-1 (10 wt. %) and maximum in compatibilised system.

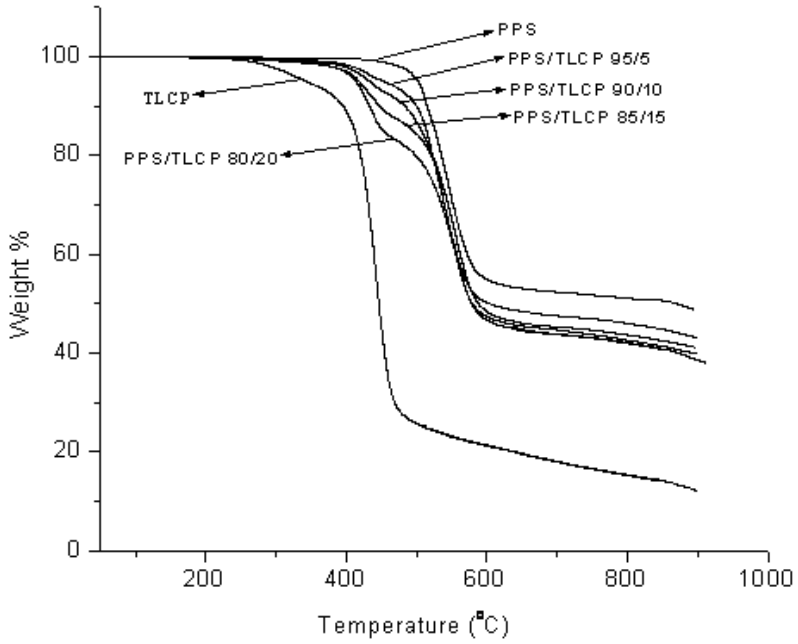

Figure 3.2: TGA thermograph of PPS/TLCP uncompatibilised blend in nitrogen atmosphere.

The temperature at which maximum rate of decomposition takes place is $T_{max.}$ In case of uncompatibilised system, as shown in Table 3.3, T_{max} is minimum for PPS/TLCP (85/15) composition. This trend is just reverse in both compatibilised systems of same composition. This indicates that the compatibilised blend system of 85/15 % composition is most stable at $T_{max.}$

The 20 % degradation temperature (20 % DT), as shown in Table 3.3, of uncompatibilised system remains constant up to 15 % TLCP composition but suddenly

drops when TLCP percent increases to 20 %. This indicates that system is stable at 20 % DT up to 15 % TLCP and then stability decreases as the percentage of TLCP increases.

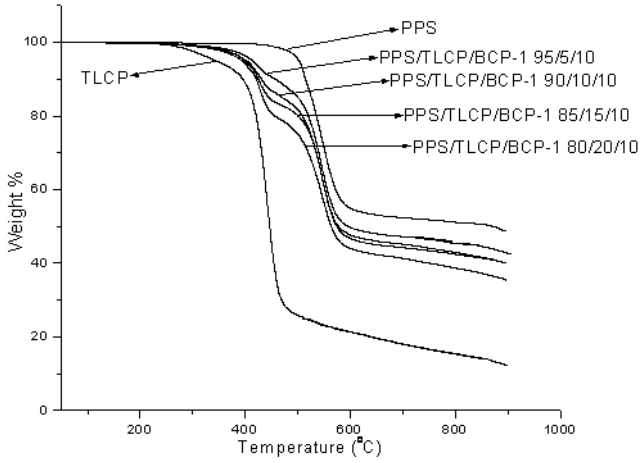

Figure 3.3: TGA thermograph of PPS/TLCP/BCP-1 (10%) blend in nitrogen atmosphere.

In compatibilised system with 5 wt.% BCP-1 the 20 % DT decreases as the TLCP increases from 5 to 20 percent, except in 15 % TLCP composition. This implies that the 85/15 composition is most stable one of the four compositions studied. In compatibilised system with 10 wt.% BCP-1 the 20 % DT decreases as TLCP increases from 5 to 20 %.

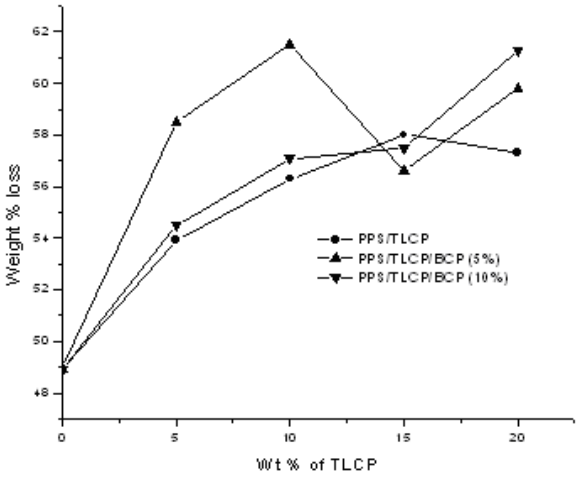

Figure3.4: Weight % loss of a) PPS/TLCP b) PPS/TLCP/BCP-1 (5%), c) PPS/TLCP/BCP-1 (10%) at 800°C.

The 40 % degradation temperature (40% DT) of uncompatibilised system, as shown in Table 3.3, does not change appreciably. There is 5^{o}C increase in 40 % DT as the TLCP percent increases from 5 to 10 % TLCP in the composition. The 40 % DT of compatibilised system with 10 % BCP-1 decreases slightly up to 15 % TLCP. However, at 20 % TLCP it decreases marginally. In case of compatibilised system with 5% BCP-1, the 40 % DT decreases to 10 % TLCP and then increases.

When the LCP percentage increases in the composition, i.e. 85/15, the weight loss of PPS/TLCP/BCP-1 (5%) is minimum and PPS/TLCP is maximum, as shown in Table 3.3. At a higher percentage of TLCP, PPS/TLCP blend system becomes more stable in the absence of compatibiliser. Thus, the stability at 800^{o}C is maximum for the blend with 15 % TLCP and reduces on further increase in TLCP, as shown in Figure 3.4.

3.2.2. Mechanical properties

Tensile bars of uncompatibilised PPS/TLCP show brittle fracture whereas compatibilised blends show ductile fracture. This is presumed to be due to crack preferentially occurring under stress at defects such as void existing at the interface between the PPS and TLCP phases in uncompatibilised PPS/TLCP blends. The compatibilised blend shows ductile fracture with improved tensile strength as a consequence of miscibility and improved stress fracture between the two phases. Tensile properties are improved on compatibilisation of PPS/TLCP blends, as shown in Figures 3.5 to 3.8. The tensile strength of the uncompatibilised 80/20 PPS/TLCP blend is 61.08 MPa whereas that of compatibilised 80/20/5 is 62.46 MPa, as shown in Table 3.4.

In uncompatibilised blends voids exist across or in between the interfaces causing a poor stress transfer between the phases and results in the inferior properties. The

enhancement in the tensile modulus of the compatibilised PPS/TLCP blends suggests improved interfacial adhesion.

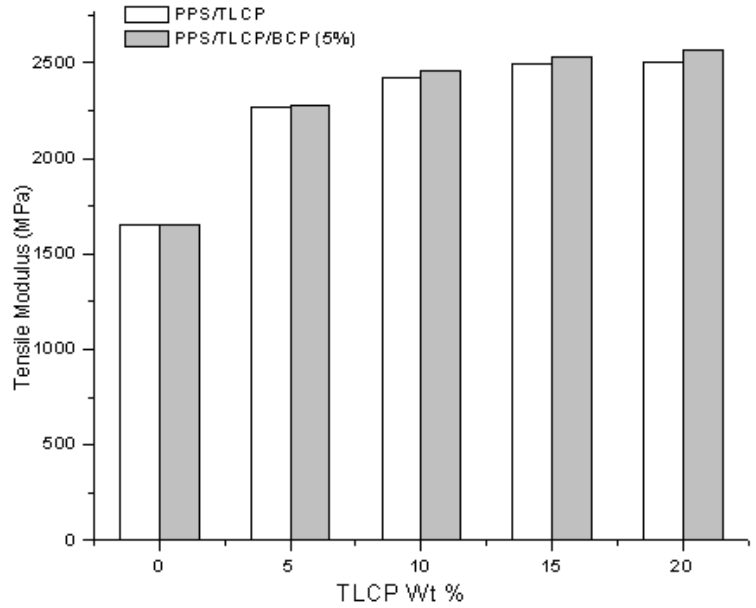

Figure 3.5: Tensile modulus of compatibilised and uncompatibilised PPS/TLCP blends.

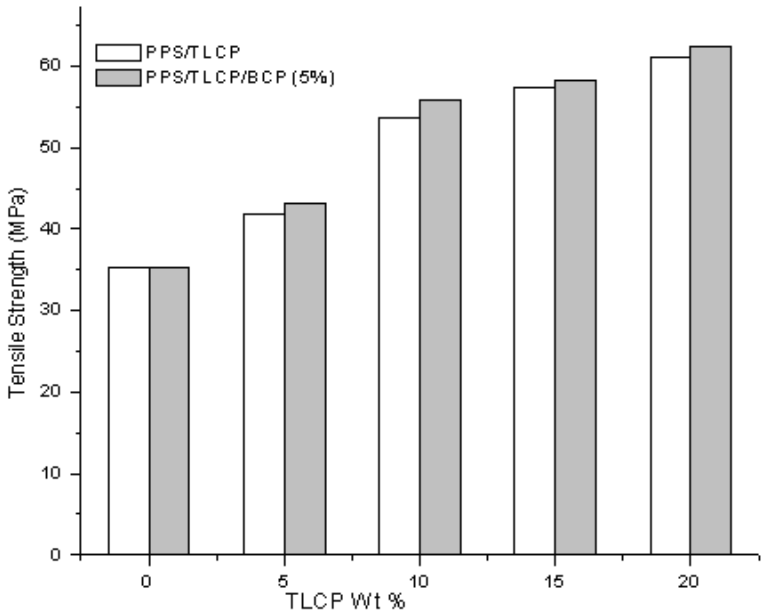

Figure 3.6: Tensile strength of compatibilised and uncompatibilised PPS/TLCP blends.

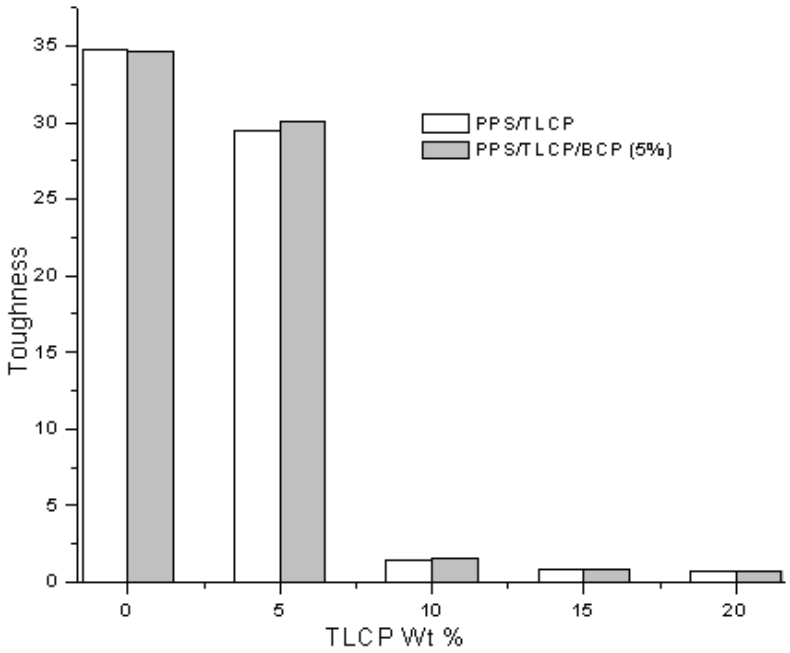

Figure 3.7: **Toughness of compatibilised and uncompatibilised PPS/TLCP blends.**

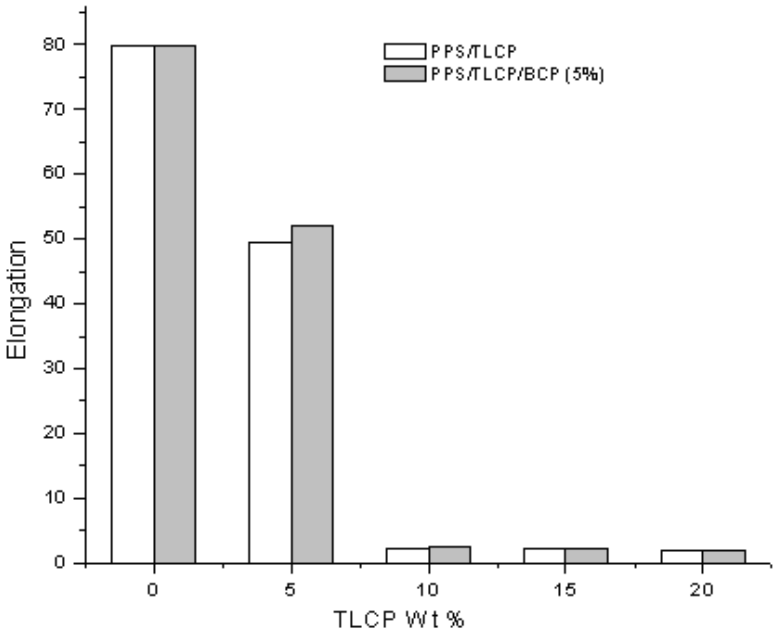

Figure 3.8: Elongation of compatibilised and uncompatibilised PPS/TLCP blends.

3.2.3. Morphology

To observe the morphology of the TLCP in the PPS matrix and to correlate with composition, scanning electron micrographs of the central area of the minitensile bars were taken. The observed surfaces were perpendicular to the direction of the flow. The

surfaces were obtained by breaking the sample during tensile test. The microscope was a *Leica Stereoscan* electron microscope, model number 440.

Figure 3.9 shows scanning electron micrograph of PPS. It shows plate like morphology of PPS with amorphous holes. Such texture is often possible when the chain and crystallite have preferential orientation, which may be due to differential applied force.

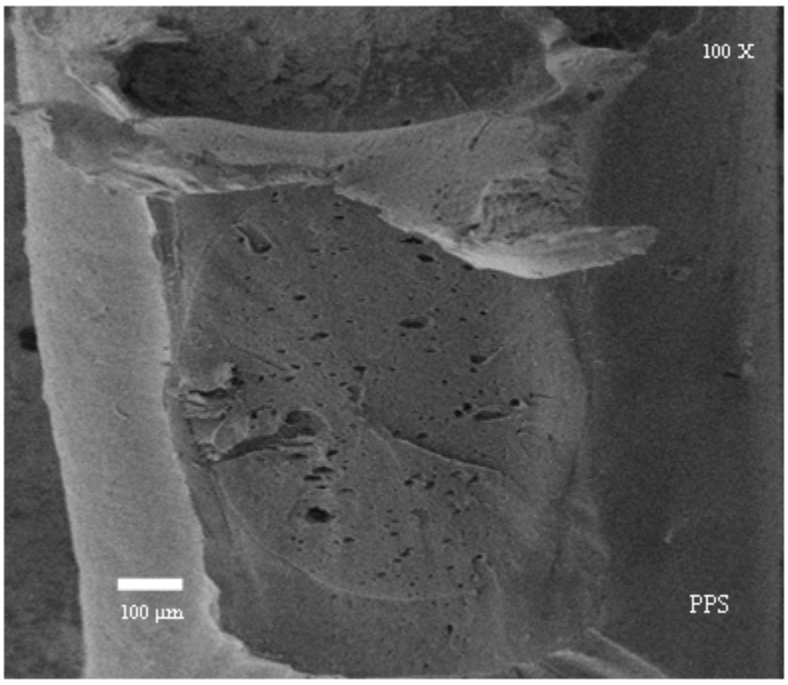

Figure 3.9: SEM micrographs showing morphology of PPS

Figures 3.10 and 3.11 show the uncompatibilised PPS/TLCP 80/20 and Figure 3.12 depicts compatibilised PPS/TLCP/BCP-1 80/20/5 blend. The TLCP dispersed droplets are almost negligible than the corresponding uncompatibilised blend. This observation supports the claims of better compatibilisation. At the core region the size of the TLCP droplets become rather small indicating an improved compatibility between PPS and TLCP.

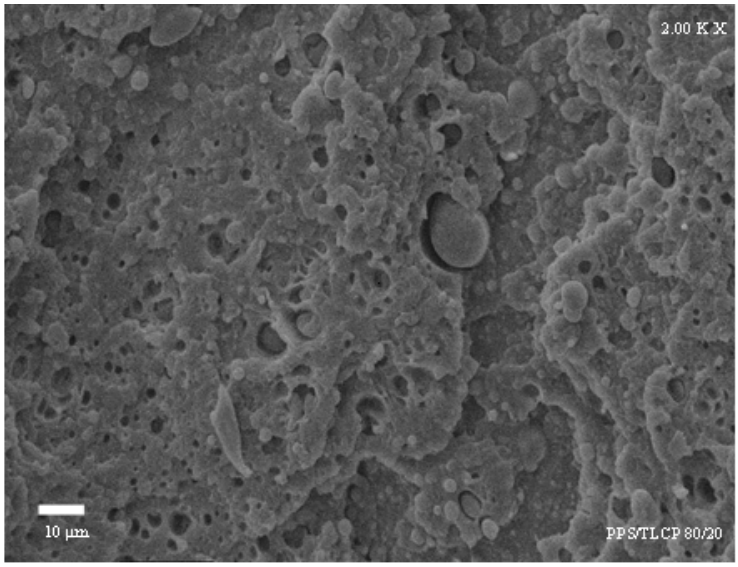

Figure 3.10: SEM micrographs showing morphology of PPS/TLCP 80/20 uncompatibilised blend.

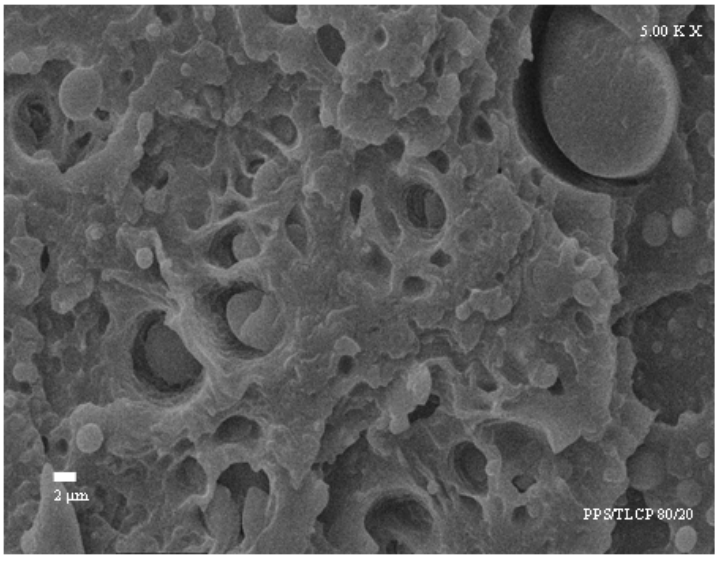

Figure 3.11: SEM micrographs showing morphology of PPS/TLCP 80/20 uncompatibilised blend.

By properly choosing the processing condition and compatibiliser composition the mechanical properties can be improved further. Earlier reports[2-6,8-13] have indicated that compatibilisation altered the fibril morphology of the TLCP phase resulting in inferior properties.

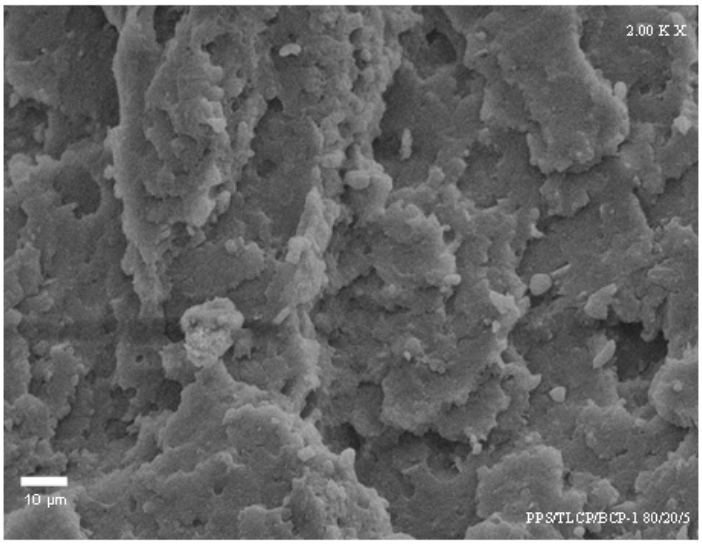

Figure 3.12: SEM micrographs showing morphology of PPS/TLCP/BCP-1 85/20/5 compatibilised blend.

Similar morphology was observed in case of uncompatibilised PPS/TLCP 85/15 and compatibilised PPS/TLCP/BCP-1 85/15/5, as shown in Figures 3.13 and 3.14.

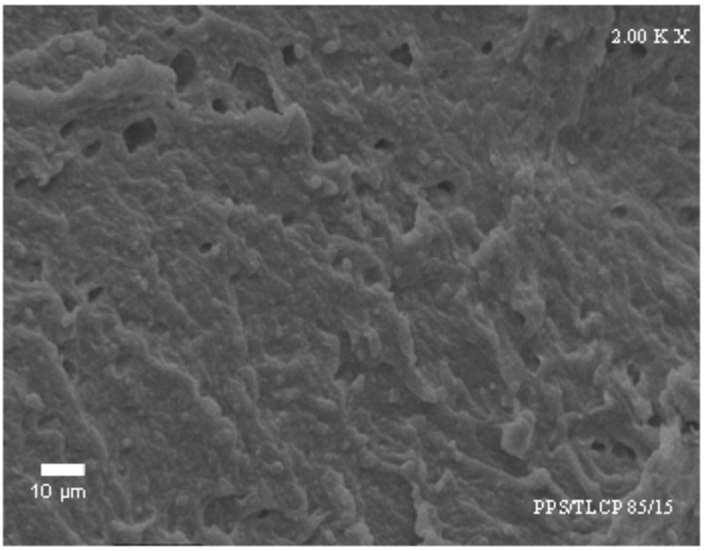

Figure 3.13: SEM micrographs showing morphology of PPS/TLCP 85/15 uncompatibilised blend.

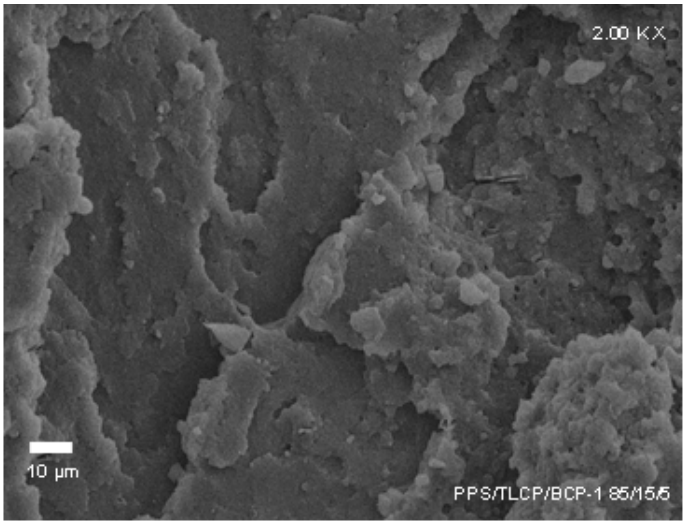

Figure 3.14: SEM micrographs showing morphology of PPS/TLCP/BCP-1 85/15/5 compatibilised blend.

3.3. Conclusion

Two loadings (5 and 10 wt.%) of poly(phenylene sulphide)-*block*-poly(ethylene terephthalate-co-oxybenzoate) block copolymer's effect on thermal properties, mechanical properties and morphology of PPS/PET-OB blends were studied. The decrease in the heat of melting, crystallisation temperature and heat of crystallisation of PPS phase in PPS/PET-OB on compatibilisation points to the presence of favourable interaction between the blend components. By increasing the loading of poly(phenylene sulphide)-*block*-poly(ethylene terephthalate-co-oxybenzoate) from 5 to 10 wt.% results in only minor changes in properties changes suggesting the optimum loading to be 5 wt.%. Marginal increase in tensile properties and toughness is noted due to increase in the interfacial adhesion between the components. Morphology studies showed that the dispersed droplets were marginally reduced in case of compatibilised blends.

3.4. References

1 Elder M., Wlochowicz A., *Polymer*, **24**, 1593, 1983.

2 Chiou Y. P., Chang D. Y., Chang F.C., *Polymer*, **37**, 5655, 1996.

3 Chiou Y. P., Chiou K. C., Chang F. C., *Polymer*, **37**, 4099, 1996.

4 Ahn T. O., Lee S., Jeong H. M., Lee S. W., *Polymer*, **34,** 4156, 1993.

5 Ahn T. O., Lee S., Jeong H. M., Lee S. W., *Polymer*, **37**, 3559, 1996.

6 Ahn T. O., Hong S. C., Jeong H. M., Kim J. H., *Polymer*, **38**, 1997, 214.

7 Maemura E., Cakmak M., White L. J., *Intern. Polym. Proc*., **3**, 79, 1990.

8 Porter R. S., Wang L. H., *Polymer*, 33, 2019, 1992.

9 Legros A., Carreau P. J., Favis B. D., Michel A., *Polymer*, **35**, 758, 1994.

10 Miller M. M., Cowie J. M. G., Tait J. G., Brydon D. L., Mather R. R., *Polymer*, **36**, 3107, 1995.

11 Ramanathan R., Blizard K. G., Baird D. G., *SPE ANTEC,* **46**, 1123, 1987.

12 Subramaniam P. R., Isayev A. I., *Polymer*, **32**, 1961, 1991.

13 Lee S., Hong S. M., Seom Y., Park T. S., Hwang S. S., Kim K. U, *Polymer*, **35**, 519, 1994.

CHAPTER-4

Compatibilised polysulphone/ poly(ethylene terephthalate-co-oxybenzoate) blends

Rajkumar Patel

National Chemical Laboratory

Chapter 4. Compatibilised polysulphone/poly(ethylene terephthalate-co-oxybenzoate) blends

Abstract

Polysulphone(n≈8)-block-poly(ethylene terephthalate-co-oxybenzoate) (BCP-2C), synthesised from dicarboxyl terminated polysulphone (n≈8) and dicarboxyl terminated poly(ethylene terephthalate-co-oxybenzoate) was used as compatibiliser[1-5] in polysulphone/poly(ethylene terephthalate-co-oxybenzoate) [PSU/PET-OB] system. Four different compositions of PSU/PET-OB were chosen. Two different loading of 5 wt.% and 10 wt.% of polysulphone-block-poly(ethylene terephthalate-co-oxybenzoate) were used. Uncompatibilised blends were characterised for thermal, mechanical and morphological properties where as compatibilised blends were characterised for thermal properties. Differential scanning calorimetry studies indicate that compatibilisation was achieved using polysulphone-block-poly(ethylene terephthalate-co-oxybenzoate). Thermogravimetric studies suggest that thermal stabilities at higher temperature are increased by compatibilising with polysulphone-block-poly(ethylene terephthalate-co-oxybenzoate). Mechanical properties increased with increasing wt.% of PET-OB.

4.2. Experimental

4.2.1. Materials

Polysulphone (PSU, GAFONE S-1300), PET/OB (55/45 mol%) and dicarboxyl terminated PET/OB, a semi-aromatic thermotropic liquid crystalline polymer, were prepared. Dicarboxyl terminated polysulphone (DCTPSU), of varying statistically average block length (n ≈ 4, 6, 8), were prepared as described in Section 2.2.1.3. The

synthesis of the block copolymer, polysulphone-*block*-poly(ethylene terephthalate-co-oxybenzoate) (BCP-2C), with block length (n≈8) was described in Section 2.2.1.6.

4.2.2. Methods

Pellets of PSU and PET/OB were manually mixed in the ratio 95/5, 90/10, 85/15, 80/20 (wt./wt.%) and dried in an air oven dryer at 100^{o}C. Polysulphone-*block*-poly(ethylene terephthalate-co-oxybenzoate) (BCP-2C) was taken at two different ratios i.e. 5 Wt.% and 10 Wt.%.

The melt blending of the PSU, PET/OB and BCP-2C were done with *DSM microcompounder*. The cylinder temperature of the microcompounder was maintained at 300^{o}C and the screw speed was 100 rpm. Uncompatibilised PPS/PET-OB blends with PET-OB content 5, 10 15 20 (wt./wt.%) were prepared under identical conditions for comparative study.

4.2.3. Processing

Injection moulding was performed with a *DSM mini injection mould.* The parent polymers were processed under conditions recommended by the manufacturers. The condition chosen for the processing of blends was a suitable compromise between those used for the respective homopolymers. The moulded specimen consisted of standard test bars for tensile and impact tests.

4.2.4. Testing and Analysis

Thermal properties of extruded PSU/PET-OB blend samples were measured by *Mettler TA4000* series differential scanning calorimeter. The apparatus was calibrated with Indium at different scanning rates. The sample mass were kept constant (6.0±0.1 mg) throughout the analysis so as to minimise the effect of mass change on the enthalpy

change. The glass transition temperature (T_g) was noted in the second heating. Thermogravimetric analysis (TGA) was carried out on a *Perkin Elmer TGA 7* under nitrogen atmosphere.

Tensile properties were measured using an *Instron testing machine* (4204). The strain rate was 50 mm/minute for tensile strength and elongation measurements. The impact strength of test specimen was determined using a *CEAST* impact testing machine with 40 kpcm pendulum. The morphology of the fractured surfaces of injection moulded tensile specimen was observed by Leica Stereoscan 440 scanning electron microscope.

4.3. Results and Discussion

4.3.1. Thermal analysis

4.3.1.1. Melting behaviour

Table 4.1 shows DSC data of polysulphone/poly(ethylene terephthalate-co-oxybenzoate) blends, with and without the compatibiliser, BCP-2C.

Table 4.1: Thermal calorimetric properties of PSU/PET-OB blends

PSU/ PET-OB	Compatibiliser (BCP-2C) (0% Wt.)		Compatibilised (BCP-2C) (5% Wt.)	
	T_{g1} ^oC	T_{g2} ^oC	T_{g1} ^oC	T_{g2} ^oC
100/0	-	184.0	-	-
95/5	29.4	161.4	26.5	160.9
90/10	29.4	161.2	-	159.3
85/15	28.2	161.0	-	157.1
80/20	-	159.7	-	157.0
0/100	63.0	-	-	-

Rate of heating 10^{o}C/min; BCP-2C:polysulphone-block-poly(ethylene terephthalate-co-oxybenzoate)

Polysulphone is highly amorphous and shows only glass transition temperature (T_g). Similarly, poly(ethylene terephthalate-co-oxybenzoate), a semi-aromatic thermotropic liquid crystalline polymer does not show clear melting transition temperature (T_m). Usually, the glass transition of blend components undergoes an inward migration on compatibilisation as a direct consequence of mutual dissolution of the components.

Neat polysulphone shows glass transition temperature (T_g) at 184.0^{o}C and PET-OB at 63.0^{o}C. In case of the uncompatibilised blend, the glass transition of both the components were observed up to PSU/PET-OB 85/15 composition. Compatibilised blends[1-9] show glass transition of both components only for one composition i.e PSU/ PET-OB/BCP-2C 85/5/5. This indicates block copolymer BCP-2C acts as a compatibiliser. Further, the glass transition temperature of the uncompatibilised system with blend composition PSU/PET-OB 80/20 shows T_g at 159.7^{o}C while its compatibilised counterpart shows at 157.0^{o}C.

4.3.1.2. Thermogravimetric analysis

Thermogravimetric curves of polysulphone/PET-OB blends are shown in Figure 4.1 and analysis is presented in Table 4.2. Polysulphone exhibits a rapid thermal degradation above 460^{o}C, and the temperature leading to maximum degradation rate is calculated to be around 544.4^{o}C. TGA study reveals that neat polysulphone exhibits better thermal stability than the blends with PET-OB below the maximum degradation temperature. Similar trend is followed in the temperature range 600^{o}C through 800^{o}C. In all the cases the stabilities of PSU/PET-OB blends is much higher than that of PET-OB. At 600^{o}C, PSU/PET-OB 80/20 shows higher thermal stability other compositions.

5% DT of compatibilised PSU/PET-OB/BCP-2C blend is less than that of the uncompatibilised system for all compositions. This shows compatibilised blends are less thermally stable than the uncompatibilised blend system at lower temperature.

As the percentage of PET-OB is increased in the PSU/PET-OB/BCP-2C (5%) blend composition, the maximum rate of decomposition temperature (T_{max}) decreases. This shows a decrease in thermal stability with increase in the PET-OB content. For PSU/PET-OB/BCP-2C (10%) and uncompatibilised blend the T_{max} changes marginally with increase in PET-OB in the blend composition.

20% DT goes on decreasing with increase in PET-OB %. The same trend is observed in both compatibilised and uncompatibilised blends. Among all the blend systems and for all compositions, uncompatibilised blends are thermally most stable as represented in Table 4.2. Similarly, 40% DT follows a similar trend to that of 20% DT. Uncompatibilised blends are thermally most stable.

The 40 % decomposition temperature (DT) is depressed at all blend compositions after addition of BCP-2C (5 Wt.%). Similar trend is noted also with blends having a 10% wt.% loading of BCP-2C.

60% DT of uncompatibilised blends goes on decreasing with increase in the relative percentage of PET-OB in the blend. This trend is not followed by the compatibilised blends. PSU/PET-OB 85/15 blend composition with 10 wt.% block copolymer (BCP-2C) is thermally most stable. Further, for 80/20 blend composition compatibilised with 5 wt.% BCP-2C is thermally most stable. This trend was also observed for weight loss % at 800^{o}C.

Table 4.2: Thermogravimetric analysis of PSU/PET-OB system under nitrogen atmosphere

PSU/ PET-OB	Compatibiliser (BCP-2C) (0% Wt.)						Compatibiliser (BCP-2C) (5% Wt.)							Compatibiliser (BCP-2C) (10% Wt.)				
	$T_{5\%}$ °C	T_{max} °C	T°C at Wt % loss			Wt loss % at 800 °C	$T_{5\%}$ °C	T_{max} °C	T°C at Wt % loss			Wt loss % at 800 °C	$T_{5\%}$ °C	T_{max} °C	T°C at Wt % loss			Wt loss % at 800 °C
			20	40	60				20	40	60				20	40	60	
100/0	528.9	544.4	536.6	548.4	584.9	66.6	-	-	-	-	-	-	-	-	-	-	-	-
95/5	480.8	543.3	529.2	547.4	575.7	69.3	452.9	538.8	525.1	542.2	574.7	68.9	432.8	536.7	524.4	541.1	570.8	71.3
90/10	456.5	544.4	527.2	546.9	574.5	69.0	433.6	536.5	520.1	538.8	569.5	69.0	420.3	538.7	521.7	541.5	570.0	70.8
85/15	438.4	545.6	518.8	545.3	574.2	70.9	417.6	535.2	513.6	536.5	566.9	70.1	408.6	538.0	513.7	538.5	580.3	68.2
80/20	429.3	543.4	511.7	540.8	568.0	68.9	414.3	529.8	504.3	531.9	576.5	67.8	397.0	538.5	-	534.9	560.4	72.7
0/100	343.8	443.4	443.1	462.3	478.0	84.7	-	-	-	-	-	-	-	-	-	-	-	-

$T_{5\%}$: Temperature at 5 % wt. Loss;Rate of heating: 10°C/min; BCP-2C:polysulphone-block-poly(ethylene terephthalate-co-oxybenzoate)

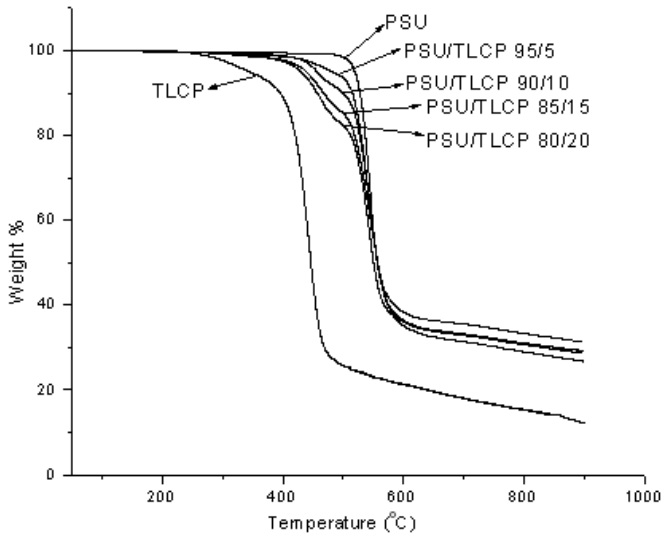

Figure 4.1: TGA thermograph of PPS/PET-OB uncompatibilised blend in nitrogen atmosphere

Figure 4.1 shows that after 600°C, the PSU/PET-OB 80/20 composition is thermally most stable and that 85/15 is the least stable one.

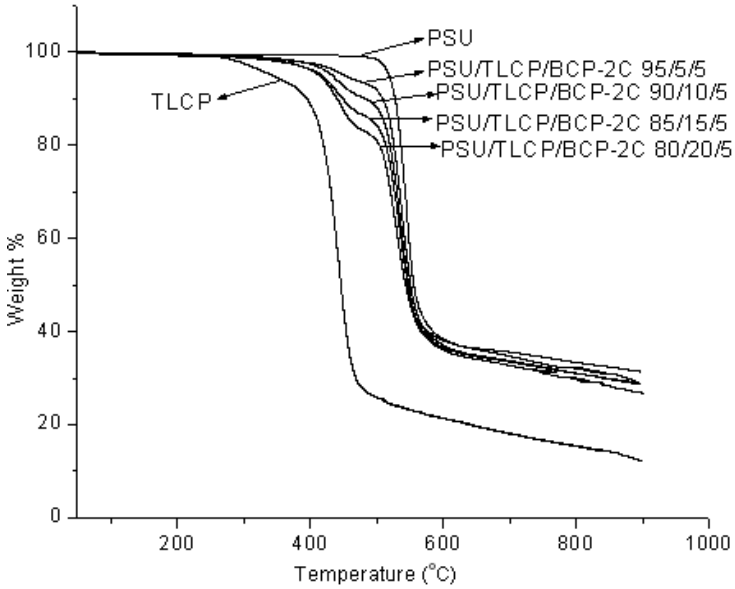

Figure 4.2: TGA thermograph of PPS/PET-OB/BCP-2C (5 Wt.%) blend in nitrogen atmosphere

Figure 4.2 shows that after 600°C, PSU/PET-OB/BCP-2C 80/20/5 composition is thermally most stable and that 85/15/10 is the least stable one.

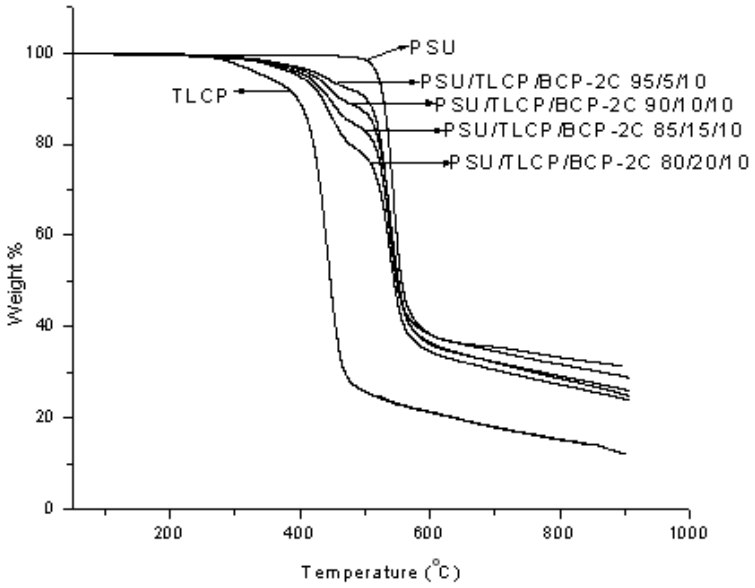

Figure 4.3: TGA thermograph of PPS/PET-OB/BCP-2C (10 Wt.%) blend in nitrogen atmosphere

Figure 4.3 shows that after 600°C, the PSU/PET-OB/BCP-2C 85/15/10 composition is thermally the most stable one and 80/20/10 is least stable one.

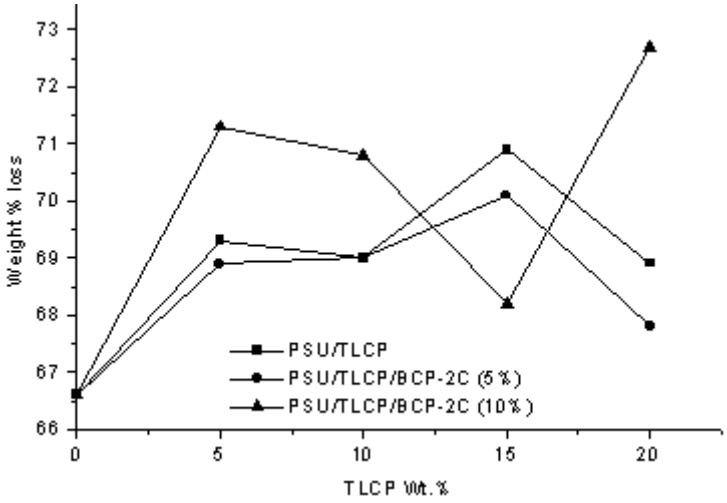

Figure 4.4: Weight % loss of i) PSU/PET-OB ii) PSU/PET-OB/BCP-2C (5%) iii) PSU/PET-OB/BCP-2C (10%) at 800°C

Figure 4.4 depicts that the weight loss at 800°C is higher for PSU/PET-OB 85/15 than PSU/PET-OB/BCP-2C 85/15/5 and 85/15/10. This implies that at this composition the thermal stabilities of the compatibilised blend is higher than that of uncompatibilised

blend and among them PSU/PET-OB/BCP-2C 85/15/10 blend composition is most stable. Further, as the PET-OB % increases, compatibilised blend PSU/PET-OB/BCP-2C 80/20/5 becomes the most stable one.

4.3.2. Mechanical properties

4.3.2.1. Tensile properties

The tensile properties (Table 4.3) of the blends were measured by Instron testing machine (Model no. 4204). In tensile measurement the cross head speed was 50 mm/min.

By increasing the PET-OB percentage, the tensile strength of PSU/PET-OB blends (Table 4.3) was increased.[10-13] In case of PSU/PET-OB 95/5 blend system, tensile strength increase was significant but as the PET-OB percentage increased further the increase in tensile strength was marginal, as shown in Figure 4.5.

Tensile modulus value of PSU/PET-OB blends is presented in Table 4.3. Neat polysulphone shows 2207 MPa and it goes up to 2417 MPa for PSU/PET-OB 85/15 blend. On further increase in PET-OB, tensile strength does not increase much, as shown in Figure 4.6. This indicates that the PSU/PET-OB 85/15 blend composition is optimum to achieve tensile modulus.

Table 4.3: Tensile test of PSU/PET-OB system

PSU/ PET-OB	Elongation at break	Modulus MPa	Tensile strength Mpa	Toughness MPa
100/0	33.64	2207	70.58	29.2
95/5	8.25	2295	83.58	8.9
90/10	3.28	2342	84.43	2.7
85/15	3.17	2417	85.53	2.3

80/20	2.62	2425	86.32	1.00

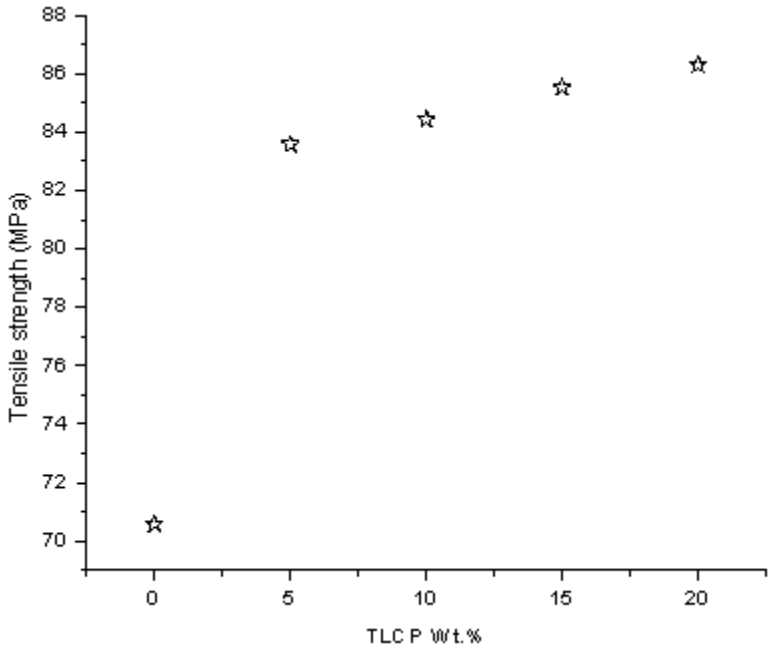

Figure 4.5: Tensile strength of PSU/PET-OB blends

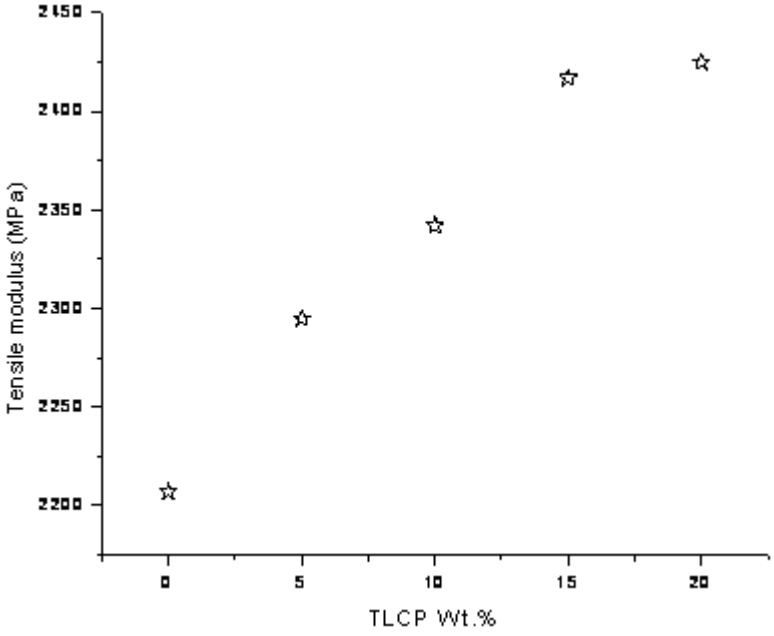

Figure 4.6: Tensile modulus of PSU/PET-OB blends

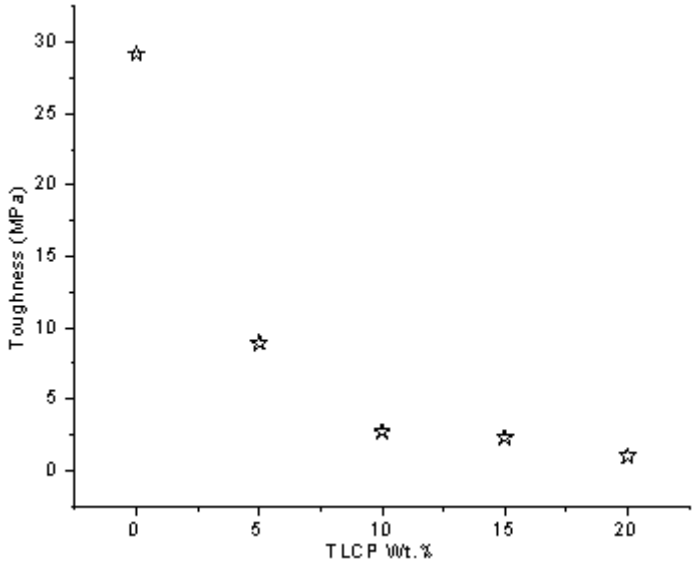

Figure 4.7: Toughness of PSU/PET-OB blends

Toughness was decreased by increasing the PET-OB percentage in the PSU/PET-OB blend, as presented in Table 4.3. This trend is along expected lines and is due to increased rigidity. This is presented in Figure 4.7.

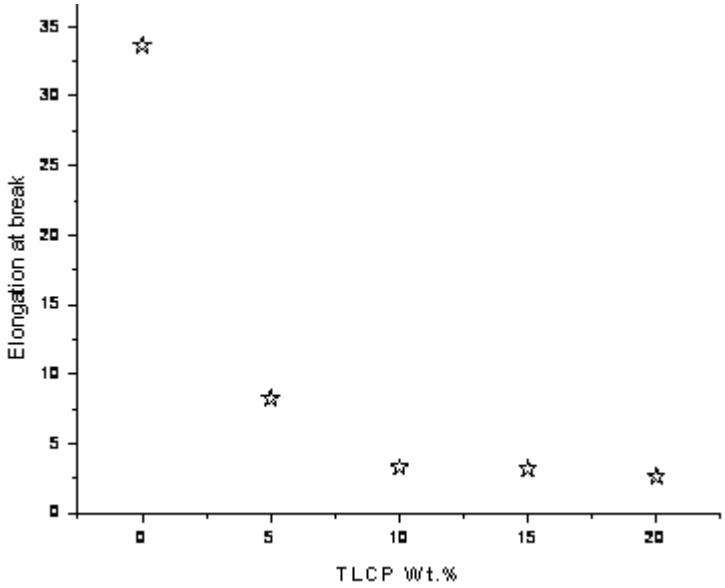

Figure 4.8: Elongation at break of PSU/PET-OB blends

As the percentage of PET-OB increases the elongation at break decreases as expected. Initially it decreases drastically but as the percentage of PET-OB increases, the decrease was small, as shown in Figure 4.8.

4.3.2.2. Flexural properties

Flexural properties of the PSU/PET-OB blend are presented in Table 4.4. Flexural strength of PSU/PET-OB blend is similar to the tensile strength. By increasing the percentage of PET-OB in the blend there is only marginal increase in flexural strength. This is shown in Figure 4.9.

Table 4.4: Flexural properties of PSU/ PET-OB system

PSU/ PET-OB	Flexural strength MPa	Modulus Mpa
100/0	35.91	2528
95/5	41.52	2573
90/10	41.93	2781
85/15	42.41	2881
80/20	42.80	2892

The trend in flexural modulus of PSU/PET-OB mirrors that observed in flexural strength. Flexural modulus increased drastically by increasing the PET-OB percentage up to 15%. Further addition of PET-OB in the blend resulted in a marginal increase. This implies the PSU/PET-OB 85/15 blend composition shows optimum properties. This is presented in Figure 4.10.

Izod impact strength of test specimen was determined using a *CEAST* impact testing machine with 40 kpcm pendulum. It shows decrease in the impact strength with

increase in the PET-OB in PSU/PET-OB blend composition, as shown in Figure 4.11 and Table 4.5.

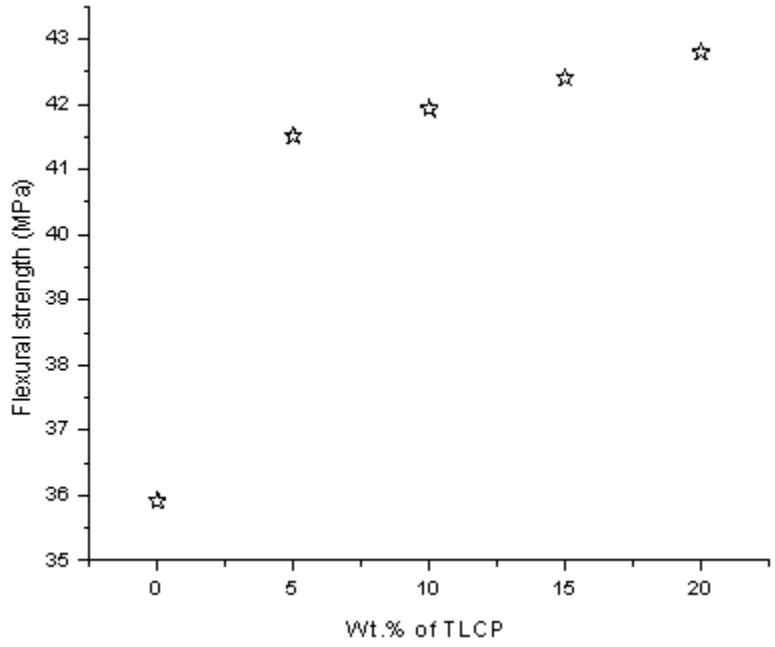

Figure 4.9: Flexural strength of PSU/PET-OB blends

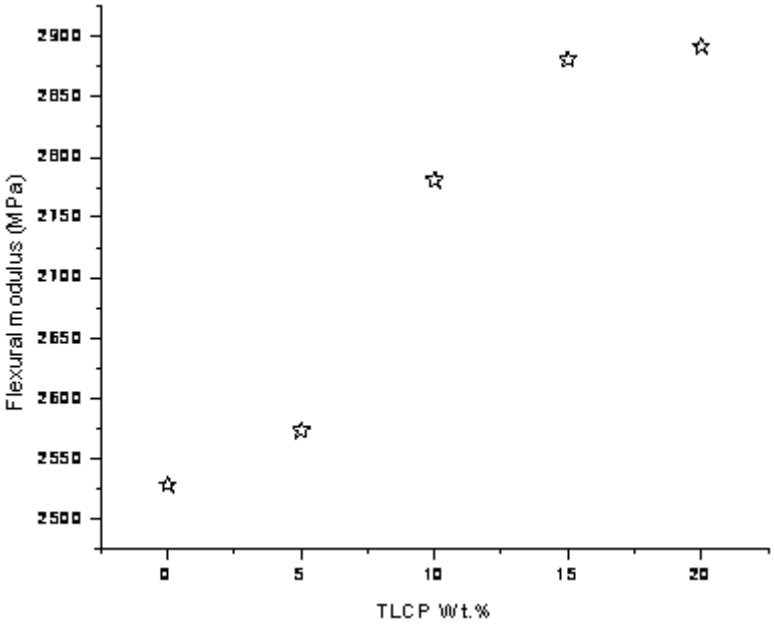

Figure 4.10: Flexural modulus of PSU/PET-OB blends

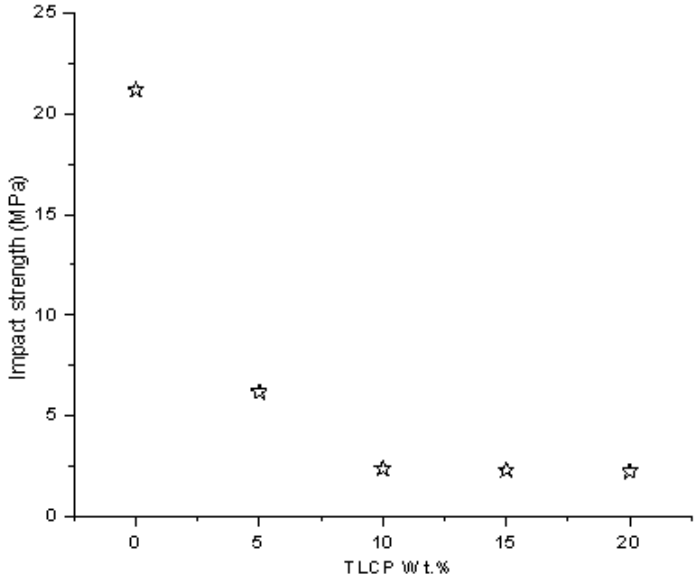

Figure 4.11: Impact strength of PSU/PET-OB blends

Table 4.5: Izod impact test of PSU/PET-OB system

PSU/PET-OB	Izod Impact strength MPa
100/0	21.18
95/5	6.18
90/10	2.38
85/15	2.31
80/20	2.24

4.3.3. Morphology

The fractured surface morphologies of the injection moulded specimen were inspected on the planes perpendicular to the injection flow direction with scanning electron microscope (*Leica Streoscan;* model 440).

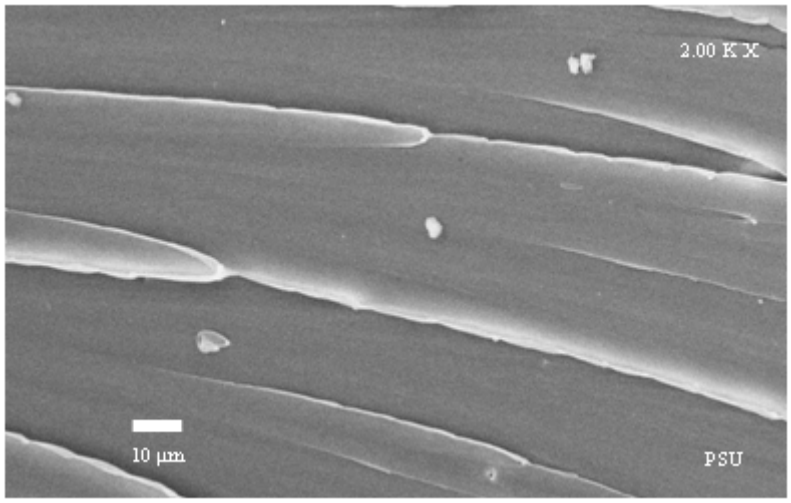

Figure 4.12: Scanning electron micrograph of neat polysulphone

Figure 4.12 shows the photomicrograph of neat polysulphone. It shows the surface to be smooth, with few defects due to errors in microtoming. Figure 4.13 shows the scanning electron micrograph of PSU/PET-OB 95/5 blend. The polysulphone matrix does not show any indication of the PET-OB phase. Figure 4.14 shows the scanning electro micrograph of PSU/PET-OB 90/10 blend. In this case also PET-OB phase is not visible.

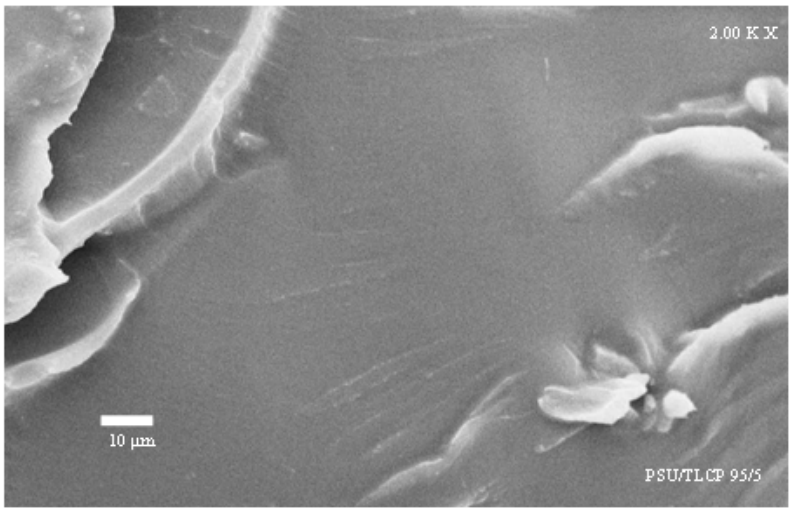

Figure 4.13: Scanning electron micrograph of PSU/PET-OB 95/5

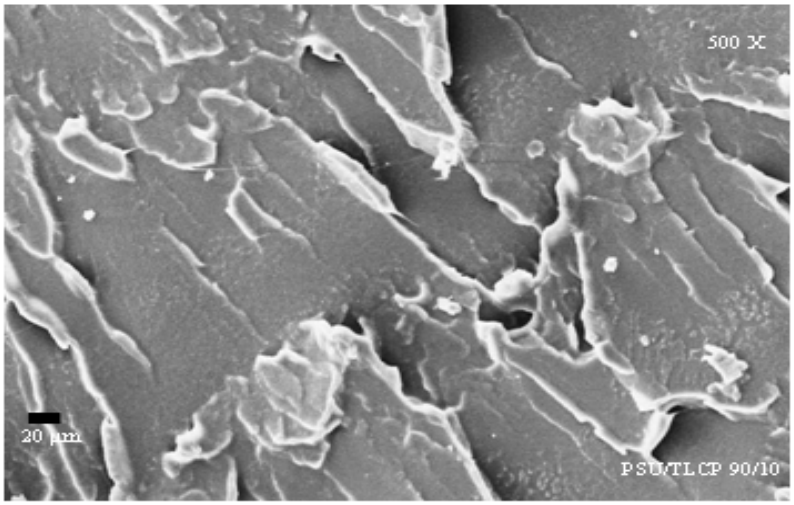

Figure 4.14: Scanning electron micrograph of PSU/PET-OB 90/10

Figure 4.15 shows the photomicrograph of PSU/PET-OB 85/15 composition. In this case small droplets of PET-OB phase are visible.[10-17] This infers the beginning of phase separation of PET-OB from the polysulphone matrix polymer.

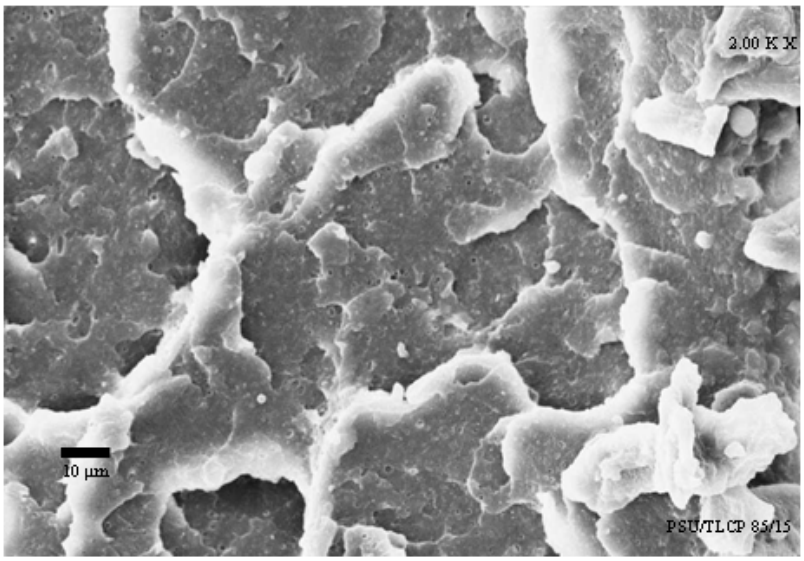

Figure 4.15: Scanning electron micrograph of PSU/PET-OB 85/15

Figure 4.16 shows the photomicrograph of PSU/PET-OB 80/20 composition. In this case droplets of PET-OB phase become more prominent. This indicates that with the increase in the PET-OB % phase separation is enhanced.

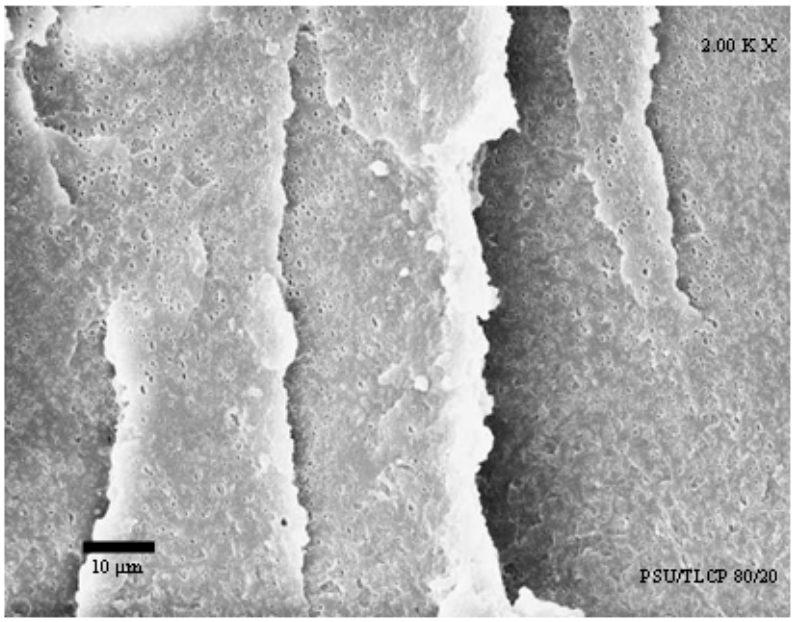

Figure 4.16: Scanning electron micrograph of PSU/PET-OB 80/20

4.4. Conclusion

The compatibilising efficiency and thermal stability of the polysulphone ($n \approx 8$)-block-poly(ethylene terephthalate-co-oxybenzoate) (PSU-*b*-PET/OB, BCP-2C) for a blend of polysulphone and poly(ethylene terephthalate-co-oxybenzoate) (PET-OB) was tested. Thermal properties, mechanical properties and morphology of uncompatibilised blend as well as thermal properties of compatibilised blends were compared using differential scanning calorimetry and thermogravimetric analyser. These studies suggest that (i) polysulphone ($n \approx 8$)-block-poly(ethylene terephthalate-co-oxybenzoate) is a suitable compatibiliser for PSU/PET-OB blend and (ii) at higher temperature the thermal

stability of PSU/PET-OB blend increases with incorporation of polysulphone ($n \approx 8$)-block-poly(ethylene terephthalate-co-oxybenzoate.

4.5. References

1 Zhang Q., Xie G., Yan H., *Polym.-Plast. Tech. Eng.,* **42**, 311, 2003.

2 Pospiech D., Haubler L., Meyer E., Janke A., Vogel R., *J. Appl. Poly. Sci.,* **64**, 619, 1997.

3 Haubler L., Pospiech D., Eckstein K., Janke A., Vogel R., *J. Appl. Poly. Sci.,* **66**, 2293, 1997.

4 Yang H., Wu X., Li S., *Poly. Eng. Sci.,* **36**, 2781, 1996.

5 Yazaki F., Kohara A., Yosomiya R., *Poly. Eng. Sci.,* **34**, 1129**,** 1994.

6 Jung H. C., Lee H. S., Chun Y. S., Kim S. B., Kim W. N., *Poly. Bull*., **41**, 387, 1998.

7 He J., Liu J., *J. Appl. Poly. Sci*., **67**, 2141, 1998.

8 Li W., Jin X., Li G., Jiang B., *Eur. Poly. J.,* **30**, 325, 1994.

9 Hong S. M., Kim B. C., Kim K. U., Chung I. J., *Poly. J.,* **23**, 1347, 1991.

10 Golovoy A., Kozlowski M., Narkis M., *Poly. Eng. Sci.,* **32**, 854, 1992.

11 He J. S., Zhang H. Z., Yuan Q., Xie P., Zhang G. Y., Xu X. Q., *Prog. Nat. Sci.,* **4**, 373, 1994.

12 Shi F., *Int. J. Polym. Mater.,* **23,** 207, 1994.

13 Wang H., Yi X., Hinrichsen G., *Poly. J.,* **29**, 881, 1997.

14 Garcia M., Eguiazabal JI., Nazabal J., *Poly. Int.,* **53**, 272, 2004.

15 Xu J., Xian W., Zeng H., *Polym. Commun.,* **32**, 336, 1991.

16 Cohen-Addad S., Stein R. S., Esnault P., *Polymer*, **32**, 2319, 1991.

17 Engberg K., Stromberg O., Martinsson J., Gedde U. W., *Poly. Eng. Sci.,* **34**, 1336, 1994**.**

CHAPTER-5

Thermotropic liquid crystalline polymer-clay nanocomposites by melt processing

Rajkumar Patel

National Chemical Laboratory

Chapter 5. Thermotropic liquid crystalline polymer-clay nanocomposites by melt processing

Abstract

Melt processing as an efficient method, for preparation of nanoscale hybrids of nematic liquid crystalline poly(ethylene terephthalate-co-oxybenzoate) {PET-OB} with montmorillonite and organically modified montmorillonite, has been investigated here. To our knowledge, this is the first report of PET-OB-clay nanocomposites. Typically crystalline and semi-crystalline polyesters require high processing temperatures which may not be suitable for preparation of nanocomposites using quaternary ammonium ion modified clays by melt processing.

Nanocomposites were prepared via batch mixing using Brabender type twin-screw mixer with roller rotors. The processing conditions were optimised such that stable intercalated nanocomposites were obtained. The nanoscale and mesoscale structure and morphology were studied by X-ray diffraction (XRD), polarised-light-optical microscopy (PLOM), transmission electron microscopy (TEM), and thermal properties were investigated using differential scanning calorimetry (DSC) and thermo-gravimetric analysis (TGA). The structural features of the intercalated nanocomposites of PET-OB and organically modified montmorillonite are presented.

Presence of clay platelets and polymer intercalation leads to a decrease in crystallisation temperature (T_c), increase in glass transition temperature (T_g) and a slight increase in the crystal-nematic transition temperature (T_{cn}) all of which can be explained on the basis of current understanding of polymer-filler hybrid materials. PLOM characterisation of the nanocomposites as well as the unfilled polymer clearly shows the existence of the nematic phase in the temperature window 190-220^oC, for 2-wt % clay in

the nanocomposite. TEM imaging performed on ultrathin microtomed samples show a homogeneous dispersion of the stacks of clay platelets throughout the polymer matrix. In addition, a heterogeneous dispersion is also observed in certain regions of the hybrid. The formation and observations in the case of nanocomposites prepared with organically modified clays having different modifier chemical structures show that favourable thermodynamic interactions exist between PET-OB and these clays. The details of nanocomposite structure, and the effect of organosilicate type and loading in polymer matrix on the liquid crystallinity and thermal stability are presented and discussed. XRD and TEM results support partial exfoliation of clay layer stacks into the LCP matrix.

5.1. Introduction

Thermotropic LCPs can be generally categorised as (i) main-chain (ii) main-chain containing spacer groups or (iii) chains containing mesogenic side-groups. Many of the LCPs of the polyester (or copolyester) family are of the main-chain type. Thermotropic melts are generally nematic in nature. Layered silicate (clay)-polymer nanocomposites (PLS), which are inorganic-organic hybrids, have been known to show unusually enhanced thermal and mechanical properties. These materials have been the considerable attention and research focus over the past decade from scientific and technological perspectives,[1-6] due to the typically nanoscale confinement and the large aspect ratio offered by the clay layers. Melt processing methods, such as mixing in an internal mixer, extrusion, injection molding and casting, to the preparation of intercalated and exfoliated nanocomposites, offer an easy and large scale preparation route compared to other existing methodologies today.[4-7] PLS nanocomposites have gained importance in recent years due to their superior thermal, mechanical and gas barrier properties as compared to

the virgin (pristine) unfilled polymer itself, all of which are achievable merely by the dispersion of only a few percent (2-10% by wt.) of either pristine or organically modified silicates into the polymer matrix. Non-reactive melt processing of polymer with organically modified layered silicates (OLS) is an effective and easy approach to the preparation of thermodynamically compatible nanocomposites. There exists the thermodynamic driving force[8,9] for polymer intercalation which is a complex interplay of entropic and enthalpy factors, apart from the effect of kinetic mixing during the preparation.

There are very few reports in the literature on the study of layered silicate based nanocomposites of thermotropic liquid crystalline polymers (TLCP).[10-14] Vaia and Giannelis,[10] have recently studied the thermal behaviour of nematic thermotropic model main chain LCP based on 4,4'-dihydroxy-α-methyl stilbene (DHMS 7,9) in melt intercalated nanocomposites prepared using dioctadecyl dimethyl ammonium modified montmorillonite, by a thermal annealing procedure of the LCP-OLS blends in the nematic state. Carter et al.[12] have studied nanocomposites prepared from the aromatic main chain LCP of poly(4-oxybenzoate-co-4-phenylene isophthalate) stabilised using dimethyl dioctadecyl tallow ammonium exchanged and dimethyl hydrogenated tallow benzyl ammonium exchanged montmorillonite and vermiculites spanning a wide CEC range, via a novel dispersion polymerisation synthetic route.

Very recently, Chang et al.[13] prepared and studied the liquid crystallinity, morphology and thermal properties of a thermotropic LCP polyester from 2-ethoxy hydroquinone and 2-bromo terephthalic acid, via the melt processing route at temperature above the melting temperature of the LCP. In all the aforementioned investigations, only

intercalated nanocomposites have been formed via melt processing. However, the level of intercalation has been found to be of varying nature.

The only study that reflects exactly the evidence of liquid crystallinity of the nanocomposite is the work of Chang et al.[13] where they have presented the optical microscopy results of the nematic phase. However, contrary to what they mention as exfoliated situation of their nanocomposites, the evidence provided by their X-ray diffraction results as well as transmission electron microscopy results clearly do not show exfoliation but rather intercalation. The mechanical modulii of the nanocomposites have been looked at and have been found higher than that of the LCP and to increase with clay loading.[14] The structure of PET-p-hydroxybenzoic acid copolymers (PET-OB), which is a well known LCP of commercial significance, originally reported by Jackson and Kuhfuss[15] and which has been widely studied by various investigating groups,[16,17] is random in nature as has been shown by NMR[15] and X-ray diffraction[18] studies originally while later work supports more of a two-phase system[19-22] in the LCP forming composition range.

The work of Wunderlich group has provided thus far the most valuable understanding of the LC structure and overall thermal phase behaviour of this polymer,[20,21] from the crystalline state to the isotropic state. Currently, there are no reports of clay-based nanocomposites and organic-inorganic hybrid materials of PET-OB and it is the main objective here is to present the first study of the nanocomposites of PET-OB.

5.2. Experimental Synthesis and Preparation

5.2.1. Clay Materials

Sodium montmorillonite (Na-MMT) and various other organically modified montmorillonites used in this study were supplied by Southern Clay Products Inc. The clays used in this study were Cloisite-Na^{+}MT (natural sodium montmorillonite, having CEC=90 meq/100 g), Cloisite-10A (the organic modifier being dimethyl benzyl hydrogenated-tallow ammonium 2MBHT, with CEC=125 meq/100 g), and Cloisite-30B (the organic modifier is methyl tallow bis(2-hydroxy ethyl) ammonium MT2EtOH, CEC=90 meq/100 g). The average agglomerate particle size (80% by volume) of the clays used varied in the range 2μ - 13μ.

5.2.2. Monomers and Polymer synthesis

4-Hydroxy benzoic acid and acetic anhydride were supplied by S. D. Fine Chemicals. Poly(ethylene terephthalate) (PET) (1676 μm) of intrinsic viscosity 0.58 (M/S Century Enka Pvt. Ltd., Pune, India) was used as received. 4-Acetoxy benzoic acid (ABA) was synthesised and characterised as described elsewhere.[15] In brief, as an example, 138.2 g 4-hydroxy benzoic acid was dissolved in 60 g of sodium hydroxide dissolved in 2 litre of cold water. Then, 150 mL of acetic anhydride was added drop-wise to the solution while maintaining stirring. Hydrochloric acid (2N) was added in order to acidify the precipitate. Subsequently, the precipitate was washed with distilled water to free from the acid. In order to remove any sodium salt, the precipitate was boiled in distilled water and then filtered. Recrystallisation from distilled methanol was performed, after which the product was dried in a vacuum oven at 70^{o}C. The yield was 130 g.

The copolyester was synthesised by the procedure reported earlier.[15,16] A 500 mL glass-lined electrically heated reactor, a larger version of the reactor used in a previous study[15] was used for synthesis and the melt transesterification reaction. Dibutyltin oxide, the most suitable catalyst in the homopolyesterification of 4-acetoxy benzoic acids,[15] was used for this transesterification reaction. PET, 4-hydroxy benzoic acid and acetic anhydride were taken in the glass-lined reactor and heating was performed on the batch.

PET melted at around 256^{o}C and degrades at around 320^{o}C on maintaining isothermally for 15 min., at atmospheric pressure. PET-OB (55/45 ethylene terephthalate to oxybenzoate mole %; random copolymer) was prepared at a reaction temperature of 275^{o}C. The purity of acetic acid formed during the reaction is best found to be 95 % (at 275^{o}C) from previous study.[15] PET and ABA were taken in the reactor and stirred at 275^{o}C under dry nitrogen blanket for 15 min. The acetic acid evolved during the reaction was collected through the distillation condenser. Application of purging and vacuum is necessary during the final stages of the reaction, in order to obtain high molecular weight copolyester.

5.2.3. PET-OB-NaMT, PET-OB-C10A, and PET-OB-C10A nanocomposites

PET-OB and all the clays (Cloisite-NaMT, Cloisite-30B and Cloisite-10A), used for the mixing experiments were dried at 65°C in a vacuum oven for 12 hours prior to mixing. PET-OB (98% by wt.) and clay (2% by wt.), for each of the nanocomposites, were dry mixed and melt blended at a temperature of 175°C in Brabender Plasticorder mixer (twin blade rotor internal mixer system) at a rotating speed of 30 rpm for a mixing time period of 10 min. The mixing was seen to be taking place very easily due to the low melt shear viscosity in the nematic phase of this LCP, which exists at this temperature.

The processing conditions were kept the same for all cases. The hybrid mass after completion of processing was taken and crushed into fine powder using a cryo-grinder for preparation of fine powder samples for the polymer as well as nanocomposites characterisation by WAXD, DSC and TGA.

5.2.4. Polymer and Nanocomposites Characterisation

Inherent viscosities were measured at 30^{o}C, using a Ubbelohde viscometer in 60:40 v/v phenol-tetrachloro ethane at a concentration of 0.5 g/dL. The copolyester and the nanocomposite samples were crushed into powder form using a cryogrinder. The powder samples were used for the characterisation by WAXD, DSC and TGA. Pellets were prepared and embedded in embedding media for performing cryo-ultramicrotomy. Microtomed samples were imaged using transmission electron microscopy. The wide-angle X-ray diffraction (WAXD) patterns were recorded on a Rigaku diffractometer using CuK_{α} radiation at 50 kV and 120 mA. The experiments were performed in a scan range of 2θ = 2 to 15° with a scan speed of 1° per min. on powder samples. d_{001} peaks were recorded. Small angle diffraction did not show any peaks.

The copolyesters and the copolyester nanocomposites were observed under a Zeiss Axioskop (Germany) polarising microscope equipped with a Linkam (TMS 92) hot stage. Imaging was performed using an Olympus lens with magnifications of 10x/0.25, 20x/0.40, and 50x/0.50. A small amount of copolyester was mounted between a slide and cover slip and was then heated on the stage at a constant rate. PET-OB copolyester was heated from 30^{o}C to 320^{o}C at a constant temperature rate of 30^{o}C/min., and maintained at 320^{o}C isothermally for 1 min. Then, the sample was cooled to 240^{o}C at a rate of 10^{o}C/min., followed by cooling at a rate of 0.1^{o}C/min., from 240^{o}C to 230^{o}C. Sample was

kept overnight at 230^{o}C in order for the slow relaxation of the polymer to take place to result in the formation of the liquid crystalline domains. Subsequent to the annealing at 230^{o}C for 24 hours, imaging was performed and the sample was cooled from 240^{o}C to 230^{o}C at a constant slow rate of 0.1^{o}C/min. Imaging was thus performed at temperatures 230^{o}C, 210^{o}C, 200^{o}C and 190^{o}C, when maintained at those temperatures during the overall stages of cooling down in the nematic phase.

In the case of the nanocomposites with NaMT, C30B, and C10A, variation of this general procedure was employed due to presence of clays layers in order to be able to let the LC phase develop, however, overall parameters and conditions remained roughly similar. Imaging was performed subsequent to annealing isothermally at the aforementioned specific temperatures during the cooling phase.

Thermo-gravimetric analysis (TGA) measurements were carried out on a Perkin-Elmer TGA-7. Samples of approximately 4 mg were heated from 50^{o}C to 650°C at a heating rate of 10°C per minute under nitrogen atmosphere. Same heating rates were used for PET-OB as well as the PET-OB-Clay hybrid samples. Thermal analysis was also carried out using Mettler DSC equipped with cold stage (to go to cryo conditions). Typically, for PET-OB (without clay), about 10.8 g of sample was heated with first scan of heating was performed at 10^{o}C/min from 30^{o}C to 300^{o}C. This step was followed by maintaining sample at 300^{o}C for 1 min., subsequently cooled from 300^{o}C to 30^{o}C at a rate of 10^{o}C/min. Alternating steps of heating and cooling were performed 4 times.

For the nanocomposites, containing organoclays, heating stage did not exceed 240^{o}C in order to avoid organic degradation from the clay surface. The correct values of glass transition temperatures were recorded during the third heating cycle. For the

nanocomposite samples the cooling step was performed till –30^{o}C followed by heating from that temperature. Three alternating cycles of heating and cooling were sufficient to obtain the value of specific heats and glass transition temperatures for the LCP as well as the nanocomposites and composite hybrid (PET-OB-NaMMT). These procedures were chosen in order to obtain reasonably accurate values of the specific heats and T_g.

5.3. Results and Discussion

5.3.1. Dispersibility of clays in the PET-OB matrix

The WAXD results presented in Figure 5.1 show a significant dispersion of clay in the LCP matrix by way of a large reduction in peak intensities accompanied by the organoclay peak shift towards higher d-spacing due to polymer intercalation. PET-OB-10A nanocomposite shows intercalation as well as partial exfoliation (supported additionally by the TEM results). PET-OB-30B nanocomposite as seen in Figure 5.1(b) is seen to be nearly exfoliated. No peaks were observed in the small angle regime of the X-ray diffraction measurements for these two nanocomposites.

The hybrid prepared by mixing Na^{+} Montmorillonite (without any organic modification) and PET-OB did not result in the formation of a nanocomposite (d-spacing in the hybrid was found to be 12.6 Å). The small peak which occurs at d=34 Å for PET-OB-10A nanocomposite (Fig. 5.1(A)) supports existence of intercalated structure in part of the region of the nanocomposite, while most of the clay layer stacks are almost completely exfoliated. This results in uniform dispersion on clay stacks with small number of layers within each stack on the average.

TEM imaging, which provides direct observation of nanoscale and mesoscale structure of nanocomposites, was utilised to ascertain the structural hierarchy. Some of

the results of images from certain regions of the exfoliated and intercalated nanocomposites are presented in Figures 5.2 and 5.3. Near exfoliated structure was obtained in these two nanocomposites of PET-OB, with Cloisite-30B and Cloisite-10A clays. The interlayer spacing in the case of nanocomposite PET-OB-10A was found to be around 32 Å by detailed image analysis (GATAN image analyser), a result which is found to go in conjunction with the result of 34 Å obtained from WAXD.

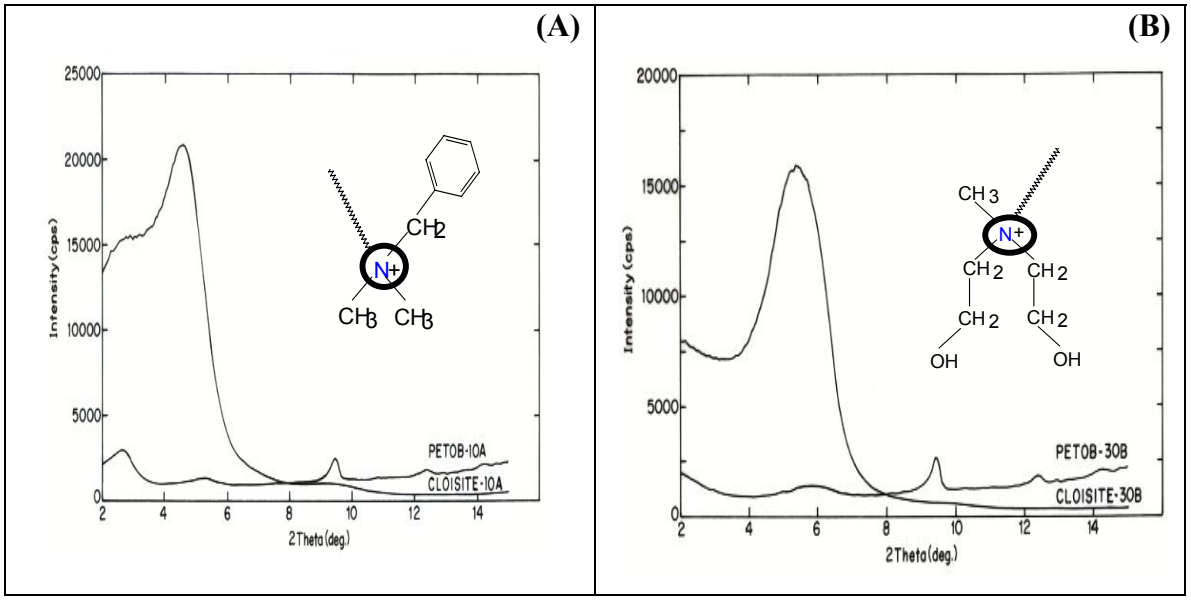

Figure 5.1: WAXD curves of PET-OB nanocomposites and organoclays. (A) Nanocomposite with Cloisite-10A organoclay. (B) Nanocomposite with Cloisite-30B organoclay.

Even though we observe and report intercalated stacks in the two nanocomposite, the evidence shows partial exfoliated structure of these nanocomposites due to the small number of clay layers per stack (we see less than 8 layers per stack in several regions with a stack size distribution which has an overall average stack thickness found to be 45 nm). This is around 13.3 intercalated clay layers per stack.

There is a distribution of various hierarchical structural distances and sizes in the nanocomposite. The distributions are, however, sharply peaked with clearly determinable

average values for quantities such as the interstack distances, stack thickness and interlayer spacing. Especially in the case of interlayer spacing the distribution is very narrow with peak value at around 4 nm, which is the sum of the thickness of a single clay layer and the interlayer distance between successive clay layers containing polymer chains. The minimum stack thickness was seen at 20 nm which are around 5 clay layers intercalating the polymer, presenting a near exfoliated situation of clay layers and stacks in the system.

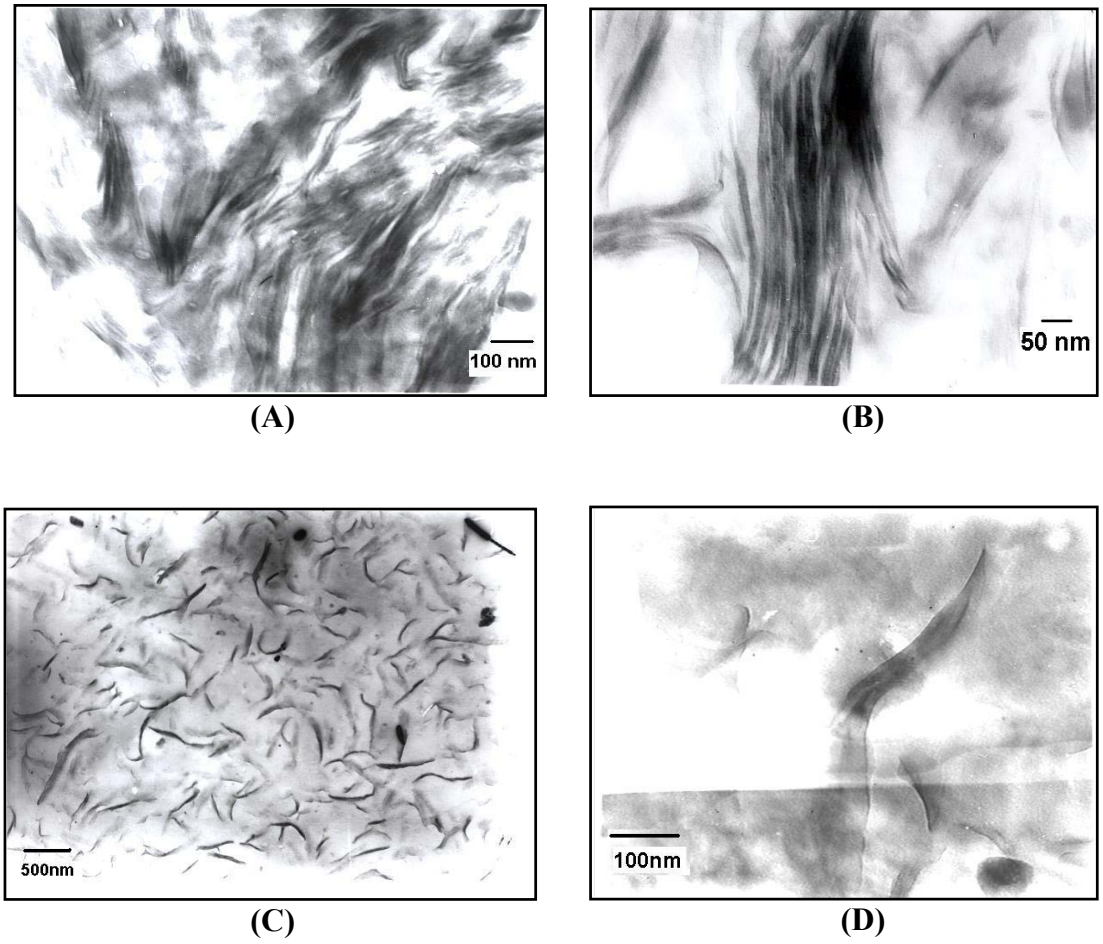

Figure 5.2: TEM images of PET-OB nanocomposites. (A), (B) PET-OB-30A nanocomposite and (C), (D) PET-OB-10A nanocomposite.

(A) **(B)**

Figure 5.3: TEM images of PET-OB-10A nanocomposite at high magnification. (A) Clay layer stacks. (B) Individual stack. Result showed interlayer spacing at 32 Å, similar to the result from WAXD of this nanocomposite.

5.3.2. Liquid crystallinity of the nanocomposites

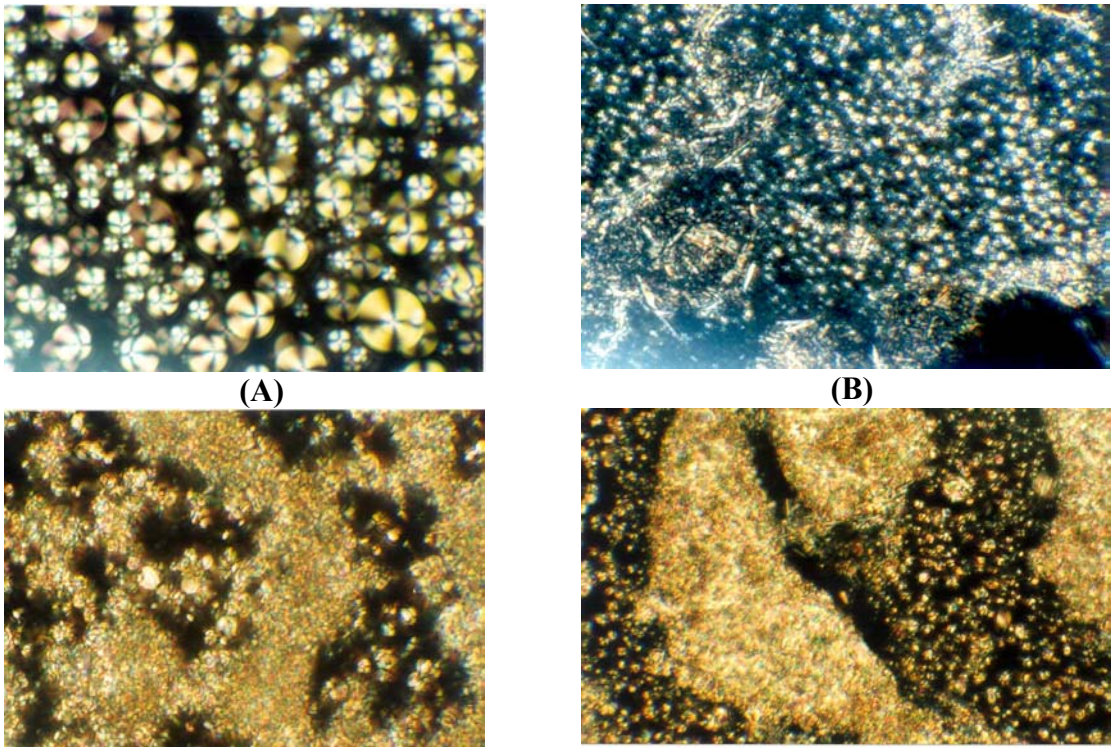

(A) **(B)**

(C) **(D)**

Figure 5.4. Optical micrographs of PET-OB and its hybrids showing textures typical of the nematic LC phase.

The nanocomposites were found to exhibit liquid crystalline behaviour. The results of the polarised light optical microscopy are presented in Figure 5.4, for two nanocomposites PET-OB-10A and PET-OB-30B. Even the composite PET-OB-NaMMT retains LC behaviour.

Since the weight loading of clay into the polymer matrix is fairly low we expected LC behaviour to be present and confirmed this by the optical microscopy characterisation. The LC behaviour was found to be retained in the similar range for the nanocomposites as compared to the LC polymer, while nematic-isotropic transition temperature was found to be lower in nanocomposites as compared to the polymer phase.

5.3.3. Thermal properties of the nanocomposites

The glass transition temperature of the composite hybrid (PET-OB-NaMMT) and the nanocomposites were found to be higher than that of the LCP. This effect is similar to that reported earlier in the literature for other LCP-clay nanocomposites. T_g increased by 10^{o}C for the nanocomposite as compared to the polymer. Figure 5.5 shows the thermooxidative degradation behaviour of the polymer and nanocomposites.

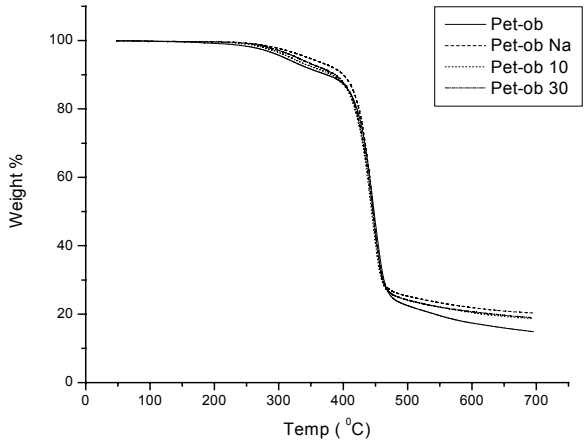

Figure 5.5: TGA curves of degradation behaviour of PET-OB and nanocomposites.

Presence of clay has a slight effect in increasing the initial degradation stability of the polymer, especially in the temperature range till 400°C, as seen by the degradation behaviour. A significant enhancement in degradation temperature is seen till about 10% weight loss. Results of thermal transitions are given in Table 5.1 and Figures 5.6 to 5.8.

Table 5.1: Thermal transitions of PET-OB LCP and its nanocomposites

System	T_g (°C)	ΔCp ($J.g^{-1}K^{-1}$)	T_{cn} (°C)	T_c (°C)	ΔH_c ($J.g^{-1}$)
PET-OB	63	0.28	170	137	9.8
PET-OB-NaMT	76	0.30	180	131	7.2
PET-OB-10A	-	-	175	132	4.7
PET-OB-30B	64	0.19	180	121	8.3

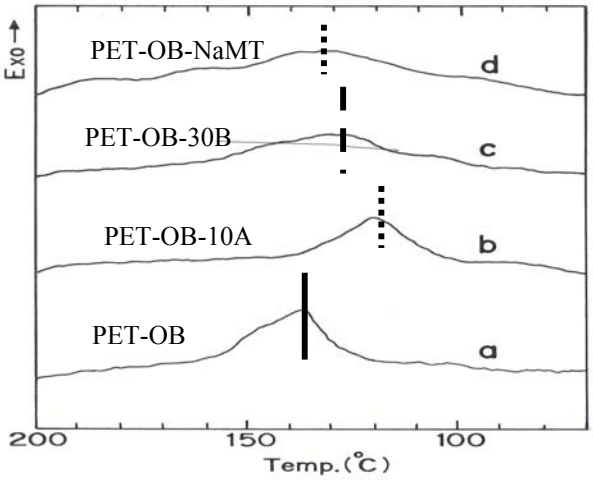

Figure 5.6. Crystallisation of PET-OB and nanocomposites

Presence of clay platelets and polymer intercalation leads to a decrease in crystallisation temperature (T_c), increase in glass transition temperature (T_g) and a slight increase in the crystal-nematic transition temperature (T_{cn}) all of which can be explained on the basis of current understanding of polymer-filler hybrid materials.

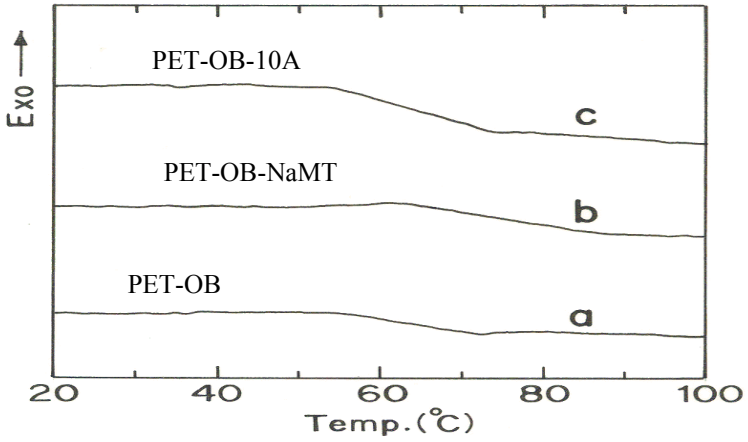

Figure 5.7. Glass transition of PET-OB and nanocomposites

The smaller heats of crystallisation are due to presence of platelet filler, the higher glass transition temperature is due to filler effect, lowering of crystallisation temperature is due to presence of filler platelets.

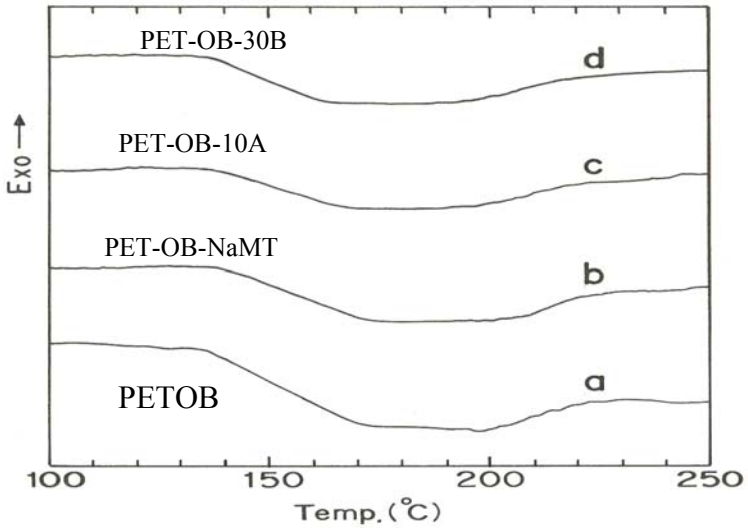

Figure 5.8. Crystal-Nematic phase transition of PET-OB and nanocomposites

Specific interactions between polymer segments and the organic modifier (containing aromatic rings), in the case of PET-OB-10A nanocomposite, lead to a

compensating effect with respect to restriction of chain mobility and thereby reducing the specific heat capacity of glass transition.

5.4. Conclusion

Nanocomposites of an semi-aromatic and random thermotropic liquid crystalline polyester PET-OB 55/45 and three clays were studied. Liquid crystallinity is retained at 2 wt% loading of clay. Presence of clay platelets decreases crystallisation temperature (T_c), increases glass transition temperature (T_g) and marginally increases crystal-nematic transition temperature (T_{cn}). TEM study shows a homogeneous dispersion of the stacks of clay platelets throughout the polymer matrix and in certain regions of the hybrid, indicating that favourable thermodynamic interactions exist between PET-OB and the clays.

5.5. References

1 Usuki A., Kawasumi M., Kojima Y., Okada A., Kurauchi T., Kamigaito O., *J. Mater. Res*., **8**, 1174, 1993.

2 Kojima Y., Usuki A., Kawasumi M., Okada A., Fukushima Y., Kurauchi T., Kamigaito O., *J. Mater. Res*., **8**, 1185, 1993.

3 Giannelis E. P., *Adv. Mater*., **8**, 29, 1993.

4 Giannelis E. P., Krishnamoorti R., Manias E., *Adv. Polym. Sci*., **138**, 107, 1999.

5 Lagaly G., *Appl. Clay Sci*., **15**, 1, 1999.

6 Gilman J. W., *Appl. Clay Sci*., **15**, 31, 1999.

7 Vaia R. A., Ishii H., Giannelis E. P., *Chem. Mater*., **5**, 1694, 1993.

8 Vaia R. A., Giannelis E. P., *Macromolecules*, **30**, 7990, 1997.

9 Vaia R. A., Giannelis E. P., *Macromolecules*, **30**, 8000, 1997.

10 Vaia R. A., Giannelis E. P., *Polymer*, **42**, 1281, 2001.

11 Cimecioglu A. L., Fruitwala H., Weiss R. A., *Makromol. Chem*., **191**, 2329, 1990.

12 Carter N., MacDonald W. A., Pitman D., Ryan T. G., *Polymer*, **40**, 7233, 1999.

13 Chang J. H., Seo B. S., Hwang D. H., *Polymer*, **43**, 2969, 2002.

14 Zhang G., Jiang C., Su C., Zhang H., *J. Appl. Poly. Sci*., **89**, 3155, 2003.

15 Jackson W. L., Kuhfuss H. F., *J. Polym. Sci. Polym. Chem. Ed*., **14**, 2043, 1976.

16 Mathew J., Bahulekar R. V., Ghadage R. S., Rajan C. R., Ponrathnam S., Prasad S. D., *Macromolecules*, 25, 7338, 1992.

17 Mathew J., Ghadage R. S., Ponrathnam S., Prasad S. D., *Macromolecules*, **27**, 4021, 1994.

18 Blackwell J., Lieser G., Gutierrez G., *Macromolecules*, **16**, 418, 1983.

19 Sawyer L. C., *J. Polym. Sci. Lett. Ed*., **22**, 347, 1984.

20 Menczel J., Wunderlich B., *J. Polym. Sci. Polym. Phys. Ed*., **18**, 1433, 1980.

21 Meesiri W., Menczel J., Gaur U., Wunderlich B., *J. Polym. Sci. Polym. Phys. Ed.,* **20**, 719, 1982.

22 Zachariadis A. E., Economy J., Logan J. A., *J. Appl. Polym. Sci*., **27**, 2009, 1982.